Impact of Curling and Warping on Concrete Pavement

Final Report
July 2016

National Concrete Pavement Technology Center

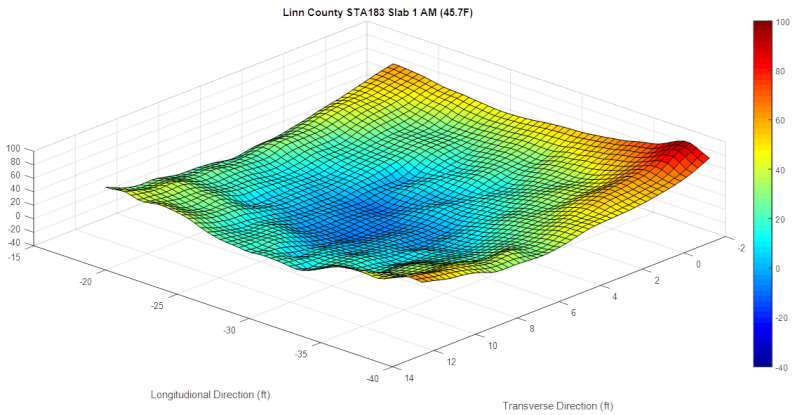

IOWA STATE UNIVERSITY
Institute for Transportation

Sponsored by
Iowa Highway Research Board
(IHRB Project TR-668)
Iowa Department of Transportation
(InTrans Project 13-486)
Federal Highway Administration

About ProSPER

The overall goal of the Program for Sustainable Pavement Engineering and Research (ProSPER) is to advance research, education, and technology transfer in the area of sustainable highway and airport pavement infrastructure systems.

About the National CP Tech Center

The mission of the National Concrete Pavement Technology (CP Tech) Center is to unite key transportation stakeholders around the central goal of advancing concrete pavement technology through research, tech transfer, and technology implementation.

About InTrans

The mission of the Institute for Transportation (InTrans) at Iowa State University is to develop and implement innovative methods, materials, and technologies for improving transportation efficiency, safety, reliability, and sustainability while improving the learning environment of students, faculty, and staff in transportation-related fields.

Disclaimer Notice

The contents of this report reflect the views of the authors, who are responsible for the facts and the accuracy of the information presented herein. The opinions, findings and conclusions expressed in this publication are those of the authors and not necessarily those of the sponsors.

The sponsors assume no liability for the contents or use of the information contained in this document. This report does not constitute a standard, specification, or regulation.

The sponsors do not endorse products or manufacturers. Trademarks or manufacturers' names appear in this report only because they are considered essential to the objective of the document.

Non-Discrimination Statement

Iowa State University does not discriminate on the basis of race, color, age, ethnicity, religion, national origin, pregnancy, sexual orientation, gender identity, genetic information, sex, marital status, disability, or status as a U.S. veteran. Inquiries regarding non-discrimination policies may be directed to Office of Equal Opportunity, Title IX/ADA Coordinator, and Affirmative Action Officer, 3350 Beardshear Hall, Ames, Iowa 50011, 515-294-7612, email eooffice@iastate.edu.

Iowa Department of Transportation Statements

Federal and state laws prohibit employment and/or public accommodation discrimination on the basis of age, color, creed, disability, gender identity, national origin, pregnancy, race, religion, sex, sexual orientation or veteran's status. If you believe you have been discriminated against, please contact the Iowa Civil Rights Commission at 800-457-4416 or Iowa Department of Transportation's affirmative action officer. If you need accommodations because of a disability to access the Iowa Department of Transportation's services, contact the agency's affirmative action officer at 800-262-0003.

The preparation of this report was financed in part through funds provided by the Iowa Department of Transportation through its "Second Revised Agreement for the Management of Research Conducted by Iowa State University for the Iowa Department of Transportation" and its amendments.

The opinions, findings, and conclusions expressed in this publication are those of the authors and not necessarily those of the Iowa Department of Transportation or the U.S. Department of Transportation Federal Highway Administration.

Technical Report Documentation Page

1. Report No. IHRB Project TR-668	**2. Government Accession No.**	**3. Recipient's Catalog No.**	
4. Title and Subtitle Impact of Curling and Warping on Concrete Pavement		**5. Report Date** July 2016	
		6. Performing Organization Code	
7. Author(s) Halil Ceylan (orcid.org/0000-0003-1133-0366), Shuo Yang (orcid.org/0000-0002-2653-5199), Kasthurirangan Gopalakrishnan (orcid.org/0000-0001-8346-5580), Sunghwan Kim (orcid.org/0000-0002-1239-2350), Peter Taylor (orcid.org/0000-0002-4030-1727), Ahmad Alhasan (orcid.org/0000-0002-0091-9899)		**8. Performing Organization Report No.** InTrans Project 13-486	
9. Performing Organization Name and Address Institute for Transportation Iowa State University 2711 South Loop Drive, Suite 4700 Ames, IA 50010-8664		**10. Work Unit No. (TRAIS)**	
		11. Contract or Grant No.	
12. Sponsoring Organization Name and Address Iowa Highway Research Board Iowa Department of Transportation 800 Lincoln Way Ames, IA 50010 Federal Highway Administration U.S. Department of Transportation 1200 New Jersey Avenue SE Washington, DC 20590		**13. Type of Report and Period Covered** Final Report	
		14. Sponsoring Agency Code IHRB and SPR Project TR-668	
15. Supplementary Notes Visit www.intrans.iastate.edu for color pdfs of this and other research reports.			

16. Abstract

Portland cement concrete (PCC) pavement undergoes repeated environmental load-related deflection resulting from temperature and moisture variations across the pavement depth. This phenomenon, referred to as PCC pavement curling and warping, has been known and studied since the mid-1920s. Slab curvature can be further magnified under repeated traffic loads and may ultimately lead to fatigue failures, including top-down and bottom-up transverse, longitudinal, and corner cracking. It is therefore important to measure the "true" degree of curling and warping in PCC pavements, not only for quality control (QC) and quality assurance (QA) purposes, but also to achieve a better understanding of its relationship to long-term pavement performance.

In order to better understand the curling and warping behavior of PCC pavements in Iowa and provide recommendations to mitigate curling and warping deflections, field investigations were performed at six existing sites during the late fall of 2015. These sites included PCC pavements with various ages, slab shapes, mix design aspects, and environmental conditions during construction. A stationary light detection and ranging (LiDAR) device was used to scan the slab surfaces. The degree of curling and warping along the longitudinal, transverse, and diagonal directions was calculated for the selected slabs based on the point clouds acquired using LiDAR. The results and findings are correlated to variations in pavement performance, mix design, pavement design, and construction details at each site. Recommendations regarding how to minimize curling and warping are provided based on a literature review and this field study. Some examples of using point cloud data to build three-dimensional (3D) models of the overall curvature of the slab shape are presented to show the feasibility of using this 3D analysis method for curling and warping analysis.

17. Key Words concrete pavement curling—concrete pavement warping—LiDAR—pavement performance—slab curvature		**18. Distribution Statement** No restrictions.	
19. Security Classification (of this report) Unclassified.	**20. Security Classification (of this page)** Unclassified.	**21. No. of Pages** 140	**22. Price** NA

Form DOT F 1700.7 (8-72) **Reproduction of completed page authorized**

IMPACT OF CURLING AND WARPING ON CONCRETE PAVEMENT

Final Report
July 2016

Principal Investigator
Halil Ceylan, Professor and Director
Program for Sustainable Pavement Engineering and Research (ProSPER)
Institute for Transportation, Iowa State University

Co-Principal Investigators
Kasthurirangan Gopalakrishnan, Research Associate Professor
Sunghwan Kim, Research Scientist
Iowa State University

Peter Taylor, Director
National Concrete Pavement Technology Center, Iowa State University

Research Assistant
Shuo Yang

Authors
Halil Ceylan, Shuo Yang, Kasthurirangan Gopalakrishnan, Sunghwan Kim,
Peter Taylor, and Ahmad Alhasan

Sponsored by
Iowa Highway Research Board,
(IHRB Project TR-668),
Iowa Department of Transportation, and
Federal Highway Administration

Preparation of this report was financed in part
through funds provided by the Iowa Department of Transportation
through its Research Management Agreement with the
Institute for Transportation
(InTrans Project 13-486)

A report from
Program for Sustainable Pavement Engineering and Research
Institute for Transportation
Iowa State University
2711 South Loop Drive, Suite 4700
Ames, IA 50010-8664
Phone: 515-294-8103 / Fax: 515-294-0467
www.intrans.iastate.edu

TABLE OF CONTENTS

LIST OF FIGURES

LIST OF TABLES

ACKNOWLEDGMENTS

The authors gratefully acknowledge sponsorship for this project from the Iowa Department of Transportation (DOT) and the Iowa Highway Research Board (IHRB), which used Federal Highway Administration (FHWA) state planning and research funds as part of their funding and provided match funds for a related study (published in January 2016/Ceylan et al. 2016 in the References).

The project technical advisory committee (TAC) members, Ben Behnami (Iowa DOT), Chris Brakke (Iowa DOT), Mark Dunn (Iowa DOT), Vanessa Goetz (Iowa DOT), Todd Hanson (Iowa DOT), Kevin Merryman (Iowa DOT), Jason Omundson (Iowa DOT), Jim Grove (FHWA), Gordon L. Smith (Iowa Concrete Paving Association [ICPA]), and John C. Cunningham (ICPA) are gratefully acknowledged for their guidance, support, and direction throughout the research.

Special thanks are due to Jonathan Miranda, Norman Miller, and Kent Nicholson from the Iowa DOT Office of Design (Surveys) for their full support during the field investigations and the collection of pavement scan data using the LiDAR device.

The authors would also like to sincerely thank Robert F. Steffes, research engineer with the National Concrete Pavement Technology (CP Tech) Center, for his timely assistance with the field investigations.

EXECUTIVE SUMMARY

Temperature and moisture variations across the depth of portland cement concrete (PCC) pavements result in unique deflection behavior that has been characterized as pavement curling and warping since the mid-1920s. Repeated slab curvature changes due to curling and warping, combined with traffic loading, can accelerate fatigue failures, including top-down and bottom-up transverse, longitudinal, and corner cracking.

Numerous studies have reported premature transverse cracking resulting from slab curling and warping in concrete pavements, such as the series of cracks recently observed in a section of I-80 in Adair County, Iowa. This cracking is not only a safety issue, but it also costs transportation agencies time and money to implement repair solutions.

It is therefore of paramount importance to measure the actual magnitude of curling and warping taking place in concrete pavements to develop performance measures and critical threshold magnitudes and to gain a better understanding of the relationship of curling and warping to diurnal and seasonal temperature/moisture changes and long-term pavement performance.

This research was designed to document the degrees of curling and warping by utilizing a light detection and ranging (LiDAR) system. Field investigations were performed at six existing sites in Iowa at different times of the day during the late fall of 2015. The sites included the following:

- STA 1422 and 2207 on US 30 in Story County
- STA 162 and 183 on US 151 in Linn County
- STA 463 on US 30 in Linn County
- STA 113 on US 30 in Tama County

These sites have PCC pavements with various ages, slab shapes, mix design aspects, and environmental conditions during construction. By using the Leica ScanStation C10 LiDAR device, point clouds for these sites were obtained. Three scans were performed at each site. The point clouds were first processed for registration and segmentation. Then, the point cloud for each slab was exported and processed in the MATLAB environment by fitting a quadratic equation to the scanned slab surface. The degree of curling and warping was then calculated along the longitudinal, transverse, and diagonal directions.

The degree of curling and warping at each site was correlated to variations in pavement performance, mix design, pavement design, and construction details at the site. Recommendations on how to minimize curling and warping are provided based on a literature review and this field study. Some examples of using point clouds to build three-dimensional (3D) models of the overall curvature of the slab shape were also presented to show the feasibility of using this 3D analysis method for PCC curling and warping analysis.

INTRODUCTION

Problem Statement

Curling and warping of portland cement concrete (PCC) pavement is a well-recognized and extensively investigated issue. Past research studies have shown that this kind of unique deflection behavior can exert tensile stresses within the slab due to restraints from the surrounding environment and has the potential to cause cracks. Although curling and warping issues have been investigated extensively, their impacts on long-term pavement performance are not well understood. While some recent studies have pointed to a strong connection between curling and warping and long-term pavement performance, others have stated that these findings may not be as significant as first thought. In order to design and construct pavements in Iowa in more cost-effective ways without sacrificing performance, the curling and warping relationship needs to be better understood.

Curling and warping occur because of differences in temperature and moisture gradients across the depth of a PCC slab. These two environmentally driven variables can lead to repeated upward or downward slab curvature. Under repeated slab curvature changes and traffic loading, concrete pavements exhibit fatigue failures, including top-down and bottom-up transverse, longitudinal, and corner cracking (Hiller and Roesler 2005). Recognizing the importance of curling and warping behavior for concrete pavement performance, the new American Association of State Highway and Transportation Officials (AASHTO) Mechanistic-Empirical Pavement Design Guide (MEPDG) and associated software (AASHTOWare Pavement ME Design) considers the impact of curling and warping behaviors on pavement performance prediction in concrete pavement design (AASHTO 2008, AASHTO 2013). Specifically in Iowa, a study sponsored by the Federal Highway Administration (FHWA) and conducted by Ceylan et al. (2007) focused on assessing the impact of curling, warping, and other early-age behaviors on concrete pavement smoothness. The overall goal of this study was to obtain detailed information about the factors affecting pavement smoothness during the critical time immediately after construction because initial smoothness can significantly affect pavement service life (Ceylan et al. 2007). Additionally, the recently completed NCHRP Project 1-47, "Sensitivity Evaluation of MEPDG Performance Prediction," concluded that concrete pavement performance predictions are highly sensitive to the properties related to slab curling and warping (Ceylan et al. 2013, Schwartz et al. 2011).

In order to better understand the curling and warping behavior of PCC pavements in Iowa, research is needed to collect data from Iowa pavements and to document the true degree of curling and warping. Such research outcomes can provide recommendations regarding how to minimize curling and warping. This understanding of research needs and goals forms the basis of the study documented in this report.

Research Objectives

The objectives of this project were as follows:

- Conduct a field investigation to survey the degrees of curling and warping in Iowa PCC pavements
- Identify the following:
    - The impact of curling and warping on the performance of Iowa PCC pavements
    - The effect of the mixture, pavement design, construction details, and climate on curling and warping behaviors
- Develop recommendations for mitigating the amount of curling and warping (guidelines are provided based on a literature review and the results of this study)

LITERATURE REVIEW

Curling and Warping Behaviors

Curling and warping of PCC pavement due to changes in environmental conditions can result in upward (concave) or downward (convex) deformation. Temperature and moisture are the two most significant environmental factors that can influence volumetric changes in PCC. The deformation induced by a non-uniform temperature gradient is referred to as curling, while the deformation induced by a non-uniform moisture gradient is referred to as warping. Usually, when the top of a PCC slab has a higher temperature or greater moisture content than the bottom, a positive gradient will be induced, and the top part of the PCC slab will experience more expansion than the bottom, resulting in downward slab curling or warping. Conversely, if the bottom of a PCC slab has a higher temperature or greater moisture content than the top, a negative gradient will occur, and the bottom part of the slab will experience more expansion than top, resulting in upward curling or warping of the slab. Furthermore, a positive temperature gradient usually occurs during daytime and a negative temperature gradient usually occurs during nighttime. Conversely, a positive moisture gradient usually occurs during nighttime and a negative moisture gradient usually occurs during daytime.

Typically, the curling effect of temperature reversals on slab deflection is diurnal whereas the warping effect of moisture on slab deflection is more seasonal, and the diurnal variation (curling) is generally larger than the seasonal variation (warping) (Chang et al. 2008, Rao et al. 2001). Furthermore, the diurnal temperature effect has a maximum impact during the nighttime and on the morning of the following day (Masad et al. 1996). However, it should be pointed out that diurnal ambient temperature changes only affect the temperature profile of the top half of a PCC slab, whereas seasonal ambient temperature changes can affect the temperature profile of the full depth of a PCC slab. The temperature difference between the mid-depth and bottom of a slab due to diurnal effects is almost negligible (Nantung 2011).

Curling and warping of the PCC slab can cause stresses as well. Once the curling and warping–induced concrete slab curvature is initiated, slab restraints will tend to exert tensile stresses in the slab that resist the differential strain response throughout the slab depth. The magnitudes of the critical tensile stresses are usually determined by sudden and drastic changes in ambient temperature (Nantung 2011). Figure 1 illustrates the tensile stresses induced in the slab due to non-uniform gradients and slab restraints.

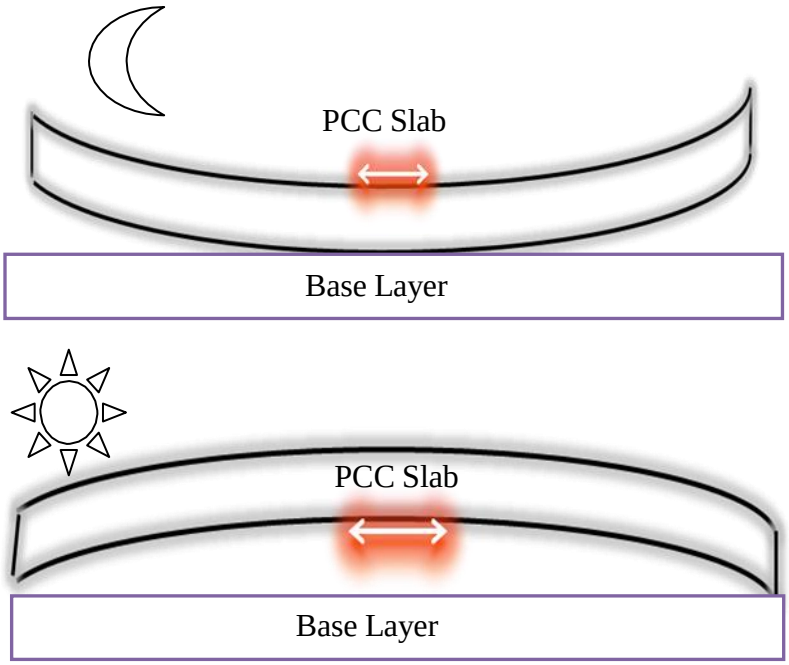

Nassiri 2011

Figure 1. Stresses exerted due to PCC curling and warping: tensile stress exerted at top of PCC slab with upward curvature (top), and tensile stress exerted at bottom of PCC slab with downward curvature (bottom)

The most common PCC pavement restraints include the self-weight of the concrete, dowel bars, the shoulder and adjacent slabs, aggregate interlock, and non-uniform friction between the PCC slab and the base (Kim et al. 2007, Rao and Roesler 2005a, Wells 2005). Furthermore, it should also be noted that the deflection of a PCC slab in the field is usually asymmetric due to varying restraints along the slab.

Curling and warping have a significant influence on overall PCC pavement performance. The stresses caused by curling and warping deflection can lead to cracking (Ahmed 1998, Hansen and Wei 2008, Lim and Tayabji 2005, Mashad 1996). Some studies also indicate that the effect of curling and warping stresses may be even more significant than the effect of traffic loads on premature cracking (Mahboub et al. 2004, Nantung 2011, Rao et al. 2001, Zhang et al. 2003).

Hveem (1949) initially investigated cracks resulting from curled PCC slabs. He defined the curling-related deflection of concrete as the "tendency of a concrete pavement to bend or warp, usually developing high joints." Hudson and Flanagan (1987) carried out a study to compare the damage due to environmental effects and due to traffic loads. Nantung (2011) conducted a study to investigate the influence of climatic changes on pavements in Indiana. In the study, mid-slab cracking on a few sections of the newly constructed jointed plain concrete pavement (JPCP) was observed even before opening to traffic (Nantung 2011). The result of curling and warping stresses can be critical for PCC pavement, especially at early ages.

Furthermore, even though the tensile stresses generated from curling may not be critical or sufficient to initiate fatigue cracking, the effect can be magnified several times when combined with traffic loads (Lee and Darter 1994a and b, Yoder and Witczak 1975). For instance, if the top of the pavement is warmer than the bottom, which results in downward curling, this can generate bottom-up cracking when combined with traffic loads. Conversely, top-down cracking can result from the combined effect of upward curling (when the top of the slab is cooler than the bottom) and traffic loads.

Curling and warping can also cause loss of contact between the slab and the subgrade. Loss of contact between the slab and the subgrade occurs at the center of the slab during downward curling and at the corners of the slab during upward curling. Loss of contact between the slab and the subgrade can increase stresses and thus aggravate pavement deterioration through repeated loading (Channakeshava et al. 1993, Rao and Roesler 2005b). Furthermore, under negative temperature gradients the PCC slab tends to curl upward and cause joint opening between adjacent slabs. The degree of joint opening can be affected by drying shrinkage and slab length (Bissonnette et al. 2007, Masad et al. 1996).

Curling and Warping Stresses

Curling Stresses

Westergaard (1926) was one of the first researchers to investigate slab curling by looking into the effect of temperature differentials on PCC pavement without traffic loads. An infinite or semi-infinite PCC slab supported on a Winkler foundation was assumed to produce the closed-form solutions for loading conditions at the corners, edges, and interior of the slab (Westergaard 1926). Westergaard (1927) also assumed that the temperature distribution was linear throughout the concrete depth. He derived numerical equations for calculating curling stresses by accounting for the positive and negative temperature gradients (Westergaard 1927). However, a study conducted by Teller and Sutherland (1935) extended Westergaard's work and revealed that temperature is, in fact, nonlinearly distributed within PCC slabs. The nonlinear distribution could be attributed to material and geometrical nonlinearities. The authors also found that the measured curling stresses can be as much as those produced by the heaviest legal wheel loads (Teller and Sutherland 1935). Further extending Westergaard's study, Bradbury (1938) derived an approximate solution to calculate the maximum stress in a finite concrete slab with all edges free. He developed a simplified chart to estimate curling stresses by applying the ratio of the slab length to the radius of relative stiffness. Based on this study, it was found that curling stresses are affected by slab length and the degree of support under the slab (Bradbury 1938).

Although both Westergaard's and Bradbury's work indicated that the stresses induced by temperature differentials alone may be comparable to the stresses induced by traffic loading under extreme climatic conditions, the PCC curling phenomenon did not receive much attention until later researchers found proof of the significance of curling stresses from field data and finite element (FE) analysis (Choubane and Tia 1992, Kuo 1991, 1998). Nevertheless, most of those numerical analysis methods still relied on Westergaard's and Bradbury's work, including the assumption of linear temperature distribution, even though it had already been realized that the

true temperature profile is highly nonlinear in realistic conditions (Liang and Niu 1998). In the later part of the 20th century, two-dimensional (2D) FE methods were used for curling analysis, which were limited to linear temperature distribution (Haril et al. 1994). Compared to the three-dimensional (3D) FE methods used later, the traditional 2D plate elements' analysis did not require as much input and execution time (Harik et al. 1994, Smith et al. 1991), but these methods had limitations with respect to predictive accuracy and visualization.

Thomlinson (1940a, 1940b) was likely the first researcher to have evaluated the curling stresses in PCC with the assumption of nonlinear temperature distribution in the concrete slab. Choubane and Tia (1992, 1995) confirmed that the temperature distribution was mostly nonlinear in the PCC slab and that the distribution could be represented fairly well by a quadratic equation to express the temperature as a function of depth. This equation was then used to characterize the respective thermal gradient components. Furthermore, the authors also concluded that if the additive effects of moisture variation at nighttime had been included, the resulting nonlinear stresses may have been much higher; thus, a nonlinear temperature distribution might affect the critical stress analysis (Choubane and Tia 1992, 1995). Harik et al. (1994) also proposed a method in conjunction with packaged 2D FE programs for the treatment of a nonlinear temperature profile through the thickness of a PCC pavement. Although this model is 2D, it is still able to superimpose the effect of the nonlinear temperature distribution on the FE solution. The authors' results clearly indicated that disregarding temperature stresses in PCC pavement design is not conservative (Harik et al. 1994).

During the 1990s, nonlinear 3D FE modeling of PCC pavement became more and more popular in curling stress investigations (Channakeshava et al. 1993, Kuo et al. 1996, Zaghloul et al. 1994). Based on 3D FE modeling, Kuo (1998) concluded that the major factors affecting curling stresses were the temperature differential, self-weight of the concrete, and support from the underlying layers. In this study, an "effective temperature differential" was proposed as that temperature differential that can cause fatigue damage equivalent to the accumulated pavement fatigue damage induced by daily curling changes. The effective temperature differential was used to avoid issues regarding the most appropriate input for curling analysis (Kuo 1998). Liang and Niu (1998) used a closed-form analytical solution to investigate the effect of temperature variations. The authors reasoned that the frequency of temperature variations, rather than the amplitude, has a greater effect on the calculated temperature distribution across the slab thickness. It was found that the magnitude of the temperature variation does not cause significant differences in the temperature distribution pattern (Liang and Niu 1998).

Warping Stresses

Slab warping due to moisture differences within a PCC slab was first reported by Hatt (1925). Carlson (1938) later conducted experiments on slabs drying from the top and observed greater moisture loss and shrinkage near the exposed surface than in other parts of the slab. However, in the 20th century warping stresses were not investigated as much as curling stresses. Hansen et al. (2008) constructed a model for warping stresses using a FE solution, which can compute concrete properties by analyzing varying environmental conditions, including moisture transport properties. The model used both surface drying at the top of the slab and wetting exposure at the

bottom to predict warping. The warping predicted corresponds to the upward movement at the center of the transverse joint of a modeled JPCP slab. In this model, an equivalent temperature gradient (ΔT_e), which causes the same magnitude of slab uplift as that caused by a moisture gradient, is determined as a function of internal relative humidity (RH), aggregate content, slab thickness, and the coefficient of thermal expansion (CTE) of concrete (Hansen et al. 2008). The authors found that wetting of the slab bottom could significantly increase the equivalent temperature gradient and consequently warping deformations.

Factors Affect Curling and Warping

Temperature Gradient

Temperature gradient within the concrete slab depth can simply be calculated by subtracting the temperature at the bottom of the slab from the temperature at the surface of the slab and then dividing it by the slab thickness, assuming linear temperature distribution. Thus, a positive temperature gradient can be induced by higher temperatures at the slab surface than at the slab bottom during daytime hours, while a negative temperature gradient can be induced by higher temperatures at the slab bottom than at the slab surface during nighttime hours. However, the actual typical temperature profile throughout a PCC slab's depth (see Figure 2) is a nonlinear temperature distribution decomposed into three components: (a) a uniform component that causes axial expansion or contraction due to uniform temperature change, (b) a linear component that causes bending of the concrete slab and (3) a zero-moment nonlinear component that causes self-equilibrating stress (Choubane and Tia 1992, Yu et al. 2004).

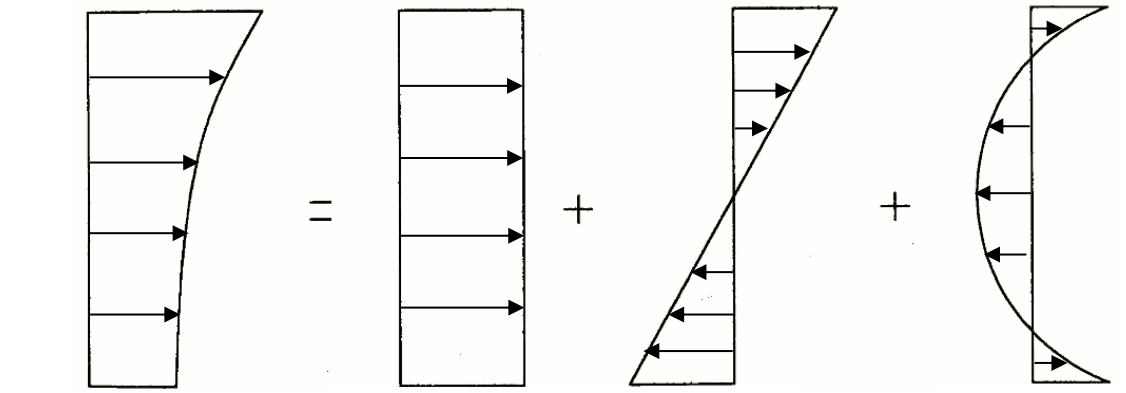

Figure 2. Typical temperature distribution throughout concrete slab depth

As discussed previously, a linear temperature distribution will result in overestimated maximum tensile stresses during the daytime and underestimated maximum tensile stresses during the nighttime compared to the results of a nonlinear temperature distribution (Choubane and Tia 1995, Masad et al. 1996). Even though it has long been realized that, in reality, slab temperature profile is nonlinearly distributed, most studies in the 20th century have assumed a linear temperature profile for easier determination (lesser computational time and effort) and for clearer

visualization of temperature gradients. Janssen and Snyder (2000) proposed the concept of "temperature-moment" to quantify pavement temperature profiles and demonstrated a method of calculating temperature-moment to quantify temperature gradients for further stress analysis..

Temperature gradient can have a more significant influence on pavement deflection than moisture gradient (McCracken 2008). Therefore, the effect of temperature gradient has been given more importance in concrete pavement design procedures because the temperature-related curling stresses can be magnified when combined with wheel load and can initiate fatigue cracking, even though the curling stresses do not exceed the allowable stresses (Choubane and Tia 1995, Harik et al. 1994, Yoder and Witczak 1975). In the Mechanistic-Empirical Pavement Design Guide (MEPDG) developed by National Cooperative Highway Research Program (NCHRP) Project 1-37A (now marketed as AASHTOWare Pavement ME Design), the effect of temperature is more thoroughly considered in concrete pavement design in order to meet the relevant performance criteria. The MEPDG uses the thermal properties of materials as direct input parameters for predicting PCC pavement performance (ARA, Inc. 2004, Chung 2012, Nantung 2011). In the design guide, all effects due to environmental conditions that influence PCC pavement performance are converted to equivalent temperature difference to quantify the impact of both temperature and moisture gradients (Yu et al. 2004).

Moisture Gradient

Harr (1958) demonstrated that moisture gradient can cause effects similar to those of temperature gradient. Similar to temperature gradient, a positive moisture gradient induced by a slab surface wetter than the slab bottom results in downward warping of the slab corners, while a negative moisture gradient induced by a slab bottom wetter than the slab top results in upward warping of the slab corners. This is because a net loss of moisture can cause contraction of concrete, while an increase in moisture up to the point of saturation for the concrete can cause volume expansion (Lederle et al. 2011). However, as noted previously, a positive moisture gradient usually occurs during nighttime hours and a negative gradient usually occurs during daytime hours, quite the opposite to the positive and negative temperature gradients. In fact, the pavement bottom is exposed to underlying layers, so its moisture content (or relative humidity) always remains around the saturation point due to the evaporation of underground water. The pavement surface, meanwhile, is exposed to the external environment, and therefore the moisture content at the top of the slab is affected by rainfall, clouds, solar radiation, and even wind. As a result, the pavement surface is typically drier than the bottom of the slab, and thus pavements usually show upward warping in the field. If it rains or snows, the surface becomes wet, and the moisture gradient tends to be zero. This may help counteract some portion of upward warping. Furthermore, moisture distribution is typically nonlinear through the concrete depth, and it mainly varies in the top two inches of the slab (Yu and Khazanovich 2001).

Previous laboratory and field studies focusing on moisture distribution have mainly used moisture sensors to measure RH, which is the percent of the water content in air compared to the saturated moisture level at the same temperature and pressure. Wei and Hansen (2011) summarized the processes of moisture distribution within the concrete slab in three ways:

external drying at the top of the concrete, water absorption at the bottom of the concrete, and self-desiccation of entire concrete sections (Wei and Hansen 2011).

External drying is the loss of moisture from the PCC pavement surface due to drying shrinkage and nonuniform moisture distribution, typically in the top two inches of the PCC slab. This process is mainly controlled by the diffusivity of the concrete, which can be affected by internal factors such as temperature, water-cement (w/cm) ratio, and concrete permeability (porosity) and external factors such as internal pore relative humidity (Yinghong 2011). During this process, moisture migrates from the moisture-rich sections to the moisture-poor sections due to the capillary force at high pore moisture contents and the gas pressure at lower pore moisture contents (Bazant 1988, Yinghong 2011). The overall movement is controlled by a diffusion equation in which moisture flux is proportional to moisture gradient (Wei and Hansen 2011). Furthermore, other studies on the diffusivity of concrete, including numerical studies, found that wetting and drying cycles can determine absorption and loss of moisture, which highly depends on ambient relative humidity and wind speed, for in-service concrete pavement (Bazant 1988, Bazant 2001, Grasley et al. 2006, Yinghong 2011, Xi et al. 1994).

Self-desiccation is the loss of moisture due to cement hydration, which can cause a uniform reduction of internal relative humidity throughout the entire concrete thickness. As a result, less of the capillary water held in the hydrating cementitious materials is free. In this process, a volumetric reduction of concrete occurs as well, which is often recognized as autogenous shrinkage (Hansen and Wei 2008). Obviously, self-desiccation is mainly affected by w/cm ratio and the degree of cement hydration. Higher degrees of hydration can aggravate self-desiccation and macroscopically lead to joint contraction (Wei and Hansen 2011).

In addition to the nonuniform and uniform reduction of internal relative humidity caused by external drying and self-desiccation, respectively, water absorption at the bottom of the concrete can cause an increase in moisture content due to capillary suction within the pore structure of the concrete (Yinghong 2011, Wei and Hansen 2011). Capillary suction dominates the transfer of moisture when concrete is at its saturation point, which is very common for the bottom portions of concrete pavements in the field because groundwater is moving up all the time due to evaporation. In the presence of water absorption, the nonuniform distribution of internal relative humidity is induced. Nevertheless, if the concrete is unsaturated, water absorption is initially conducted through instantaneous surface suction when water is introduced. Subsequently, capillary suction will continue to force the concrete to absorb water. In the end, water will fill the smaller pore structure of the concrete due to water diffusion (Wei and Hansen 2011).

Studies have demonstrated that moisture variations throughout the concrete can influence pavement performance, especially at the early ages of pavement life. During the early life of a concrete pavement, changes in moisture gradient, similar to changes in temperature gradient, have a greater influence on the behavior of the PCC slab as well as on long-term pavement performance (Jeong and Zollinger 2005). However, past studies (and even a majority of current studies) on curling and warping have focused more on investigating the effects of temperature gradient. In part, this is because temperature gradient is easier to measure, which is true even today due to the lack of commercially available moisture sensors for reliable long-term

measurements in concrete pavement (Yang 2014). The other important reason for the focus on temperature gradient is the lack of comprehensive understanding of the moisture transport phenomenon in concrete (Wei and Hansen 2011). Nevertheless, moisture effects are considered and given equal importance to temperature effects in the MEPDG (Yu et al. 2004).

Moisture gradient can be affected by concrete shrinkage (both drying and autogenous shrinkage), w/cm ratio, concrete permeability (porosity), pavement drainage conditions (subbase layer), and atmospheric climatic conditions such as temperature, relative humidity, wind, rainfall, and snow (Asbahan 2009). Figure 3 illustrates the effect of external drying, autogenous shrinkage, and water absorption on moisture gradient.

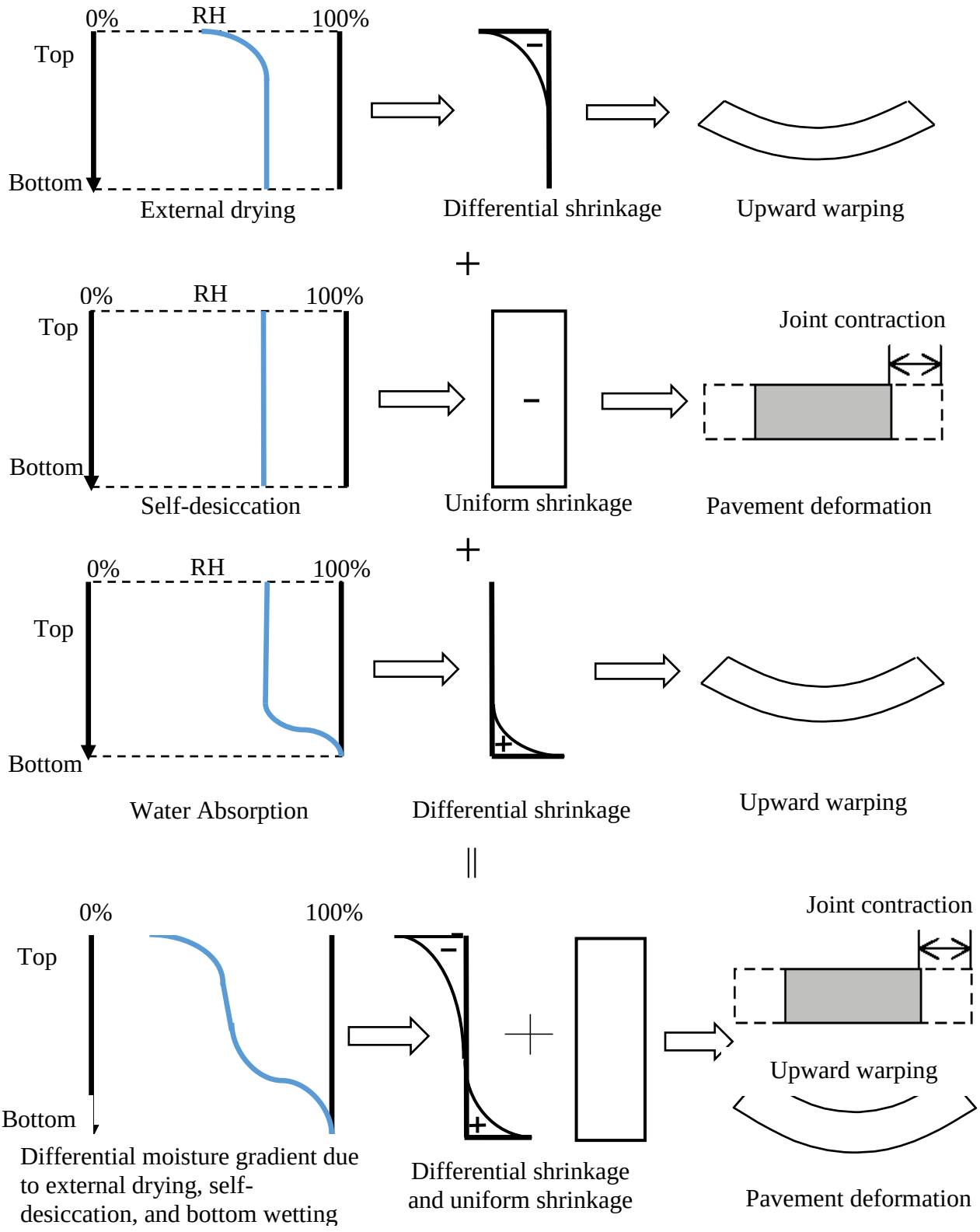

Adapted from Wei and Hansen 2011

Figure 3. Typical pavement deformation under different moisture gradients

Shrinkage

Shrinkage is one of the most significant factors that influences the warping of concrete slabs. Concrete shrinkage occurs when the concrete undergoes a decrease in either length or volume (Kosmatka et al. 2002, Rivero-Vallejo and McCullough 1976). Shrinkage can be affected by concrete mix design, ambient moisture content, the saturation level of underlying layers, and curing conditions (Rao and Roesler 2005a). Differential shrinkage due to moisture can be the main contributor to slab warping. The total moisture loss can be seen as a result of drying shrinkage and autogenous shrinkage (Hansen and Wei 2008, Wei and Hansen 2011).

Drying shrinkage, also called external drying, is the volume change as a result of moisture loss from the concrete surface (Hansen and Wei 2008). During drying shrinkage, moisture loss occurs due to the evaporation of capillary water near the surface rather than cement hydration because of the proximity of the surface to the air. During the construction of concrete pavements in the field, drying shrinkage usually occurs in the top portion of the PCC pavement rather than the bottom portion, which causes a high water content in the pores at the pavement bottom. As a result, this moisture differential can cause upward warping at the slab corners relative to the slab center due to the negative moisture gradient that persists during PCC hardening. The volume change caused by moisture loss usually manifests as a significant irreversible deformation (referred to as permanent warping) after rewetting, as illustrated in Figure 4. However, dry shrinkage–related deformation can still partially be reversed if the top surface of the concrete is exposed to a significantly higher moisture content. This usually occurs on rainy days during the pavement's service life.

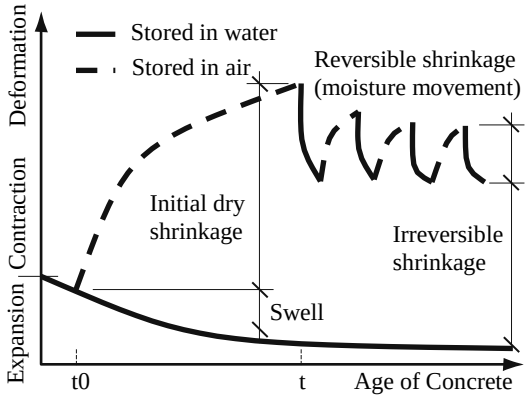

Recreated from Cement Concrete & Aggregates Australia 2002

Figure 4. Typical volume behavior of concrete drying and wetting

Generally, drying shrinkage is limited to the top two inches of the PCC slab (Franta 2012, Hansen and Wei 2008, Rao and Roesler 2005b, Suprenant 2002). It can increase upward pavement deflection and thus generate higher and lower tensile strains at the top and bottom of the PCC slab, respectively (Jeong and Zollinger 2005). Drying shrinkage can be seen as a function of the saturation of cement paste (internal pore humidity) and the concentration of volumetric aggregates (Mindess et al. 2003, Wei and Hansen 2011). Typically, a lower degree of saturation of the cement paste can aggravate drying shrinkage, while a higher degree of

saturation of the cement paste can restrain drying shrinkage (Mindess et al. 2003). Additionally, coarse aggregates in concrete are able to restrain drying shrinkage. It has been found that increasing the coarse aggregate content in a concrete mix design can improve the restraint and thus lower the level of drying shrinkage (Powers 1959).

Unlike drying shrinkage, which results from surface evaporation, autogenous shrinkage is the macroscopic reduction in volume due to cement hydration in fresh concrete. This type of shrinkage does not involve internal moisture movement. During cement hydration, internal moisture content in the capillary pores decreases. If it is assumed that the concrete is completely sealed during cement hydration, then the moisture gradient and relative humidity distribution is uniform throughout the concrete depth (Hansen and Wei 2008). As a result, no warping develops due to the zero moisture gradient. Moreover, cement hydration can generate capillary discontinuity, which can hinder moisture movement as well (Powers et al. 1959).

Usually, concrete shrinkage can be reduced if less water and cement are used in the concrete mix design (Shadravan et al. 2015). In addition to making adjustments to the concrete mix design, some modifications to concrete pavement construction practices can be made to reduce shrinkage. Altoubat and Lange (2001) investigated the impact of the use of curing compound on early age shrinkage. It was found that the use of curing compound can delay the free shrinkage rate of newly constructed pavement, but it cannot eliminate the shrinkage stresses. The authors recommend that wetting the pavement surface periodically could more effectively delay early-age shrinkage (Altoubat and Lange 2001).

Altoubat and Lange (2001) also found that extended and continuous wet curing may increase dry shrinkage, a finding similar to the observations made by Perenchio (1997). The extended curing period can reduce the permeability of the concrete and consequently lead to a higher degree of saturation due to smaller pores. As a result, extended curing can cause higher warping deflection during severe drying periods (Hajibabaee and Ley 2015). More importantly, when the curing compounds are removed, the rate of drying shrinkage may increase, which may lead to early cracks as well (Altoubat and Lange 2001, Lederle et al. 2011). Instead of using an extended wet curing period, shrinkage-reducing admixture can be used to reduce early-age shrinkage by approximately 30% to 40% and thus decrease the potential for early age cracking (Altoubat 2010). Moreover, in order to minimize the effect of early-age shrinkage during concrete construction, most state agencies specify a maximum ambient temperature for concrete paving (Schindler and McCullough 2002).

Built-in Curling

It has been observed that daily and seasonal environmental changes influence curling and warping–related PCC slab deflection. This kind of deformation is generally characterized as transient curling and warping and is repeatable and reversible via temperature and/or moisture gradient changes (Kim et al. 2011). However, a PCC slab will most likely curl or warp during its service life even without temperature and/or moisture gradient changes; a zero temperature gradient therefore does not necessarily preserve the concrete slab in a flat condition. This behavior is referred to as built-in curling, and it can occur during the setting of PCC (Kim et al.

2010, Nassiri 2011). The setting time of PCC is the time it takes for the poured concrete to become hard. During this period, concrete gains strength and loses moisture and flowability. If a temperature gradient develops inside of a fresh PCC slab due to a high ambient temperature during the curing period prior to final set, upward slab curvature can develop. This built-in curling can significantly influence early-age concrete behavior.

New PCC pavement is typically constructed during daytime hours in summer months, conditions that result in a warmer slab surface during setting time. Consequently, the PCC slab will begin to harden and stay flat with a positive temperature gradient. Once the ambient temperature starts cooling, upward curling will be induced as the temperature gradient tends to become zero or negative. In other words, a negative temperature gradient develops within the concrete when the PCC slab has a cooler surface (Hansen and Wei 2008, Rao and Roesler 2005a, Yu and Khazanovich 2001). In addition, this upward curling due to the negative temperature gradient can decrease the positive temperature gradient during daytime hours and increase the negative gradient during nighttime hours. Furthermore, the slab may revert back to a flat condition only when a sufficient positive gradient develops again to mitigate the negative gradient developed during concrete hardening (Lederle et al. 2011). The critical time for built-in curling is the first night after concrete paving because the low ambient temperature at night forces the pavement surface to remain cooler. Significant stresses tend to develop during this period while the strength gained is still low (Lim and Tayabji 2005). As a result, this built-in curling may cause cracks before the pavement is opened to traffic and initiate crack propagation from the top portion of the slab, producing top-down cracks, after the pavement is opened to traffic.

Generally, built-in curling is affected by ambient temperature, concrete setting, and pavement design factors, including joint spacing, dowel bars, sublayer type, and the thermal coefficients of the materials used (Rao et al. 2001, Rao and Roesler 2005a, Yu and Khazanovich 2001). The temperature difference during final set can also significantly influence the conditions of slab-base contact during the service life of the PCC pavement (Hansen and Wei 2008). As noted above, Hansen and Wei (2008) proposed the concept of "effective temperature difference" to represent the influence of the built-in curling on the diurnal temperature difference. The effective temperature difference can be calculated in equation (1) as follows:

$$T_{effective} = \left(T_{top,daily} - T_{bottom,daily}\right) - \left(T_{top,final\ set} - T_{bottom,final\ set}\right) \quad (1)$$

Where

$T_{effective}$: Effective temperature difference resulting from the combined effects of daily temperature difference and built-in temperature difference
$T_{top,daily}$: Top surface temperature due to diurnal ambient temperature cycles
$T_{bottom,daily}$: Bottom surface temperature due to diurnal ambient temperature cycles
$T_{top,final\ set}$: Top surface temperature at final set
$T_{bottom,final\ set}$: Bottom surface temperature at final set

Several researchers have also suggested equations or models to quantify the built-in curling in terms of temperature difference or gradient. These equations or models, conceptually similar to

each other, are referred to as "effective built-in temperature difference" (EBITD) (Rao and Roesler 2005a), "built-in equivalent temperature difference" (Vandenbossche et al. 2010), and "permanent curl/warp effective temperature difference" (ARA Inc. 2004).

Although built-in curling has been recognized and investigated for a long time, it is still difficult to estimate it with certainty due to many influencing factors, such as temperature gradient during set, differential shrinkage, creep, wind, and moisture content (Merritt et al. 2015, Rao et al. 2001). In the MEPDG/AASHTOWare Pavement ME Design model for curling, the built-in curling during concrete set and the diurnal curling during the service life of the concrete pavement are integrated as performance criteria (Yu and Khazanovich 2001).

Creep

Creep is a fundamental material property that describes the time-dependent deformation behavior of a concrete pavement subjected to a sustained load or stress. Creep strain induced within the top portion of the pavement is able to generate a shift in the movement of the concrete slab under strain cycles with respect to time (Jeong and Zollinger 2005). Nevertheless, the development of creep within a concrete structure is complex. On the microstructural level, creep in concrete can be seen as a result of the diffusion flux of the components that form solid matter and water along the hindered adsorbed layers in cement gel (Bazant and Wu 1974). Mehta (1986) indicated that creep is the result of a combination of moisture transport and the nonlinearity of the stress-strain in concrete. PCC pavement experiences shrinkage over its lifetime, and it usually occurs simultaneously with creep, especially during concrete placement (Kovler 1999). Once shrinkage occurs, tensile stresses can develop due to the restraints from the concrete's self-weight and from adjacent slabs and shoulders. These tensile stresses can further induce creep to counteract the effects of shrinkage deformation (Jeong and Zollinger 2005). If concrete paving is conducted during daytime hours, the potential for dry shrinkage increases due to the rapid drying of the surface because of the relatively higher ambient temperature. Subsequently, creep induced during concrete drying is prone to reduce upward curling and warping. The degree of upward built-in curling at the slab corners will decrease over time because of the viscous effects of creep (Lederle et al. 2011, Rao et al. 2001, Yu and Khazanovich 2001)

In addition to its effects during concrete placement, creep can affect concrete curling over the service life of a pavement as well (Lederle et al. 2001, Nantung 2011). Creep tends to cause stress relaxation in pavements, which reduces the effects of curling and warping and makes the concrete slab prone to partial recovery over time (Nassiri 2011, Rao et al. 2001). This stress relaxation can be defined as a time-dependent stress decrease in response to a constant change in strain. The tensile stresses developed at the top of the slab due to substantial drying shrinkage will experience stress relaxation over time, thereby reducing slab curling (Lederle et al. 2011, Park et al. 2015). Figure 5 illustrates the effect of creep on concrete deformation under loaded and unloaded cycles.

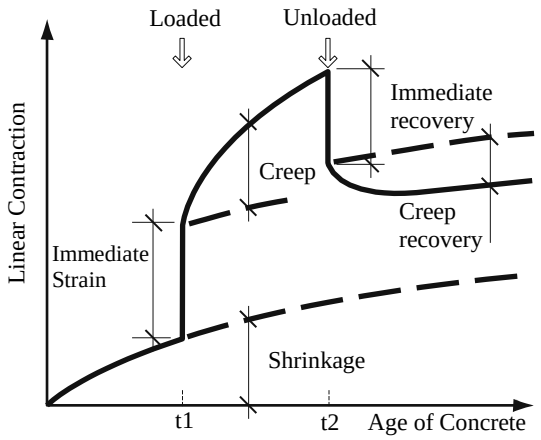

Cement Concrete & Aggregates Australia 2002

Figure 5. Effect of creep on concrete deformation

Creep can be seen as a function of mix characteristics and restraint conditions. It can be affected by coarse aggregate content, w/cm ratio, age of loading, concrete self-weight, load transfer between adjacent slabs and/or shoulders, and friction from the underlying base layer (Jeong and Zollinger 2005, Rao and Raesler 2005a, 2005b). Temperature can affect creep as well. Typically, higher temperatures can lead to an overall increase in the creep rate (Bazant et al. 2004).

Slab Geometry

Slab geometry, such as slab thickness and length, has a significant influence on JPCP curling and warping stresses. Generally, an increase in slab thickness can lead to lower curling stresses (Cement Concrete & Aggregates Australia 2006, Lee 1999, Rao and Roesler 2005a, Siddique and Hossain 2005). Thinner concrete slabs are more susceptible to curling and warping because of lower self-weight from the concrete itself and more drying shrinkage. However, all PCC pavement thickness design methods before MEPDG did not consider the effects of curling resulting from temperature gradients (Chung 2012).

Childs and Kapernick (1958) observed that curling deflection decreased by 50% when the slab thickness was changed from 6 inches to 8 inches. Nantung (2011) investigated JPCP stresses based on field measurements acquired from data collection instruments. It was found that thinner slabs typically had higher stresses than thicker slabs under the same joint spacing. Compared to thicker concrete slabs, thinner slabs have a smaller moment of inertia and therefore are more prone to bending (Nantung 2011).

A decrease in slab length can lead to lower curling stresses as well (Cement Concrete & Aggregates Australia 2006, Masad 1996, Rao and Roesler 2005a). However, slab length was initially thought to be of little importance to curling stresses based on the results of Westergaard's equations and Bradury's chart. Slab length may not affect curling stresses in PCC pavement without dowels because dowels in transverse joints can bend to resist the contraction of concrete slabs (William and Shoukry 2001). As a result, extra tensile stresses are induced

during contraction due to temperature change. Furthermore, the uniform temperature component (see Figure 2) can cause axial expansion or contraction, and thus curling and warping stresses can be initiated due to the restraints from the underlying support. The restraints due to the degree of support can vary by the ratio of joint spacing to the radius of relative stiffness. Therefore, a longer slab length and/or stiffer underlying layer can lead to higher stresses (Darter and Barenberg 1977, Jeong and Zollinger 2005). Ytterberg (1987) found that upward curling increases when the slab length increased from 15 to 20 ft. Similarly, Eisenmann and Leykauf (1990) observed that upward curling tends to increase as slab length increases. Furthermore, Nantung (2011) observed that shorter joint spacing leads to less curling stresses in JPCP, especially stresses in the longitudinal direction.

Concrete Materials Characteristics

Concrete modulus of elasticity, denoted as E, can simply be defined as the ratio of the stresses to the corresponding strain. Concrete modulus of elasticity can have an influence on curling and warping because it is correlated with concrete creep and stress relaxation behavior. Concrete with higher elastic modulus values may exhibit more curling, which is probably due to greater self-desiccation, less creep, and less downward relaxation of the curled slab over time (Lederle et al. 2011, Rao and Roesler 2005a). Concrete modulus of elasticity mainly depends on the coarse aggregate stiffness. Typically, aggregates with higher stiffness values produce concretes with higher E values. Table 1 summarizes the E values of concretes with different aggregate types, as investigated by Aitcin and Mehta (1990). According to this table, concrete with limestone has a slightly higher E value than concretes with other types of aggregates.

Table 1. Modulus of elasticity of concrete with different aggregates

Age	E, GPa			
(days)	Diabase	Limestone	Gravel	Granite
28	36.6	37.9	33.8	31.7
56	37.9	40.7	35.9	33.8

Source: Aitcin and Mehta 1990

In addition to elastic modulus, the CTE of concrete also has an influence on curling and warping. CTE is a measure of volume contraction or expansion in response to temperature variations. Typically, PCC pavements with higher CTE values undergo greater volume changes when subjected to similar temperature gradients. Consequently, more curling deflection occurs. Furthermore, a drastic difference in CTE values between the PCC layer and the subsequent underlying layer causes significant curling stresses. This is because the strain magnitudes are different for the two adjacent layers, which generates large frictional stresses and ultimately leads to significant curling stresses as well (Asbahan 2009, Wells 2005). The CTE of concrete mainly depends on aggregate type and degree of saturation. Typically, concrete with limestone has a relatively lower CTE value compared to concrete with other types of aggregates.

In recent years, the thermal properties of concrete or aggregates, such as CTE, thermal conductivity (TC), and heat capacity (HC), have received attention as important material

properties for controlling PCC pavement curling. They have been accepted as fundamental factors in mechanistic-based thickness design procedures, such as the MEPDG/AASHTOWare Pavement ME Design procedures, for predicting PCC pavement performance (ARA Inc. 2004, Chung 2012).

Underlying Layer

As noted previously, curling and warping stresses develop due to restraints caused by the underlying layer. Generally, higher friction due to restraint leads to higher curling stresses. Rivero-Vallejo and McCullough (1976) found that high friction between the top PCC layer and the underlying layer was the main factor influencing crack propagation. Masad et al. (1996) utilized a 3D FE model and interface elements to model the interaction between a PCC slab and its underlying layer. It was found that the frictional coefficient was larger in shorter slabs than longer slabs, and the maximum stresses were generated at the slab center (Masad et al. 1996). This finding agreed with the conclusion by Huang (2004) that friction is proportional to slab length but independent of slab thickness. Furthermore, friction is also affected by the weight of the concrete.

As shown in Figure 6, the PCC slab does not necessarily fully reflect the condition of the underlying supporting layer because the underlying layer is not necessarily flat (Yu et al. 2004).

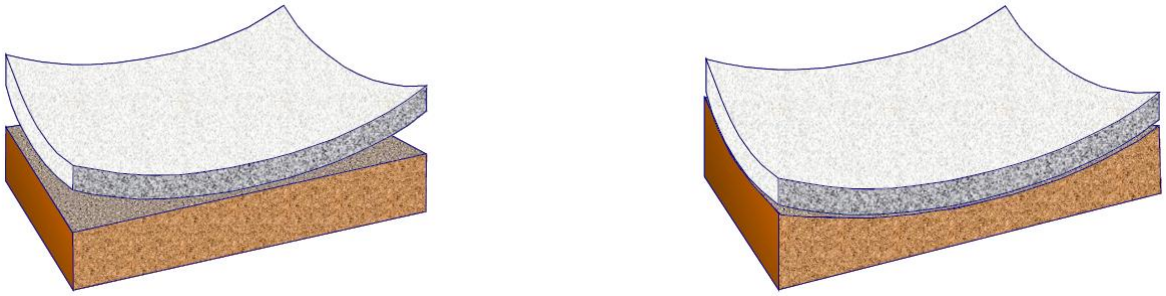

Yu et al. 2004

Figure 6. Illustration of support conditions under PCC slabs: assuming idealistic flat foundation (left) and more realistic representation, including the effects of settlement (right)

However, a stiff underlying layer generates more stresses when the slab deforms. When curling occurs, a stiff underlying layer resists the settlement of the slab into underlying layer (Ytterberg 1987). In contrast, a soft underlying layer can generate less curling stresses due to the "bedding" effect, which reduces the effect of the restraint from the underlying layer (Eisenmann and Leykauf 1990). However, when taking traffic loads into account, critical tensile stresses may be higher in a PCC pavement with a soft base because traffic loads can cause larger deflections due to the lower resistance from the underlying layer compared to the deflections caused by temperature and moisture gradients only (Dere et al. 2006).

Additionally, good drainage of the underlying layers can help minimize warping because it can help reduce the saturation of the pavement foundation. Slabs built on poorly drained layers are more susceptible to influence from moisture-associated warping and erosion (Hansen and Wei 2008). Curling and warping–induced loss of subgrade support can cause voids beneath the PCC, which can easily result in pumping and structural deterioration (Nantung 2011).

In Situ Weather Conditions

In situ weather conditions, such as solar radiation and wind speed, also have an influence on curling and warping. Solar radiation has a direct influence on pavement temperature distribution. Furthermore, solar radiation may also impact joint load transfer, freezing and thawing cycles, and crack widths (Chung and Shin 2015). Depending on the absorptivity of the concrete, absorbed heat can be partially stored in and inherited by the concrete under the top layer. The amount of heat absorbed is determined by both solar radiation and the short-wave surface absorptivity (SR) of the PCC pavement. The SR usually varies within concrete depending on pavement characteristics such as texture and color. The total heat loss or gain under the solar radiation effect can vary in different seasons. Typically, during the winter there is a net heat loss due to the extremely cold ambient temperature, while during the summer there is a net heat gain because of the strong solar radiation. Yinghong (2011) investigated the effect of SR on the distribution of temperature and thermal stresses in JPCP using a one-dimensional heat transfer model. It was found that SR at the pavement surface is the main factor determining the distribution of temperature and thermal stresses, and higher SR values can result in higher maximum tensile stresses. Furthermore, the impact of heat history is negligible on the surface of the concrete layer but remarkable at the bottom of the concrete layer (Yinghong 2011).

Wind speed greatly impacts heat convection at the PCC pavement surface by affecting heat transfer and temperature distribution (Chung and Shin 2015). Furthermore, it is well known that wind can accelerate water evaporation and thereby lead to severe drying shrinkage during concrete placement. Holt and Leivo (2004) charted the relationship among wind speed, water evaporation, and shrinkage. They showed that strong wind results in greater water evaporation and drying shrinkage. Moreover, Yinghong (2011) investigated the influence of wind speed on temperature and thermal stress distribution and the heat convection coefficient in JPCP. It was found that the impact of wind speed on stress distribution varied seasonally and was dependent on pavement location. For instance, if the pavement is built in a lower latitude region or during hot weather, wind draws more heat from the pavement surface to reduce the temperature difference, and thus less thermal stress is induced (Yinghong 2011).

In addition to solar radiation and wind, other environmental conditions, such as ambient temperature and RH, can affect curling and warping. During pavement construction, high ambient temperatures can result in significant built-in curling. As for the ambient RH, low ambient RH can result in high shrinkage, which will lead to a high potential for warping as well. The best practices for PCC pavement construction to mitigate curling and warping are discussed in the next section.

Seasonal changes can also influence the degree of curling and warping. By using strain

measurements, McCracken et al. (2008) reported the results shown in Figure 7 for both restrained and unrestrained slabs in Pennsylvania, along with following observations:

- Temperature-induced strain measurements were the dominant factor contributing to the development of total strain in the concrete slabs.
- Higher temperature-induced strain measurements were observed in the winter due to the greater slab contraction resulting from ambient temperature drops.
- The strain measurements induced by moisture and other factors were higher in the fall than in other seasons in both the restrained and unrestrained slabs.

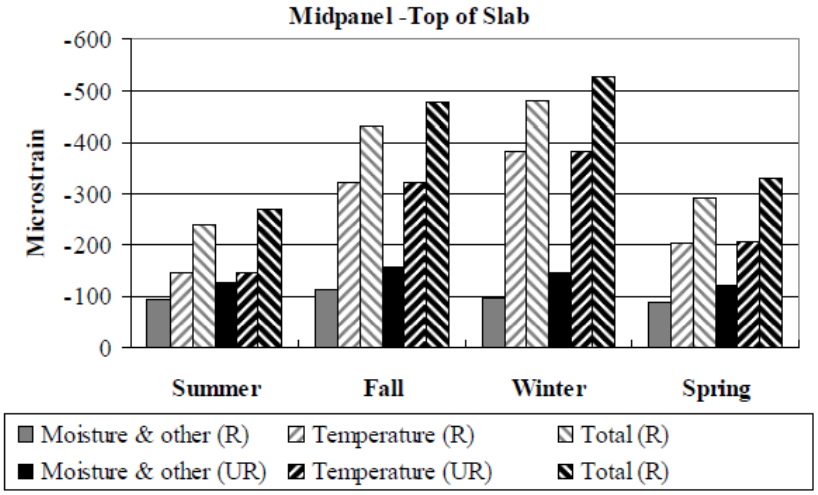

Note: the degree of curling and warping were measured using strain gages installed in the longitudinal direction at mid-panel.

McCracken et al. 2008

Figure 7. Seasonal contributions to the degree of curling and warping in restrained and unrestrained slabs

These results (based on strain measurements) indicate that the overall degree of curling and warping can be higher in winter than other seasons. McCracken et al. (2008) also utilized surface profile (i.e., dipstick) measurements, and the measurement results (based on a dipstick) indicated that the overall degree of curling and warping can be higher in the summer, which was contradictory to the findings from the strain measurements. However, diurnal curling and warping changes in both sets of measurement results were at their lowest in the winter. This is due to the prevailing seasonal temperature patterns and the length of daylight periods (Wells 2005).

Methodologies to Mitigate PCC Curling and Warping

Although PCC curling and warping cannot be completely removed in realistic conditions, enough attention should still be paid during material selection, mix design, pavement design, and construction to minimize the effect as much as possible. This section summarizes some general methods for reducing the impact of PCC curling and warping.

Materials Selection

As discussed previously, concrete thermal properties have an influence on curling. A concrete thermal property such as CTE is related to heat transfer within the concrete. Concrete CTE is mainly determined by the coarse aggregates used in concrete. Concrete produced using coarse aggregates with low CTE values also has a low CTE, which thus reduces the potential curling. Table 2 illustrates that concrete with andesite, basalt, and limestone has the lowest CTE values.

Table 2. CTE of concrete with different aggregate types

Primary Aggregate Class	Average CTE (/°F × 10^{-6})	Primary Aggregate Class	Average CTE (/°F × 10^{-6})
Andesite	4.32	Granite	4.72
Basalt	4.33	Limestone	4.34
Chert	6.01	Quartzite	5.19
Diabase	4.64	Rhyolite	3.84
Dolomite	4.95	Sandstone	5.32
Gabbro	4.44	Schist	4.43
Gneiss	4.87	Siltstone	5.02

Source: Hall and Tayabji 2011

The shrinkage behavior of concrete is directly related to moisture-induced warping. Taylor and Wang (2014) summarized the factors that influence shrinkage. Typically, using aggregates that absorb less water leads to less warping due to less shrinkage. Coarse aggregates with low water absorption values (< 0.5%) are preferred (Babaei and Purvis 1995). Table 3 illustrates the percentage of shrinkage of different aggregate types over one year (Burrows 1998). It can be seen that quartz and limestone have a lower potential for shrinkage than other aggregate types and thus result in less warping. However, quartz has a higher potential for curling due to its relatively higher CTE (see Table 3).

Table 3. Dry shrinkage of different aggregates over one year

Coarse Aggregate	Shrinkage, %
Sandstone	0.097
Basalt	0.068
Granite	0.063
Limestone	0.050
Quartz	0.040

Source: Burrows 1998

Concretes with higher elastic modulus values have less potential for shrinkage (Taylor and Wang 2014). However, if the concrete's modulus of elasticity is high, it may induce more curling deflection according to observations made by Leonards and Harr (1959) and Al-Nasra and Wang (1994) based on computation and FE simulation.

In summary, it is desirable to use coarse aggregates with lower CTE and water absorption values for mitigating PCC curling and warping (Cement Concrete & Aggregates Australia 2002). The coarse aggregate should also be hard, dense, durable, tough, and not moisture sensitive to resist crack propagation and should be free of clay or other fine materials to reduce shrinkage (Rao and Roesler 2005a, Smiley and Hansen 2007, Wilson and Kosmatka 2011). Based on Table 2 and Table 3, limestone is preferred because it has a lower CTE and less potential for shrinkage. Moreover, in order to minimize curling and warping deflection, coarse aggregates with high specific gravity (SG) values can increase concrete self-weight and thus restrain vertical deflection. However, in such cases the curling and warping stresses may increase as well due to the greater restraint.

In addition to coarse aggregates, the other components in concrete mixture, such as fine aggregate, cement, and mixing water, also have effects on the curling and warping of PCC pavement.

Babaei and Purvis (1995) recommended that the fine aggregates used in PCC should have absorption values less than 1.5% to generate less shrinkage. Furthermore, coarser sand is desired to reduce the potential for shrinkage. However, it should be noted that the amount of fine aggregate needs to be controlled within the desired range because an excessive amount of fine aggregates can result in higher water demand to achieve target slump during mixing (Chung 2012). As a consequence, more water has to be used, which can increase the risk of shrinkage.

As for cement, the coarseness and tricalcium aluminate (C_3A) content of cement can impact shrinkage behavior. It is recommended to use cement with high dicalcium silicate (C_2S), low C_3A, and low alkali content, such as Type II cement, in order to reduce autogenous shrinkage and warping in concrete. The other types of cement, such as Type I and Type III cement, may generate higher shrinkage due to their higher C_3A content. Furthermore, coarser cement is preferred because fine-ground cement leads to higher shrinkage and warping later (Rao and Roesler 2005a). Additionally, shrinkage-compensating cement, which causes expansion of concrete during curing to counteract the effect of volume contraction caused by shrinkage, can be used to replace traditional cement in concrete mix design. During the volume expansion due to shrinkage-compensating cement, the surrounding restraints generate compression at the early age to balance out the shrinkage stresses (Rao and Roesler 2005a).

Mix Design

Concrete mix proportions should be designed to minimize the shrinkage and heat released during the cement hydration process in order to minimize curling and warping. A high degree of cement hydration can lead to a high concrete mix temperature, which can easily induce positive temperature gradients during summer construction. Then, negative built-in temperature differences/gradients can be induced at nighttime when the surface temperature becomes cooler but the bottom still remains hot. Therefore, it should be ensured that the concrete mix temperature always stays below the allowable maximum temperature specified during construction (Rao and Roesler 2005a, Smiley and Hansen 2007). Hence, supplementary

cementitious materials (SCMs) such as fly ash and ground granulated blast furnace slag (GGBFS) are recommended for PCC pavement mix design (Nantung 2011).

In order to minimize warping in PCC pavement slabs, large maximum coarse aggregate size and volume are desired. Usually, a larger amount of cement paste in the concrete mixture can cause greater shrinkage. The result of using a larger coarse aggregate size in concrete mix design is that less cement paste remains in the mixture. As a result, less shrinkage and warping is induced (Rao and Roesler 2005a, Smiley and Hansen 2007).

Moreover, a relatively low w/cm ratio is preferred because it can help prevent rapid moisture escape from the PCC pavement surface. A study conducted by Yinghong (2011) indicated that the changes in RH along the PCC slab are not proportional to the changes in the w/cm ratio and that a lower w/cm ratio may result in less moisture loss during the life of the pavement surface and make the pavement less susceptible to the wetting and drying cycles (see Figure 8).

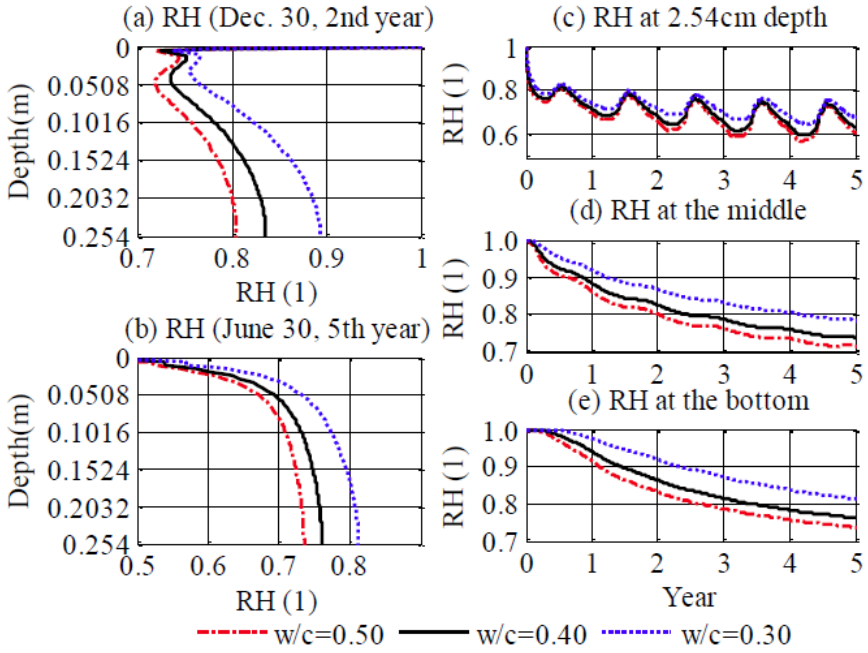

Yinghong 2011

Figure 8. Effect of various w/cm ratios on RH distribution within a concrete slab

Furthermore, variations in the w/cm ratio can greatly impact the moisture at the bottom of the slab but rarely impact the moisture near the pavement surface because surface moisture is mainly dominated by the boundary conditions (Yinghong 2011). In mix design, the controlling w/cm ratio should be neither too high nor too low. As explained above, a high w/cm ratio can facilitate moisture loss, thus aggravating drying shrinkage, while a very low w/cm ratio may increase autogenous shrinkage of the concrete slab. Hence, a moderate w/cm ratio is preferred to induce less drying shrinkage and less autogenous shrinkage and thus reduce the total shrinkage stresses that develop (Yinghong 2011, Rao and Roesler 2005a). Additionally, it is also recommended that

the sum of the volume fraction of the mixing water and cement content should be less than 27% in terms of the total volume of the concrete (Schmitt and Darwin 1999).

Chemical admixtures that can reduce shrinkage can help minimize warping as well. Shrinkage-reducing admixtures can help reduce early-age shrinkage by approximately 30% to 40% (Altoubat 2010). It was noted above that less water in concrete mixture can lead to less warping. However, chemical admixtures such as water reducers or superplasticizers, which can reduce the water demand but still maintain the desired workability, may not obviously reduce the induced shrinkage. Sometimes the total shrinkage may even be increased if too much superplasticizer is used because of the increased autogenous shrinkage resulting from the lower w/cm ratio (Rao and Roesler 2005a). Babaei and Purvis (1995) recommended that the mix water not exceed 12 lb/ft^3 to avoid excessive autogenous shrinkage. Furthermore, chemical admixtures containing calcium chloride should not be used because they can increase drying shrinkage (Cement Concrete & Aggregates Australia 2002).

Pavement Design

Pavement design factors such as concrete slab geometry, type of underlying layer, and dowel bars should account for their effects on curling and warping.

Shorter slab lengths and greater slab thicknesses can be adopted to minimize curling and warping stresses, as explained above. Typically, most pavement design procedures recommend that slab length be proportional to slab thickness. If a shorter slab length is adopted, sufficient attention should be paid to the support from the underlying layers because shorter slabs seem to be more susceptible to mid-slab or mid-panel cracking if loss of support occurs (Smiley and Hansen 2007).

Dowel bars play an important role in pavement design and restrict pavement deflection, especially at the joints. Typically, PCC pavements with dowel bars exhibit less curling and warping deflection than pavements without dowel bars (Nassiri 2011, Wells 2005). However, restraints due to the presence of dowel bars may induce higher curling and warping stresses as well. Additionally, load transfer in concrete pavements without dowel bars relies on aggregate interlock. Using dowel bars in PCC pavements can improve load transfer efficiency and restrain curling deflection in JPCP (Lederle et al. 2011). Davids (2001) carried out 3D FE analysis to investigate the load transfer efficiency in curled PCC pavements with dowels. Furthermore, dowel bars can also make slab length less of a factor in curling and warping behavior (Nassiri 2011, Vandenbossche 2003).

Additionally, proper selection of the underlying layers of a PCC pavement is also important for minimizing curling and warping because the underlying layers have direct influence on stress development, degree of support, and EBITD (Rao and Roesler 2005a). Usually, a stiffer base leaves a larger portion of the concrete slab unsupported during curling and warping because a stiff base resists the slab's downward movements (Smiley and Hansen 2007). A soft base can provide a "bedding" effect to counteract the slab's downward movements but can cause higher deflection when taking traffic loads into account. Therefore, the tradeoff between curling and

warping effects and traffic loading effects on PCC pavement performance should be considered when selecting the underlying layers.

Drainage is the main function of the base or subbase course in a PCC pavement system. Poor subsurface drainage can be a major cause of permanent joint uplift in JPCP. Therefore, the underlying layers should be designed to have good drainage to avoid moisture accumulation at the bottom of PCC slabs and thus help minimize warping.

Construction Practice

The ambient temperature has a major influence on built-in curling during concrete setting. Therefore, special attention needs to be paid in selecting the time of paving to reduce the thermal impacts on built-in curling. Considerations include paving season, time, and weather conditions during construction. Although completely eliminating built-in curling is difficult, the above considerations and related strategies should be taken into account to minimize it as much as possible.

The local climate pattern should be considered in selecting the proper paving season because this decision can elongate the longevity of PCC pavements. Generally, the construction of PCC pavements mostly occurs during the summer season and in the daytime. The ambient temperature is high during the summer or in hot and dry weather, which can easily lead to upward built-in curling in PCC slabs. Hansen et al. (2006) found that pavements built during late fall in Michigan exhibited less built-in curling.

Daytime construction in the summer should be avoided because built-in curling is prevalent when concrete placement occurs on summer mornings (Lederle et al. 2011, Rao et al. 2001, Smiley and Hansen 2007). If the PCC pavement is built in the morning, then the concrete will set and harden in the afternoon. In this case, the maximum effective negative built-in temperature gradient is likely to develop. Therefore, nighttime paving is recommended (Kim et al. 2008, Lederle et al. 2011, Merritt et al. 2015). Rao et al. (2001) compared pavements constructed during daytime and nighttime periods and found that nighttime construction can prevent significant built-in curling (Rao et al. 2001).

Construction during hot and dry weather should be avoided because of the high potential for effective negative temperature gradients. Actually, many states have provisions regarding the maximum ambient temperature allowed for hot weather construction. States usually do not allow the ambient temperature to exceed 90 to 95°F during concrete placement (Merritt et al. 2015). The temperature difference between the top and bottom of the PCC layer should be controlled so as not to exceed 10°F during concrete placement. Moreover, strong solar radiation and wind should be avoided during pavement construction because these can lead to an overheated base course before paving and aggravate the temperature difference (Smiley and Hansen 2007).

Additionally, PCC pavement construction should be avoided on days that may have sudden or dramatic changes. For example, sudden changes of weather from warm to cold in the early

winter can lead to high maximum curling stress (Nantung 2011). Maintaining a relatively uniform temperature through the concrete thickness is desirable to minimize curling stress (Hansen and Wei 2008).

Maintenance of proper conditions for the underlying layers during PCC pavement construction is important for minimizing curling as well. The maximum and minimum temperatures of the base should be kept close to temperature of the concrete during paving in order to reduce curling (Merritt et al. 2015).

In order to reduce warping, strong solar radiation and wind need to be avoided as well during pavement construction. Solar radiation and strong wind can accelerate moisture loss and shrinkage at the surface of the PCC slab after concrete placement. Furthermore, the ambient RH also has an impact after concrete setting because a low ambient RH can facilitate moisture loss from the pavement surface, resulting in greater drying shrinkage and warping (Rao and Roesler 2005a). For construction in arid climates, a thicker slab and/or shorter joint spacing should be adopted to minimize drying shrinkage (Yinghong 2011).

Cloudy days with low and weak winds and a relatively high ambient RH are desired for paving (Yinghong 2011). Rains are best after the end of concrete curing. The subsequent wetting cycles after the concrete reaches a stabilized stage can help reduce the stresses from shrinkage and reduce moisture gradients.

Curing has an effect on warping, but the effect may not be significant. Actually, curing cannot prevent warping or affect the degree of warping, but the duration of curing indeed has as influence on warping (Suprenant 2002). An extended curing period can delay the occurrence of warping, but the reduction of warping is almost negligible, and sometimes delaying curing can even increase the drying shrinkage that occurs later after curing (Perenchio 1997). Nevertheless, the delay of warping can reduce the stress developed at the early stage, which helps the concrete avoid early-age cracks before it obtains sufficient strength (Rao and Roesler 2005a).

In addition to the duration of curing, the type of curing can also have an effect on pavement performance. Curing methods that use membrane-forming curing compounds or other types of sealants to lock in moisture may lead to early cracks. This is because the rate of drying shrinkage can dramatically increase when the curing compounds wear off or gradually degrade due to environmental effects and time (Lederle et al. 2011). Therefore, other types of curing compounds, such as poly(alpha-methylstyrene), can be adopted because they can reduce shrinkage more effectively than other wax- or resin-based conventional curing compounds (Zeller 2014). To sum up, adequate and proper curing methods can be used to reduce or delay warping. Excessive curing should be avoided because this can cause negative effects. Furthermore, if a wetting method is adopted, it is better to perform the wetting hourly (Altoubat and Lange 2001, Lederle et al. 2011).

PCC pavement should be built on a dry base or subbase course to avoid rapid moisture accumulation at the interface between the top PCC layer and the underlying base course (Rao and Roesler 2005a). Furthermore, if the underlying layer has a wet surface, a membrane can be

used to avoid excessive moisture at bottom of the slab. If an impermeable membrane is used, three inches of sand can be placed on top of the membrane to reduce the moisture differential due to the accumulation of moisture at the bottom of the concrete during paving (Lafarge North America 2016).

Additionally, prior to concrete paving the contractor should ensure the shortest travel time from the central mix plant to the job site and the fewest agitating revolutions after complete mixing is achieved (Rao and Roesler 2005a). During pavement construction, the curb, gutter, and/or shoulder should be constructed at the same time as the lanes are paved in order to avoid exposing more of the surface along lane/shoulder joint to drying shrinkage (Wells 2005).

Summary

Curling and warping are unique bending behaviors of PCC slabs associated with temperature and moisture gradients. Tensile stresses are generated due to slab restraints and can be magnified several times when combined with traffic loading. These stresses may initiate top-down or bottom-up cracking. Many studies have investigated the effects of curling and warping on the early-age behavior of concrete. Based on the results of the literature review, it was found that many factors can affect PCC curling and warping. These include temperature gradients, moisture gradients, ambient environmental conditions, mix design, the properties of the constituent materials, pavement structural design, and construction practices. All of these factors should be considered for mitigating curling and warping in order to achieve better performing PCC pavements in Iowa in a cost-effective manner. Based on the comprehensive literature review, Table 4 summarizes the strategies for minimizing PCC curling and warping.

Note

Parts of this literature review were previously published by the Institute for Transportation at Iowa State University in Ceylan et al. (2016).

Table 4. Summary of mitigation strategies for PCC curling and warping

Categories	Factors	Specific factors	Strategies for minimizing curling and warping
Material Properties	Coarse aggregate (CA)	Type	CA with lower water demand (water absorption < 0.5%) can reduce warping, and CA with lower CTE can reduce curling; CA with higher specific gravity can result in less curling and warping.
		Gradation	Increase of coarse aggregate content can result in decreased shrinkage, which can result in decreased warping.
		Fines	Decreased fine materials (i.e., clay) result in decreased shrinkage, thus decreased warping.
	Fine aggregate (FA)	Type	The FA with lower water demand (water absorption < 1.5%) can result in less warping.
		Gradation	Coarser sand can result in less warping.
	Cement	Chemistry	Cement with lower C_3A and alkali can reduce autogenous shrinkage, thus decreasing warping.
		Fineness	Coarser cement is preferred because fine-ground cement leads to higher warping.
	Supplementary cementitious material	Fly ash	Fly ash potentially decreases warping.
		Slag	Still controversial, depends on other factors such as paste content.
	Chemical admixtures	Superplasticizer	May not obviously reduce the warping induced; sometimes it even increases the total warping due to increased autogenous shrinkage if excessive superplasticizer is used.
Mix Design	w/cm ratio		Moderate w/cm ratio is preferred because higher w/cm ratio can lead to higher drying shrinkage while lower w/cm ratio can lead to higher autogenous shrinkage, which results in greater warping.
	Paste content		Lower paste content for a given w/cm ratio can reduce warping.
	Aggregate content		Higher CA content is desired to reduce warping, and moderate FA content is desired because excessive FA will increase water demand to maintain slump, thus increasing warping.
Pavement Design	Slab geometry	Slab thickness	Thicker slab can result in lower curling and warping.
		Slab length	Shorter slab length can result in lower curling and warping.
	Dowel bar		Dowel bar can restrain vertical curling deflection at joints; however, it can also increase curling and warping stresses by restraining vertical deflection.
	Underlying layer	Type	Soft underlying base course leads to less curling while base with good drainage results in less warping; therefore, open-graded base course is preferred; however, when traffic loading is taken into account, more tensile stresses may be induced in soft base course.
Construction Practice	Environment conditions	Temperature	High ambient temperatures during paving can result in greater curling and warping.
		RH	High ambient RH during paving can reduce moisture loss from surface, which can reduce warping.
		Solar radiation	Strong solar radiation during paving can increase curling, so cloudy days are preferred.
		Wind	Lower wind speed during paving can induce less shrinkage, thus causing less warping.
	Paving time		Paving in the later fall season and paving at night can minimize curling.
	Curing	Duration	Extended curing period may increase warping later; therefore, excessive curing should be avoided; furthermore, curing in an hourly manner is preferred to reduce warping if wet curing is used.

FIELD INVESTIGATION SUMMARY

To obtain the degree of curling and warping in in-service PCC pavements, several field surveys were conducted at six identified sites in Iowa using a light detection and ranging (LiDAR) device. The surveys were mainly carried out during the late fall of 2015 due to the availability of equipment for field surveys, Iowa Department of Transportation (DOT) scheduling conflicts, and the project's duration. These sites had different concrete mixtures and construction designs. Table 5 summarizes the basic information of the sites visited. A detailed summary of field investigation activities follows.

Table 5. Basic information of the sites visited for field investigation

No.	Site	Route	Direction	MP[1]	CY[2]	AADTT[3]	Project
1	Ames, Story County	US 30	Eastbound	152.20	2013	952	NHSX-030-5(239) --3H-85
2	Nevada, Story County	US 30	Westbound	159.85	1995	764	NHS-30-5(71) --19-85
3	Cedar Rapids, Linn County	US 151	Southbound	32.75	1999	1930	NHS-151-3(87) --19-57
4	Cedar Rapids, Linn County	US 151	Southbound	33.15	1999	1930	NHS-151-3(87) --19-57
5	Cedar Rapids, Linn County	US 30	Westbound	261.2	1999	1120	NHSX-30-7(94) --3H-57
6	Toledo, Tama County	US 30	Eastbound	194.6	2005	744	NHSX-030-5(146) --3H-64

MP[1] is the mile post number and CY[2] is the constructed year. AADTT[3] is average annual daily truck traffic in 2013.

Light Detection and Ranging (LiDAR) System: Theory and Measurement Methodology

LiDAR is an active optical remote sensing technology that measures the properties of pulsed laser beams reflected from an object to acquire relevant information such as x, y, and z coordinates; range; and direction (FDOT 2012). LiDAR is currently the most significant geospatial data acquisition technology. Its extremely intensive point cloud data set enables 3D visualization of a scanned area or object, so it is widely used as an investigating tool for topographic inspection and geomaterial mapping (e.g., flood insurance rate mapping, forest and tree mapping, and coastal change mapping). In addition to these conventional applications, the current use of LiDAR has also been extended to transportation infrastructure design and management, such as investigation of airport site obstructions, site characterization, traffic flow estimation, and highway design.

Compared to conventional topographic investigating methods, LiDAR offers the competitive advantages of scanning large areas in a very short time, high accuracy (up to 0.001 in.), and incredibly dense collections of data points. It can emit hundreds of thousands of laser beams in one second and determine associated x, y, z coordinates from their reflections. The point cloud made up of the coordinates and associated intensity values from each laser can then be obtained.

In this way, a 3D map consisting of hundreds of thousands of data points can be created. LiDAR is sometimes described as a 3D laser scanner. Because of its capability of producing accurate and directly georeferenced spatial information describing the surface characteristics of a scanned object, LiDAR-based platforms have vast potential to be used in characterizing both longitudinal and transverse pavement profiles and pavement surface conditions.

The LiDAR device used for pavement profile measurement is also called terrestrial laser scanner (TLS), which is a type of stationary LiDAR system that includes a rotary laser device mounted on a support tripod. TLS can be classified based on distance measurement methods into time-of-flight–based, phase-shift–based, and waveform processing–based systems, although their fundamental principles are similar in that they utilize the speed of laser beams and the time of travel to determine the distances from an object to the laser scanner (Caltrans 2011). A time-of-flight–based LiDAR is the most common type of scanner available on the market; a schematic diagram of such a system is given in Figure 9.

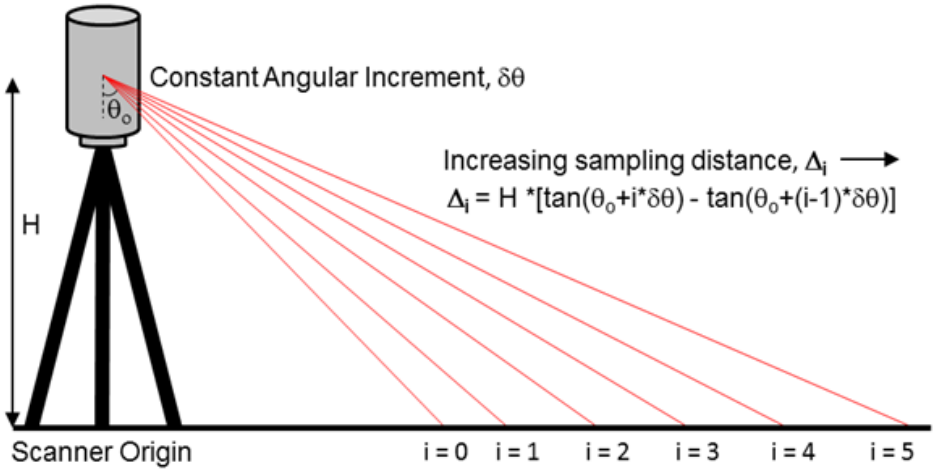

As modified by Olson and Chin 2012

Figure 9. Theory of using time-of-flight–based LiDAR system

From this figure, it can be seen that laser beams are pulsed from the scanner and deflected at different angles through a rotating mirror. Because the speed of the laser beam is already known, distance can be determined simply by measuring the travel time of the pulsed beams. A time-of-flight–based LiDAR system can commonly provide 50,000 points per second (pts) with a working range from 125 to 1,000 m. A phase-shift–based LiDAR system emits a laser beam with multiple phases with sinusoidally modulated optical power. A phase shift is induced due to reflection from the object, and the change in the phase shifts of the returned beam can be determined to calculate the distance according to the unique properties of each individual phase. A phase-shift–based LiDAR has a shorter working range, from 25 to 75 m, but a higher data collection rate. Waveform processing–based LiDAR, sometimes called "echo digitization," combines time-of-flight and internal real-time waveform processing technology to capture the reflected beams. Waveform processing–based LiDAR usually has a working range similar to that of time-of-flight–based LiDAR but has a much higher scan rate, up to 300,000 pts (Caltrans 2011, FDOT 2012).

TLS is the LiDAR platform most widely used by researchers for pavement inspection applications like International Roughness Index (IRI), surface texture, cross slope, and crack detection. Compared to other platforms such as airborne laser scanners (ALS) and mobile laser scanners (MLS), TLS is a type of stationary scanning method that usually provides a smaller scanning range but a higher accuracy (0.001 in.) and denser scan; it therefore has more potential to describe the "true profile" of a pavement surface. In this project, the Leica ScanStation C10 TLS device produced by Leica Geosystems was used. It can provide high-accuracy and long-range scanning and has the advantage of fast, full-dome interior scanning. Figure 10 illustrates the Leica ScanStation C10 used in this project. Table 6 summarizes the basic properties of this device.

Figure 10. Leica ScanStation C10 LiDAR device

Table 6. Leica ScanStation C10 data sheet

Categories	Specific Aspect	Description
Accuracy	Position Distance Angle (horizontal/vertical)	± 6 mm at 50 m ± 4 mm at 50 m 60 μrad / 60 μrad (12" / 12")
Noise	N/R	2 mm
Target acquisition	N/R	2 mm std. deviation
Laser class	N/R	3R (IEC 60825-1)
Range	N/R	300 m @ 90%; 134 m @ 18% albedo (minimum range 0.1 m)
Scan rate	N/R	50,000 points/second
Scan resolution	Spot size	From 0 – 50 m: 4.5 mm (FWHH-based); 7 mm (Gaussian-based)
	Point spacing	Fully selectable horizontal and vertical; < 1 mm minimum spacing, through full range; single point dwell capacity
Field of view	Horizontal/vertical	360°/270°

N/R: Not required

Site 1 – US 30 near Ames, Story County, STA 1422 (MP 152.20)

Pavement Design and Construction

During the summer of 2013, new JPCP construction projects were carried out on US 30 under the supervision of the Iowa DOT. The project site was located near the southeast area of Ames, as shown in Figure 11.

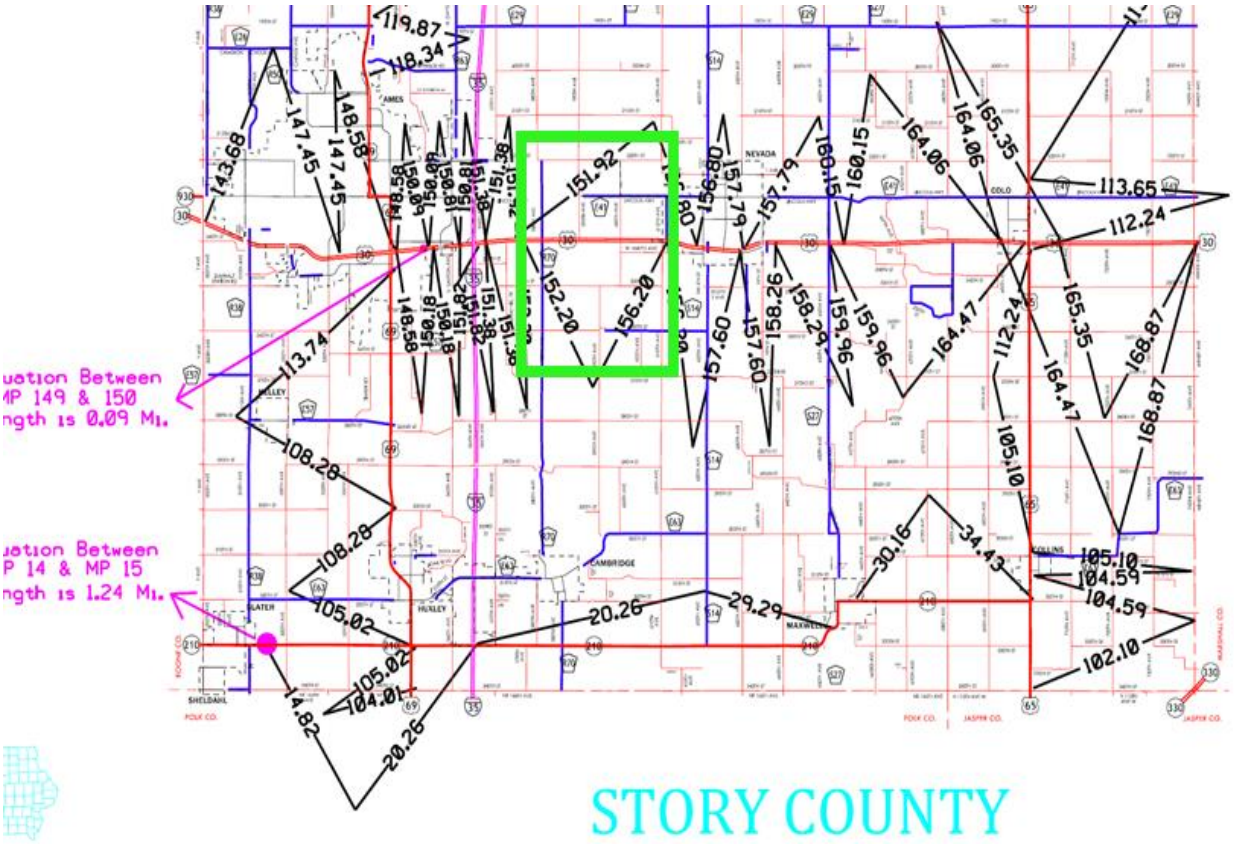

Iowa DOT 2014 Milepost book

Figure 11. Site 1 on US 30 near Ames, Story County, eastbound

The newly constructed pavement section was approximately 10 in. thick and constructed above a granular subbase with a thickness ranging from 6 to 10.3 in. The PCC pavement was crowned with a 2.0% transverse slope and had designed widths of 12 ft and 14 ft for the passing lane and travel lane, respectively. The transverse joint spacing was set at 20 ft, reflecting general practice in Iowa. The joints were sealed by asphalt sealant. Dowel bars with baskets were placed on the subbase before concrete paving.

Concrete paving started in the early morning of May 24, 2013, with a maximum ambient temperature of 85°F and a minimum ambient temperature of 72°F during the day. A slipform paver moved from west to east to pour fresh concrete on the subbase. A vibrator followed the paver to consolidate the fresh concrete using vibration tubes. Surface smoothing was performed manually. A slipform paver dragging a piece of burlap was used to create texture for the pavement surface, and a chemical curing compound was sprayed on the paving surface. A heavy rain occurred just a few days after concrete paving but before shoulder paving, and a heavy rain occurred one day after construction. Shoulder backfilling was conducted 14 days after concrete paving; a 6 in. thick and approximately 4.5 ft wide hot-mix asphalt (HMA) shoulder was then placed on June 10, just three days after shoulder backfilling. One day later, a granular shoulder was added to the pavement. The constructed pavement was opened to traffic on June 14, 2013. Figure 12 presents some snapshots during the pavement construction at this site.

Figure 12. Site 1 pavement construction: PCC placement (left) and shoulder paving (right)

Pavement Materials

Table 7 summarizes the materials used in the concrete mixture.

Table 7. Mix design of STA1422 on US 30 near Ames, Story County

Component	Description	Batch Weight
Portland cement	Lehigh Type IL (SG =3.14)	448 lbs/yd^3
GGBFS		
Fly ash	Council Bluffs FA004C Class C (SG =2.62)	112 lbs/yd^3
Coarse aggregates	Ames Mine Gradation No.5 (SG =2.68, Absorption= 1.1%)	1,403 lbs/yd^3
Intermediate aggregates	Halletts PEA Gravel (SG =2.66)	477 lbs/yd^3
Fine aggregates	Halletts Gradation No.1 (SG =2.65)	1,307 lbs/yd^3
Water		225 lbs/yd^3
Admixture 1	Brett AEA-92	12.07 oz/yd^3
Admixture 2	Brett WR-91	3.0 fl. oz/cwt
Water/cementitious ratio		0.40
Air content		7.2%

fl. oz/cwt = fluid ounces per hundred pounds of cement

It can be seen that intermediate aggregates were used in addition to coarse and fine aggregates. Specific gravity (SG) is also listed. Class C fly ash was added to replace 20% cement by weight in the final mixing. Furthermore, water reducer was used to help maintain workability, with an average w/cm ratio of 0.40. Air entraining agent was added to the concrete mixture as well, and the final air content was 7.2%.

Field Investigation Description

Field investigations at Site 1 on US 30 in Story County near Ames were conducted in the early morning at 8:00 a.m. and in the afternoon at 3:30 p.m. on October 28, 2015 to measure variations in slab deflection throughout the day. At this site, the Leica ScanStation C10 was used to scan the selected PCC slabs. No pavement cracks were observed at this site. Figure 13 presents some pictures of the activities performed during this field investigation.

Figure 13. Field investigation on US 30 near Ames, Story County, STA 1422 (MP 152.20)

Activities at the site included the following:

- Record location information such as station number, milepost number, and GPS coordinates
- Measure slab geometry
- Record joint type and shoulder type
- Measure slab surface temperature by infrared temperature gun
- Check for the presence of cracks
- Use the LiDAR device to scan the pavement surface

Data Analysis and Key Findings

The output from the TSL Leica ScanStation C10 is a point cloud data set composed of x, y, and z coordinates. Three scans were conducted at different locations at this site to obtain a dense data set for all the slabs at the site and sufficient overlap between the point clouds acquired from the different locations. After scanning, scans were processed in the Leica Cyclone SCAN software for registration and segmentation. Registration can overlap the three scans to construct an overall set of 3D point cloud data for the site. Segmentation removes the noise points from the data, such as the presence of sun, passing vehicles, and people. Then the processed point cloud data are exported as a PTS file for further data analysis using software such as CloudCompare and MATLAB. The detailed analysis procedure is as follows:

1. Use CloudCompare software to "dig" the slab out from the point cloud, and then find the coordinates at every slab corner (see Figure 14).

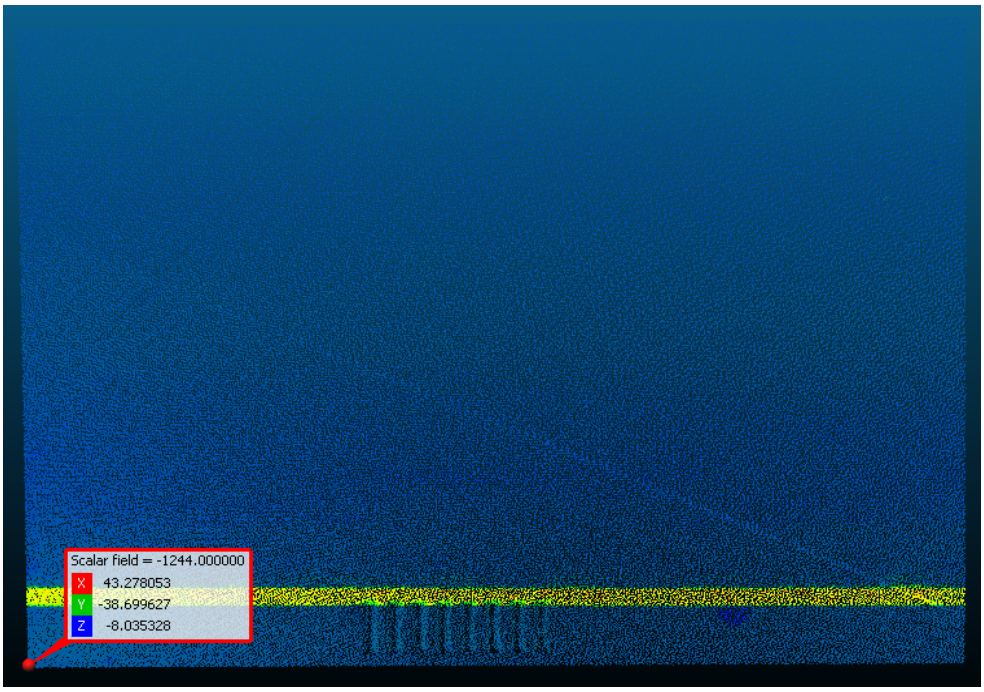

Figure 14. 3D point cloud of a single slab

2. Process the point cloud data of the slab in MATLAB.

3. Fit the scan of the slab surface using quadratic equation (2) (see Figure 15) as follows:

$$z = a * x^2 + b * y^2 + c * x * y + d * x + e * y + f \quad (2)$$

Where a, b, c, d, e, and f are coefficients obtained from MATLAB.

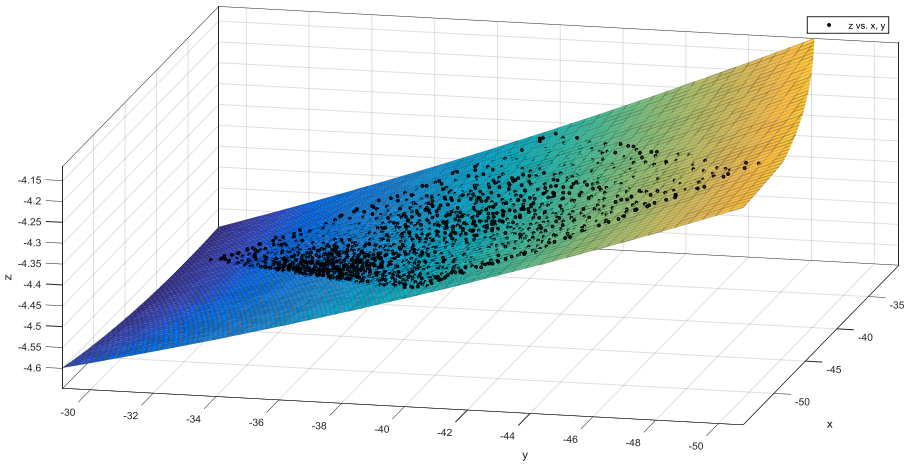

Figure 15. Fitting quadratic equation to the 3D point cloud

4. Obtain the linear equation for the selected directions (i.e., longitudinal, transverse, and diagonal directions) in the x-y plane only (see Figure 16).

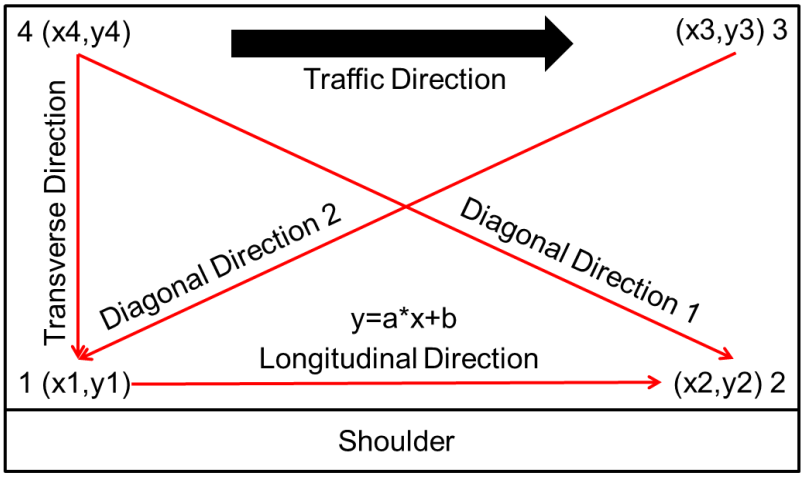

Figure 16. Schematic diagram of directions for a single slab

5. Use the x coordinate to calculate the corresponding y and z coordinates according to the linear equation (for y coordinates) and the quadratic equation (for z coordinates).

6. Calculate relative deflection by subtracting the elevation of the reference line between two corners along the selected directions from the calculated z coordinates (see Figure 17).

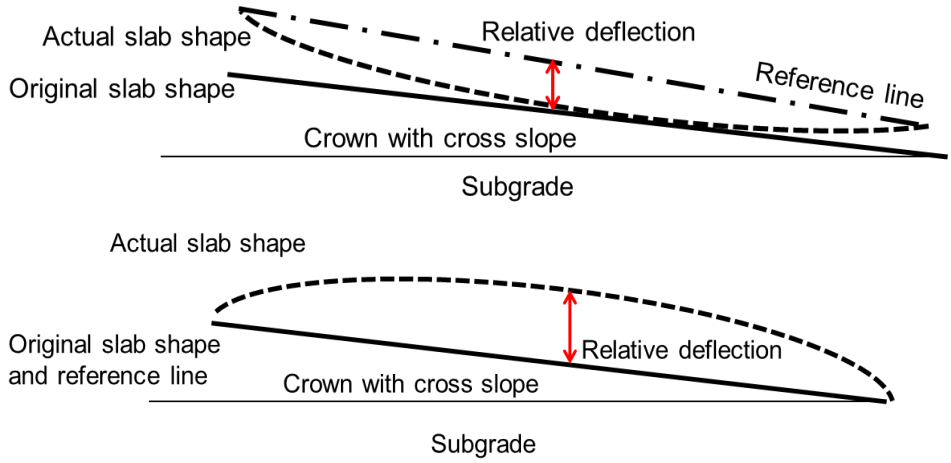

Figure 17. Calculation of relative deflection: upward curling and warping (top) and downward curling and warping (bottom)

Analysis of data acquired from all six sites investigated in the field followed the exact procedure described above. A calculated positive relative deflection represents downward curling and warping while a negative relative deflection represents upward curling and warping. In this site near Ames, Story County, four slabs were selected to calculate relative deflection in the specific directions illustrated in Figure 16. Scans from both the morning and afternoon of October 28, 2015 were analyzed to compare daily variations in curling and warping. Figure 18 through Figure 21 illustrate the relative deflection calculated in the specific directions.

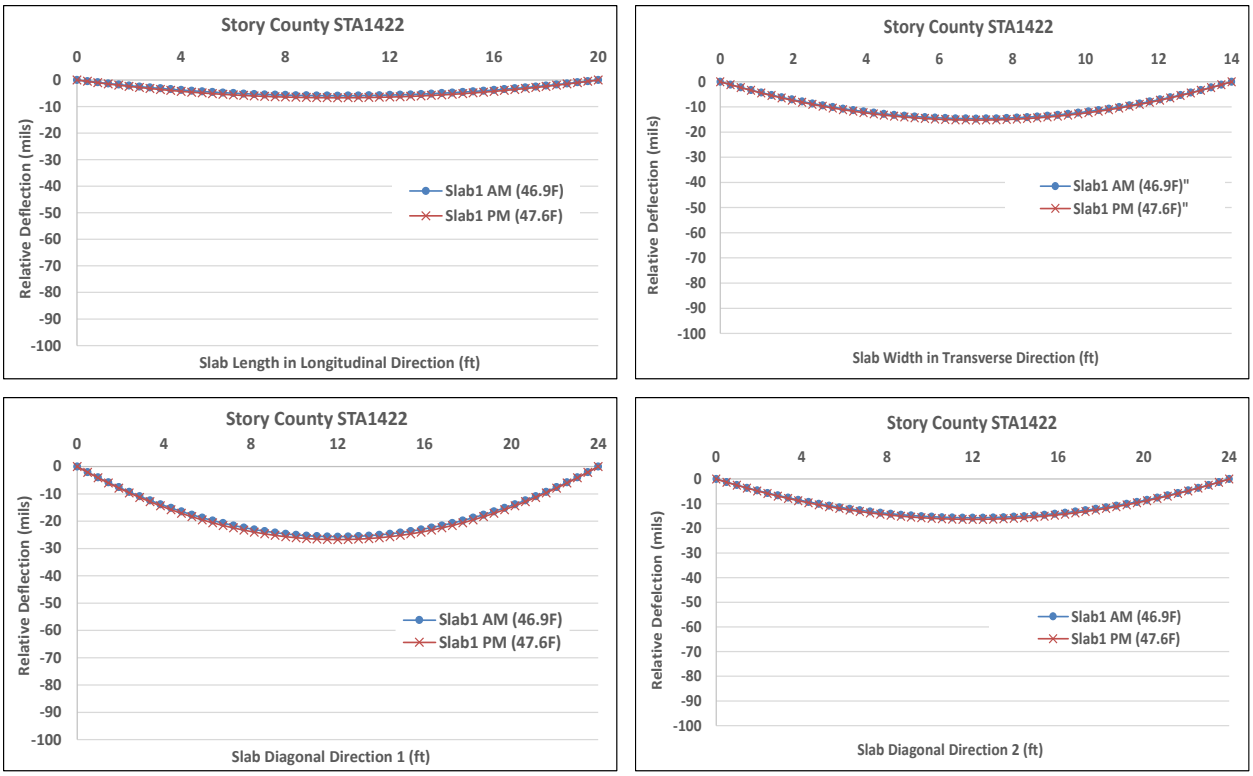

Figure 18. Morning and afternoon relative deflection of Slab 1 at Site 1: longitudinal (top left), transverse (top right), diagonal 1 (bottom left), and diagonal 2 (bottom right)

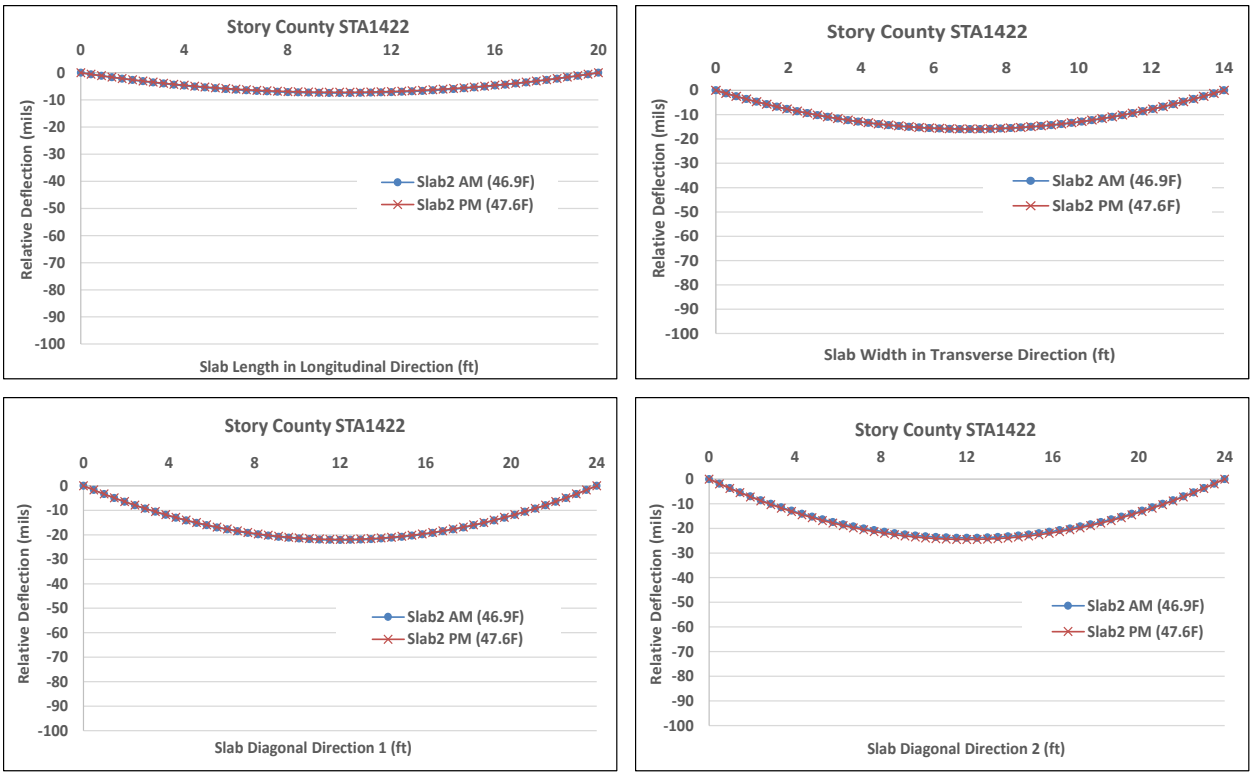

Figure 19. Morning and afternoon relative deflection of Slab 2 at Site 1: longitudinal (top left), transverse (top right), diagonal 1 (bottom left), and diagonal 2 (bottom right)

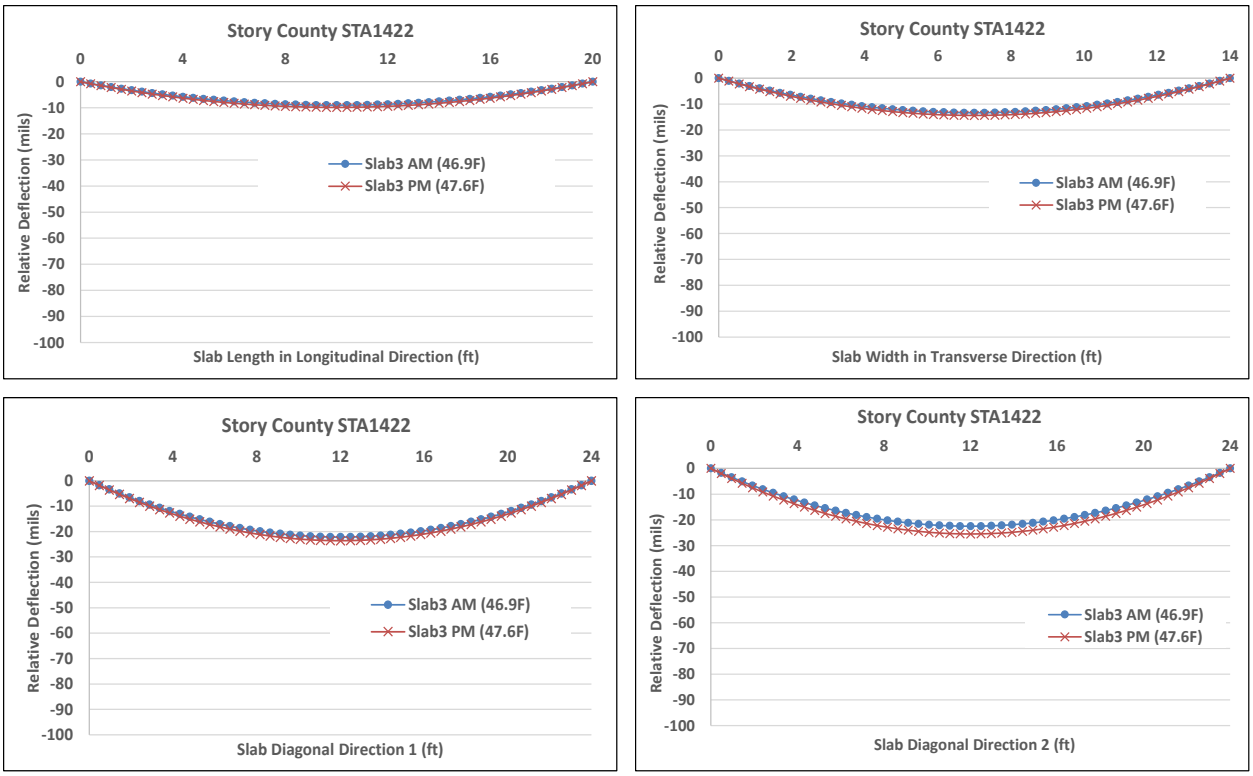

Figure 20. Morning and afternoon relative deflection of Slab 3 at Site 1: longitudinal (top left), transverse (top right), diagonal 1 (bottom left), and diagonal 2 (bottom right)

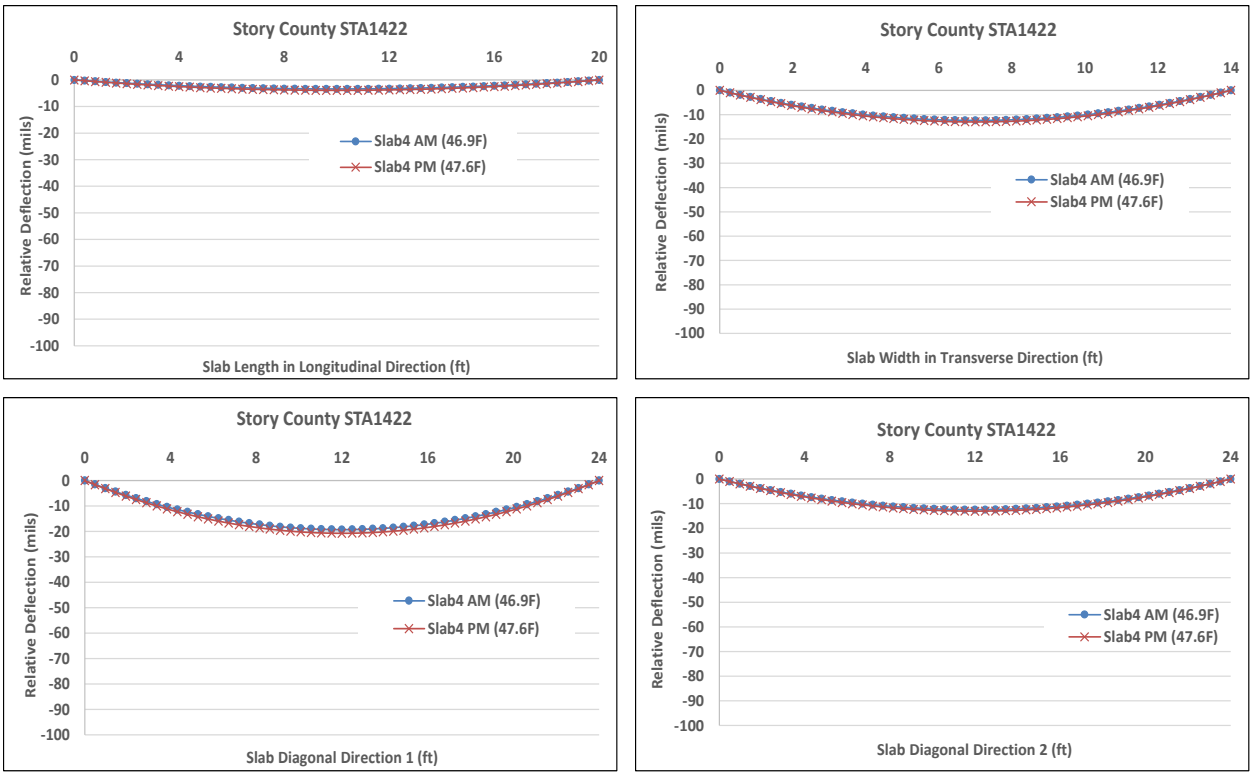

Figure 21. Morning and afternoon relative deflection of Slab 4 at Site 1: longitudinal (top left), transverse (top right), diagonal 1 (bottom left), and diagonal 2 (bottom right)

In Figure 18 through Figure 21 it can be seen that all the slabs showed upward curling and warping during field investigation, indicated by a negative value of the calculated relative deflection. The key findings for this site are as follows:

- Along the longitudinal direction, the relative deflection is in the range of -9.8 to -3.4 mils.
- Along the transverse direction, the relative deflection is in the range of -15.9 to -12.4 mils.
- Along the diagonal directions, the relative deflection is in the range of -26.7 to -12.4 mils.
- The diagonal directions have the highest upward curling and warping compared to the longitudinal and transverse directions.
- The difference in relative deflection between the adjacent slabs is within 6 mils.
- Surface temperature was measured during the investigation. The average temperature calculated for these slabs was 46.9°F in the morning and 47.6°F in the afternoon.
- The relative deflection in the afternoon is about 0.2 to 1.5 mils, which is higher than the relative deflection in the morning. This difference may be due to the small amount of rain that occurred in the morning, which made the surface wetter and thus reduced the degree of upward curvature.

Site 2 – US 30 near Nevada, Story County, STA2207 (MP 159.85)

Pavement Design and Construction

At this site, a 10 in. thick PCC layer was paved over a 10 in. granular subbase layer. The PCC pavement was crowned with a 2.0% transverse slope and had designed widths of 12 ft and 14 ft for the passing lane and travel lane, respectively. Skewed joints were adopted for this site. The transverse joint spacing was set at 20 ft. In addition to the lanes, an approximately 9.5 ft wide granular shoulder was added beside the PCC pavement.

The PCC pavement at this site was built in June 1995. Figure 22 illustrates the location of this site.

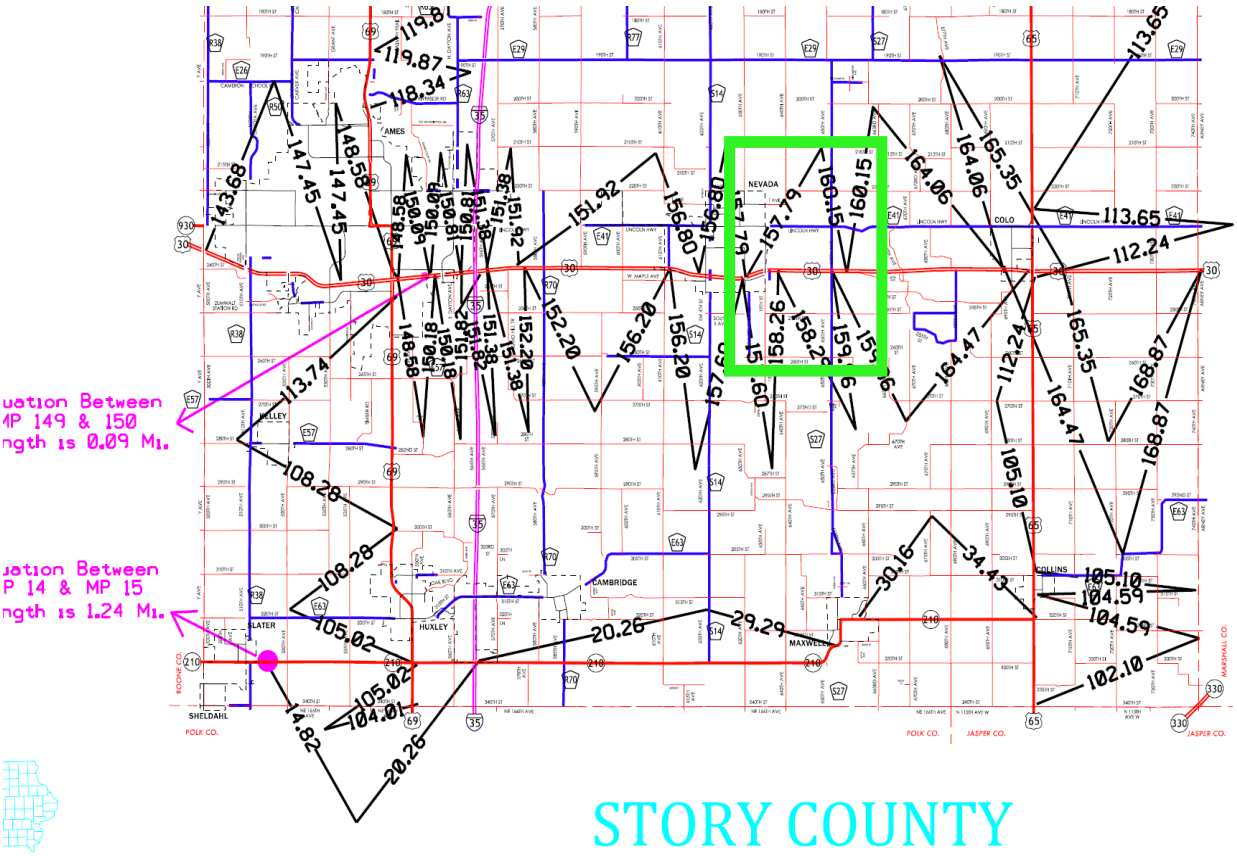

2014 Iowa DOT Milepost book

Figure 22. Site 2 on US 30 near Nevada, Story County, westbound

Prior to pavement construction at this site, the moist subgrade was covered. The construction started in the early morning around 7:00 a.m., and transit mixing was used for concrete mixing. On the day of construction, the weather was sunny, with a maximum ambient temperature of 78°F during the daytime. At night, the ambient temperature decreased to 48°F. After concrete

placement using a slipform paver, white-pigmented curing compound was used for surface curing, and broom grooving was used to create surface texture.

Pavement Materials

Table 8 summarizes the materials used in the concrete mixture for the pavement at this site.

Table 8. Mix design of STA2207 on US 30 near Nevada, Story County

Component	Description	Batch Weight
Portland cement	Ash Grove Type I (SG =3.14)	457 lbs/yd^3
GGBFS		
Fly ash	Kenosha Type C (SG =2.67)	114 lbs/yd^3
Coarse aggregate	Martin Marietta, Ames Mine Gradation No.5 (SG =2.59, Absorption= 2.6%)	1,653 lbs/yd^3
Fine aggregate	Halletts (SG =2.68)	1,446 lbs/yd^3
Water		250 lbs/yd^3
Admixture 1	Daravair	Not available
Admixture 2	Plastocrete-161	Not available
Water/cementitious ratio		0.44
Air content		7.8%

It can be seen that 20% Class C fly ash was added to improve concrete properties such as workability and durability. Furthermore, water reducer was used, which produced an average w/cm ratio of 0.44. The maximum w/cm ratio was 0.49 among the different mixes. Furthermore, air-entraining agent was added to the concrete mixture as well, and the average air content was 7.8%.

Field Investigation Description

Field investigations at Site 2 on US 30 in Story County near Nevada were conducted in the morning at 9:00 a.m. and in the afternoon at 2:30 p.m. on October 28, 2015 to measure variations in slab deflection throughout the day. No pavement cracks were observed at this site. Field investigation activities conducted at this site were the same as those conducted for Site 1. Figure 23 shows some of the activities performed during the field investigation.

Figure 23. Field investigation on US 30 near Nevada, Story County, STA2207 (MP 159.85)

Data Analysis and Key Findings

Figure 24 through Figure 27 illustrate the calculated relative deflections at STA2207, US 30 near Nevada, Story County. Four slabs were selected to compare the measurements from both the morning and afternoon.

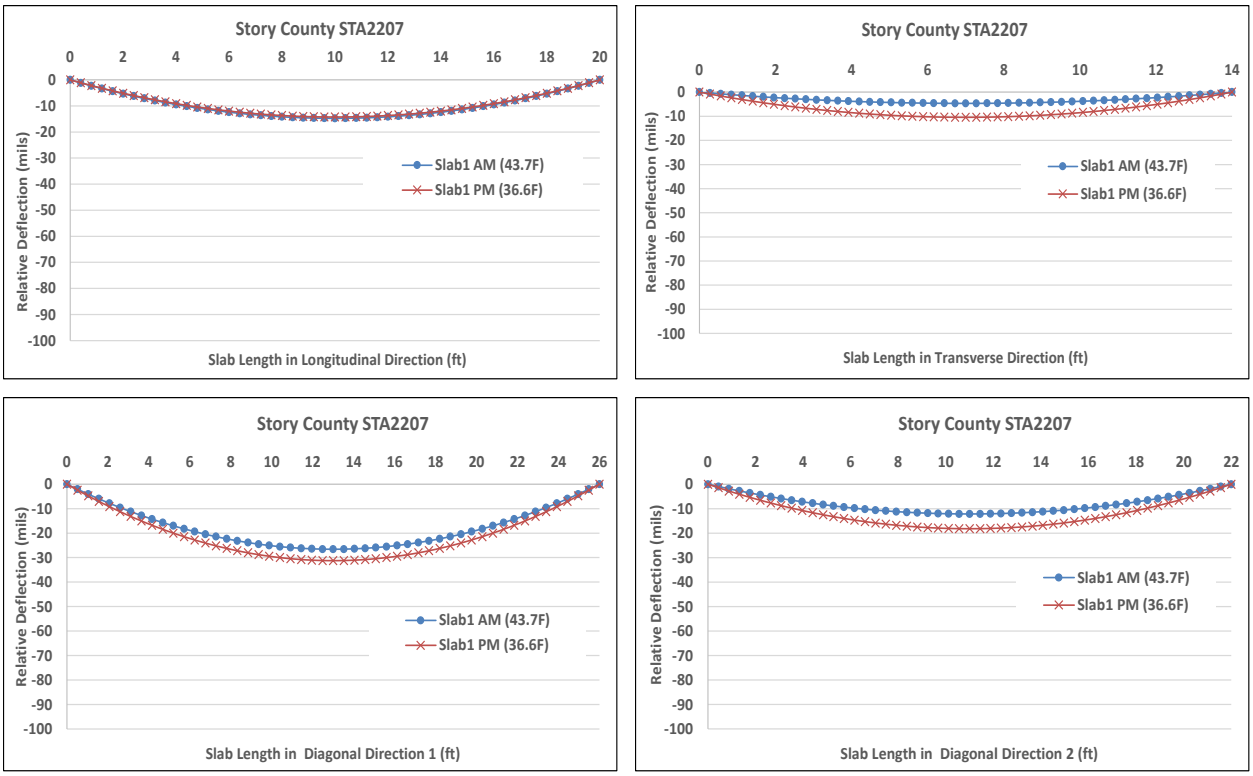

Figure 24. Morning and afternoon relative deflection of Slab 1 at Site 2: longitudinal (top left), transverse (top right), diagonal 1 (bottom left), and diagonal 2 (bottom right)

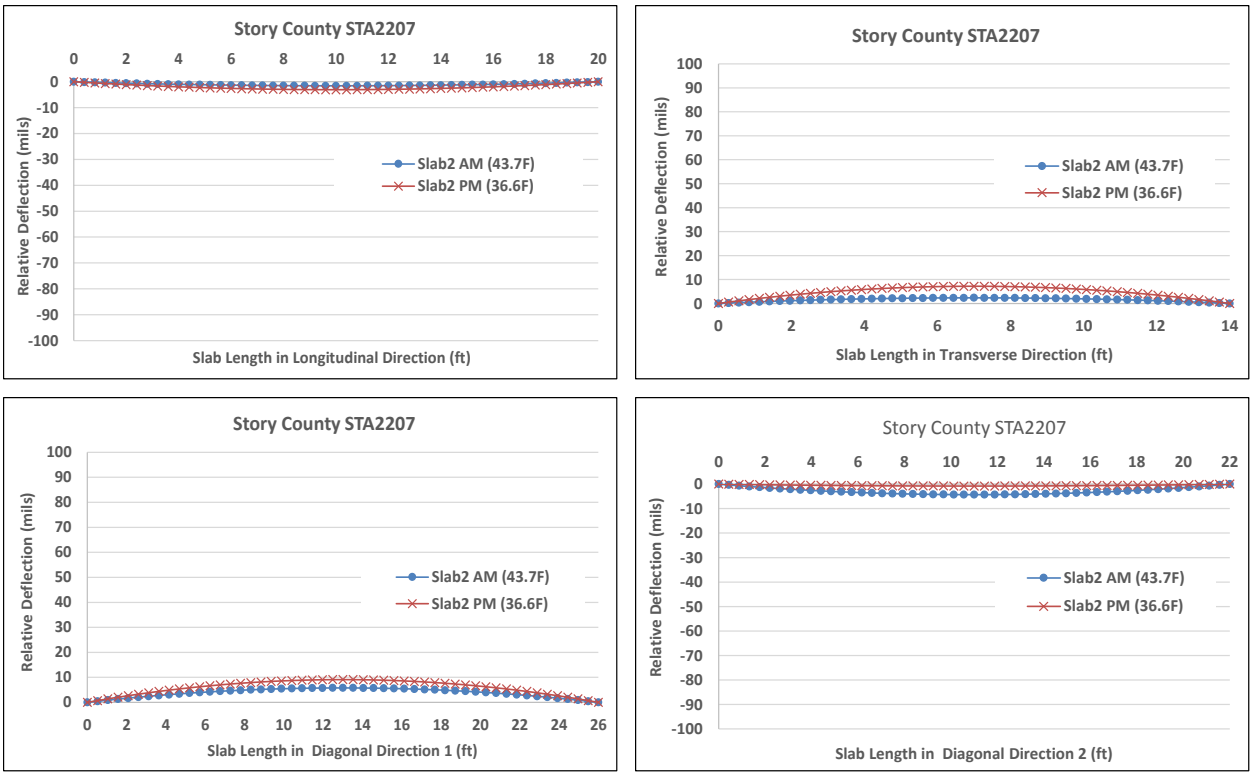

Figure 25. Morning and afternoon relative deflection of Slab 2 at Site 2: longitudinal (top left), transverse (top right), diagonal 1 (bottom left), and diagonal 2 (bottom right)

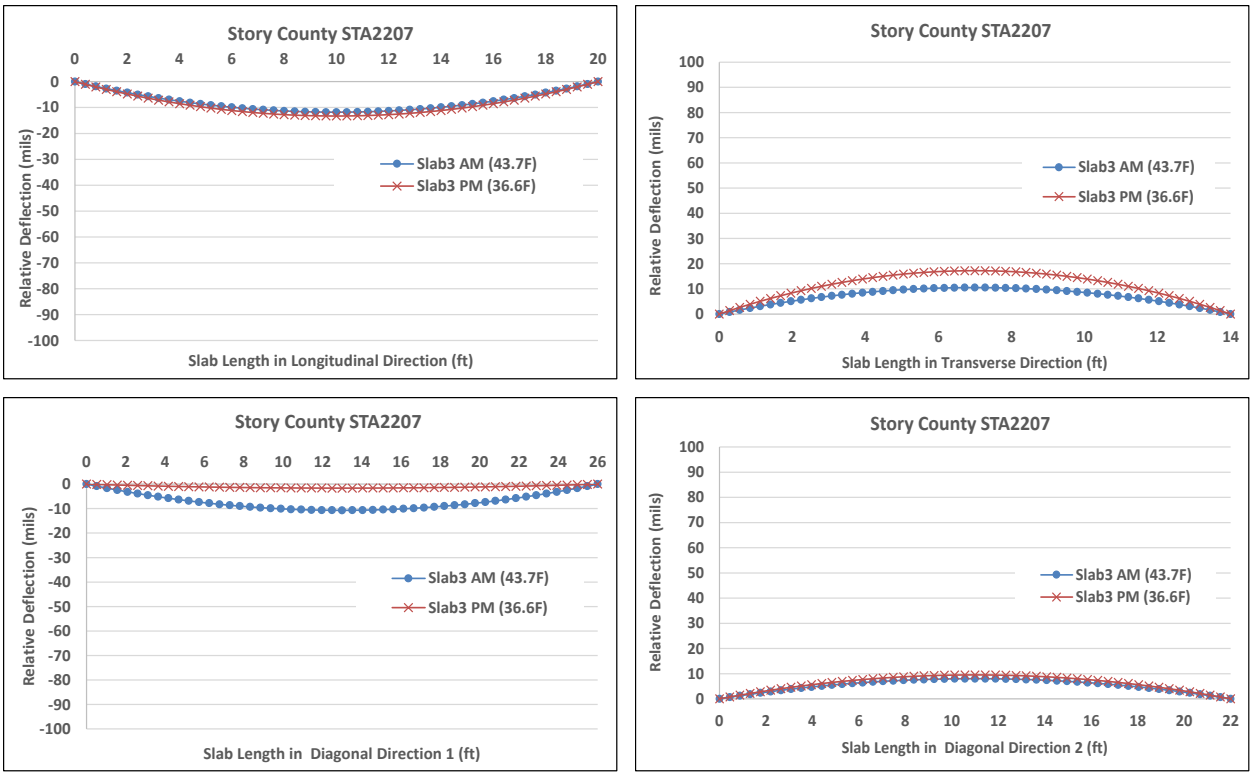

Figure 26. Morning and afternoon relative deflection of Slab 3 at Site 2: longitudinal (top left), transverse (top right), diagonal 1 (bottom left), and diagonal 2 (bottom right)

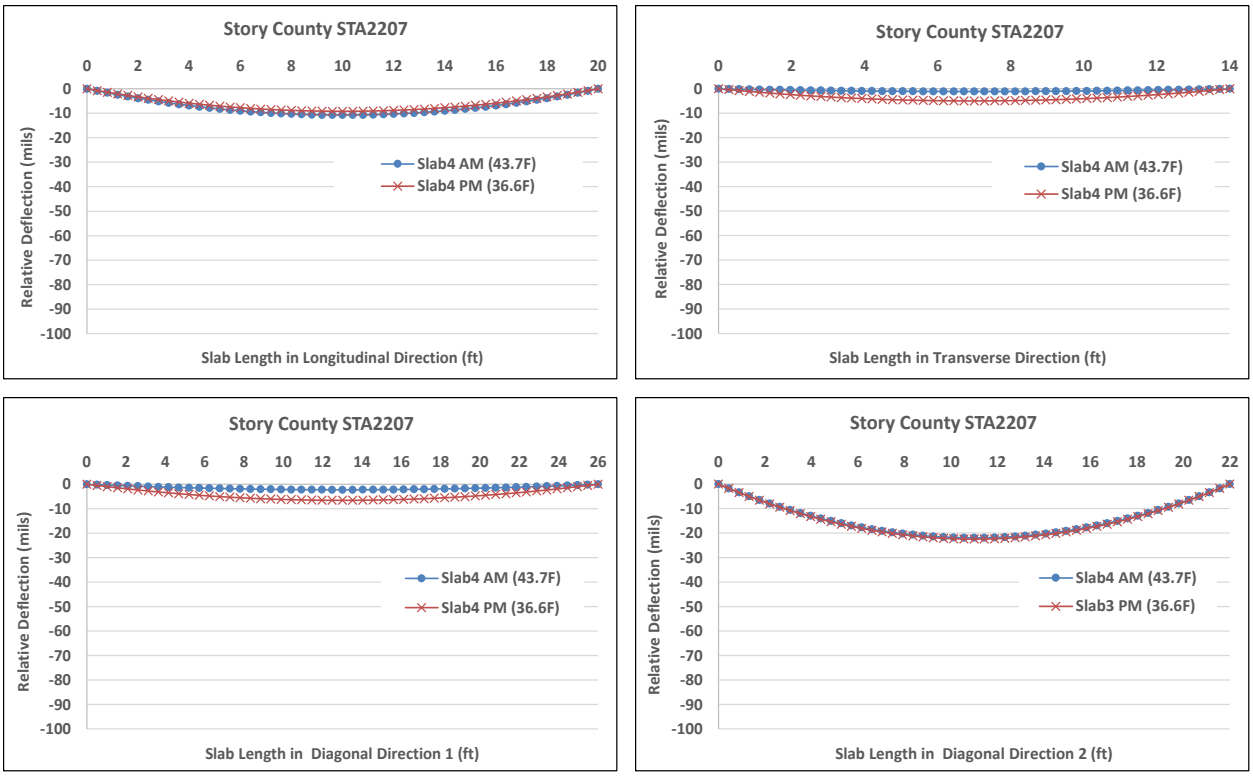

Figure 27. Morning and afternoon relative deflection of Slab 4 at Site 2: longitudinal (top left), transverse (top right), diagonal 1 (bottom left), and diagonal 2 (bottom right)

In Figure 24 through Figure 27, it can be seen that Slabs 1 and 4 at this site show upward curling and warping. Slabs 2 and 3 show upward curling and warping along the longitudinal direction and downward curling and warping along the transverse direction. For the two diagonal directions 1 and 2 (see Figure 16) of Slabs 1 and 4, one diagonal direction shows upward curling and warping while the other shows downward curling and warping. The key findings for this site are as follows:

- Along the longitudinal direction, the relative deflection is in the range of -1.6 to -14.8 mils.
- Along the transverse direction, the relative deflection is in the range of -10.4 to +17.2 mils.
- Along the diagonal directions, the reflective deflection is in the range of -31.3 to +9.5 mils.
- The diagonal directions have the highest upward curling and warping while the transverse direction has the highest downward curling and warping among the slabs.
- The difference in relative deflection between adjacent slabs is within 20 mils.
- Average surface temperature was 43.7°F in the morning and 36.6°F in the afternoon. The lower temperature observed in the afternoon was due to the small amount of rain that occurred at noon on that day.
- The relative deflection in the afternoon is about 1.5 to 7 mils more than the relative deflection in the morning. This difference may be due to the short rain shower that occurred in the morning, which made the surface wetter and thus reduced the degree of upward curvature.

Site 3 - US 151 near Cedar Rapids, Linn County, STA162 (MP 32.75)

Pavement Design and Construction

The PCC pavement at this site was constructed on November 1, 1999. Figure 28 illustrates the location of this site.

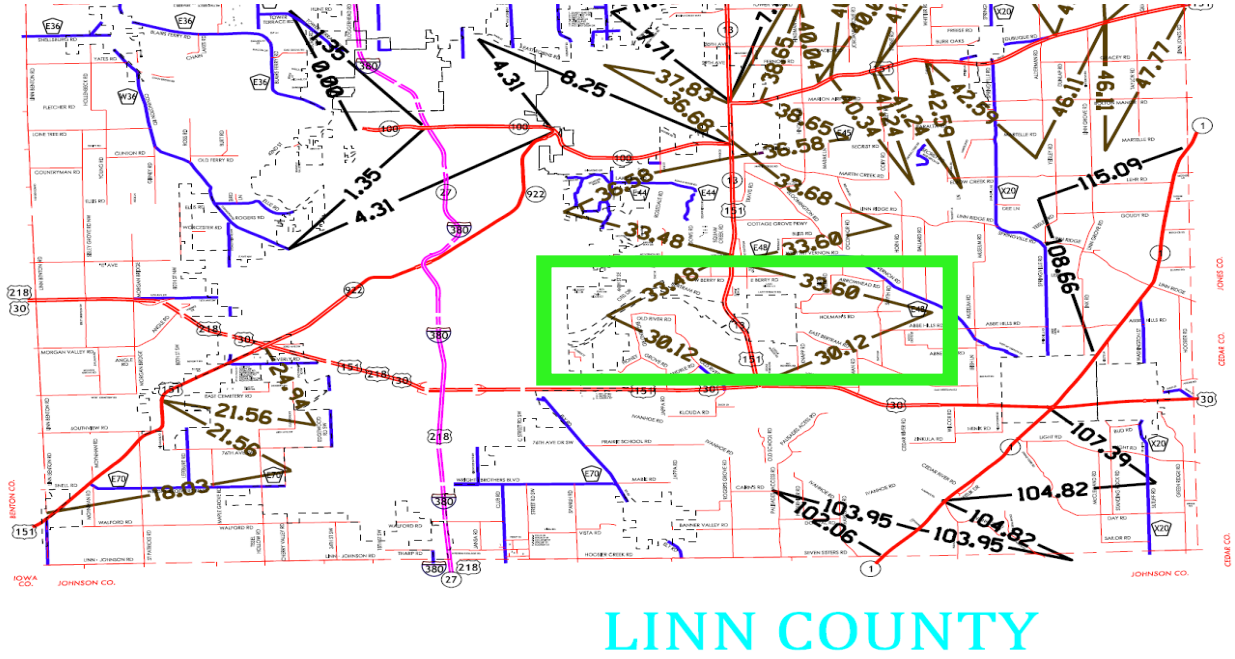

2014 Iowa DOT Milepost book

Figure 28. Site 3 at US 151 near Cedar Rapids, Linn County, southbound

The PCC layer was 10 in. thick and built on top of a 10.5 in. thick granular subbase. The travel lane was 14 ft wide. Furthermore, some portions of the lanes were cut to have skewed joints, with 20.5 ft wide joint spacing. The joints were sealed by an asphalt sealant. Moreover, it should be noted that a right-turn lane had recently been added beside the slab sections. The granular shoulder was 9 ft wide.

Construction at this site started in the early morning around 8:00 a.m. A slipform paver was used, and cold weather protection was adopted. A vibrator was used after slipform paving for consolidation. The day of construction was sunny but cold, with a maximum ambient temperature of 67°F and a minimum ambient temperature of 45°F. During concrete mixing, the maximum mix temperature was 67°F, which was the same as the ambient temperature at that time. At noon, the paving was interrupted because the contactor ran out of cement.

Pavement Materials

Table 9 summarizes the materials used in the concrete mixture for this site.

Table 9. Mix design of STA162 on US 151 near Cedar Rapids, Linn County

Component	Description	Batch Weight
Portland cement	Lafarge Cement Type SM (SG =3.10)	479 lbs/yd^3
GGBFS		
Fly ash	ISG RES-Louisa Type C (SG =2.68)	85 lbs/yd^3
Coarse aggregate	SO. Cedar Rapids Crushed Limestone #4 (SG =2.63, Absorption= 2.6%)	1,675 lbs/yd^3
Fine aggregate	T-203 A-57506 Grad #1 (SG =2.64)	1,415 lbs/yd^3
Water		222 lbs/yd^3
Admixture 1	Brett AEA 92	2.0 fl. oz/cwt
Admixture 2	Brett WR-91	2.0 fl. oz/cwt
Water/cementitious ratio		0.40
Air content		7.8%

fl. oz/cwt = fluid ounces per hundred pounds of cement

It can be seen that 15% Class C fly ash was added to improve concrete properties such as workability and durability. Furthermore, water reducer was used, which produced an average w/cm ratio of 0.4. The maximum w/cm ratio was 0.49 among the different mixes. Furthermore, air-entraining agent was added to the concrete mixture, and the average air content was 7.8%.

Field Investigation Description

Field investigations at Site 3 on US 151 in Linn County near Cedar Rapid were conducted in the morning at 9:00 a.m. on October 29, 2015. Because diurnal temperature fluctuation is typically small in the late fall, another field investigation was performed in the afternoon at 3:30 p.m. on November 10, 2015 when the weather became a little warmer (Wells 2005). A newly added right-turn lane was found next to the surveyed slabs in the traffic lane. This right-turn lane is composed of PCC slabs with rectangular joints, which are not the same as the skewed joints adopted for the passing lane. Furthermore, longitudinal cracks that went through several slabs were found in the traffic lane. One slab also showed transverse cracking. Field investigation activities conducted at this site were the same as the activities at Site 1. Figure 29 shows some of the activities performed during this field investigation, as well as the longitudinal cracking.

Figure 29. Field investigation on US 151 near Cedar Rapids, Linn County, STA162 (MP 32.75)

Data Analysis and Key Findings

Figure 30 through Figure 33 illustrate the calculated relative deflections at STA162, US 151 near Cedar Rapids, Linn County. Four slabs were selected to compare the measurements acquired in the morning of October 29, 2015 and in the afternoon of November 10, 2015.

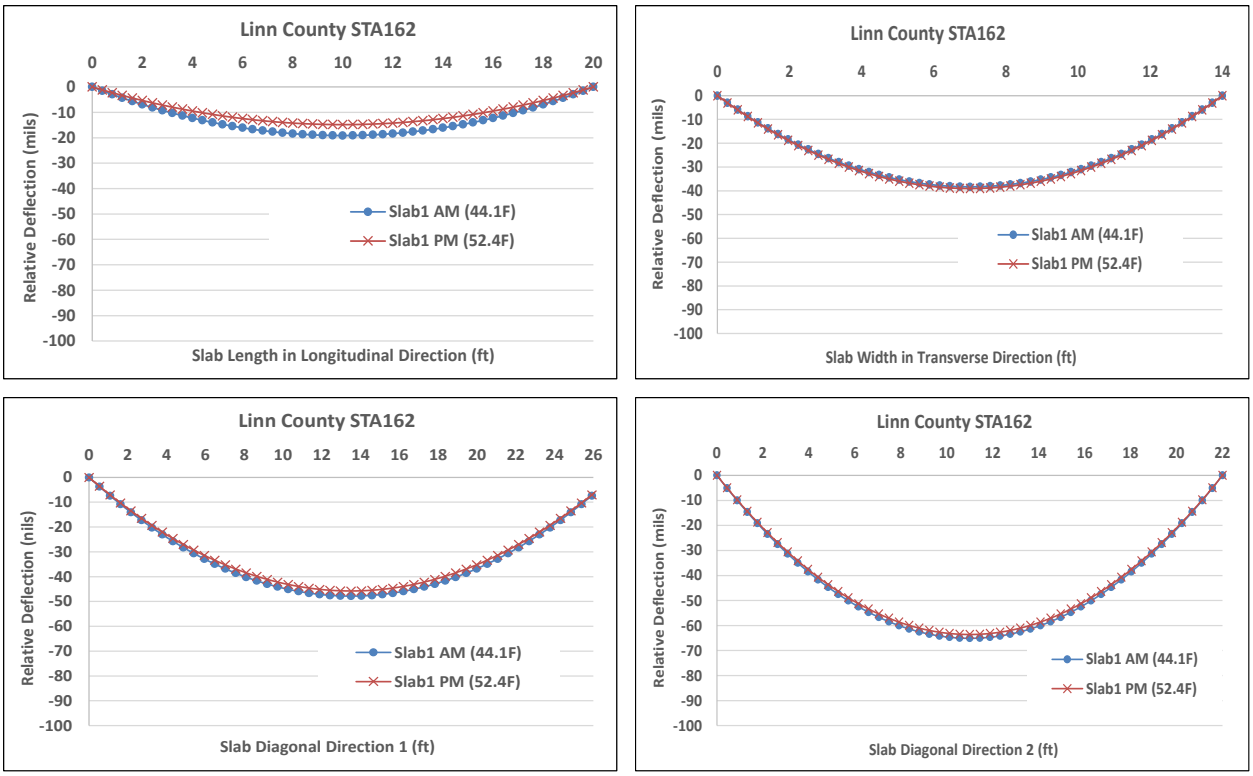

Figure 30. Morning and afternoon relative deflection of Slab 1 at Site 3: longitudinal (top left), transverse (top right), diagonal 1 (bottom left), and diagonal 2 (bottom right)

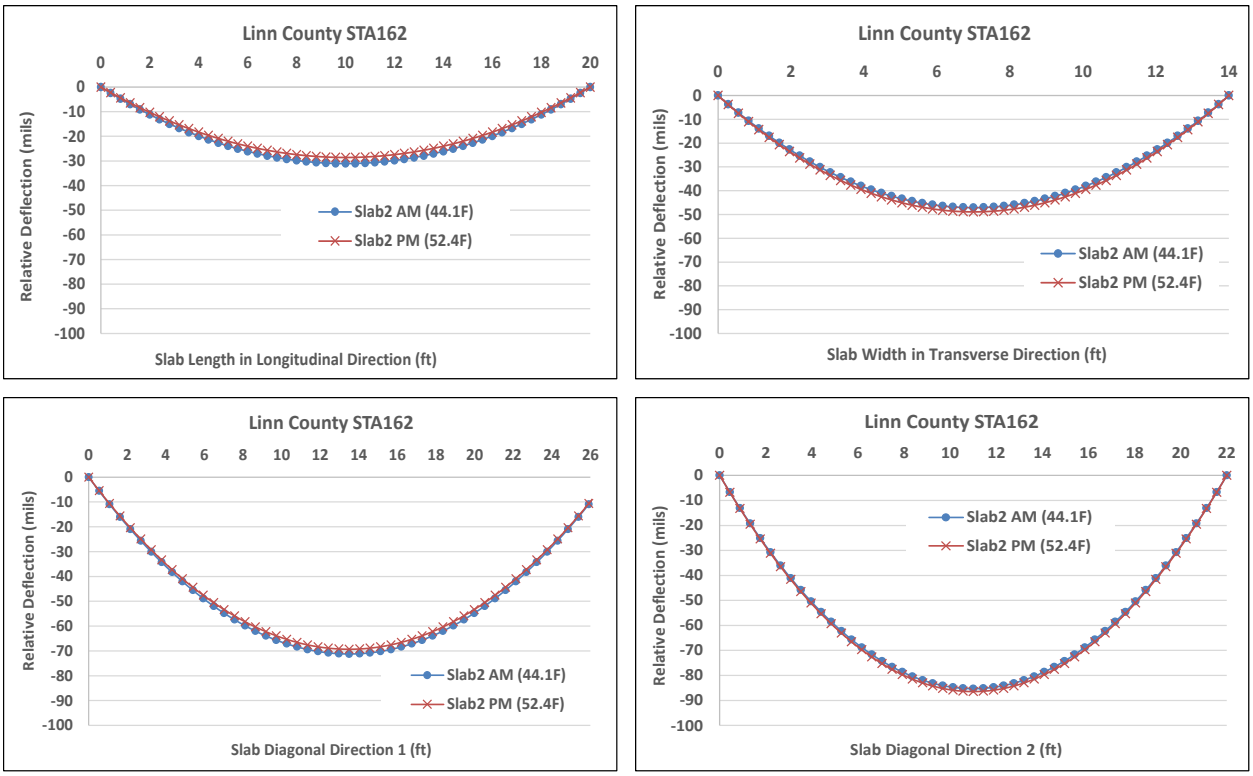

Figure 31. Morning and afternoon relative deflection of Slab 2 at Site 3: longitudinal (top left), transverse (top right), diagonal 1 (bottom left), and diagonal 2 (bottom right)

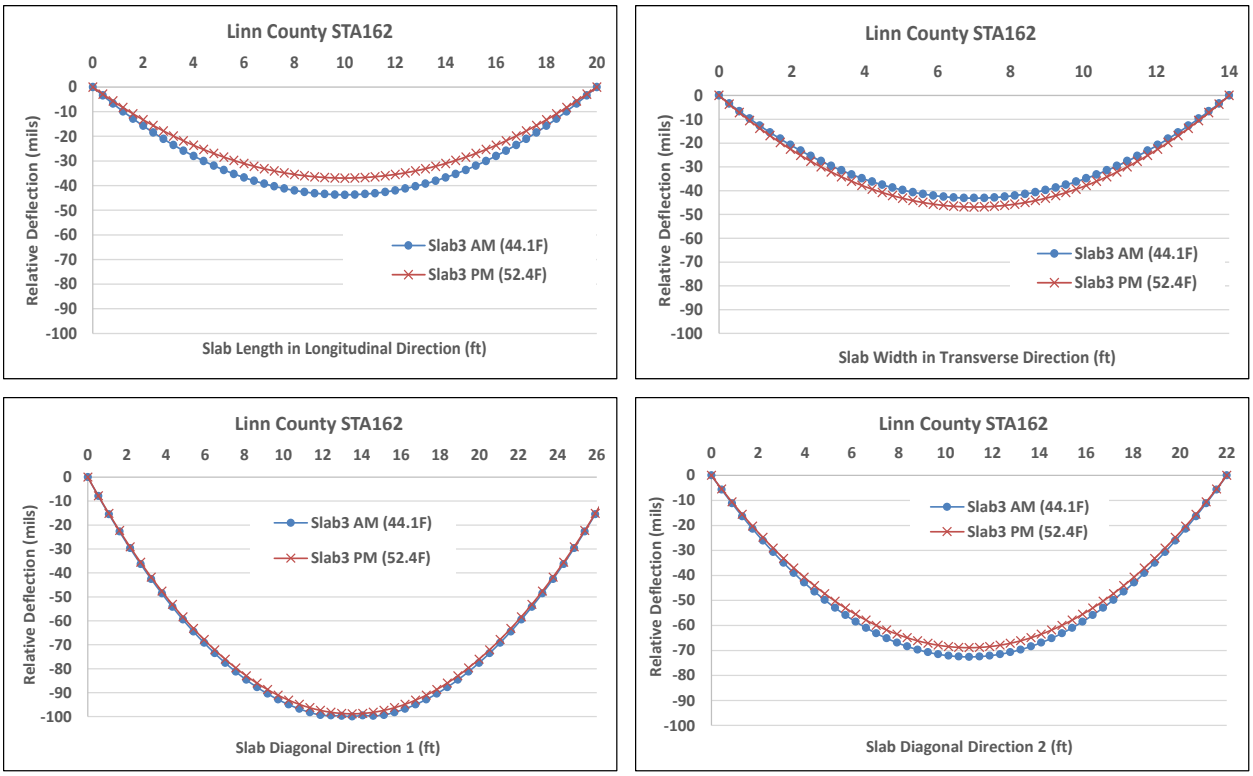

Figure 32. Morning and afternoon relative deflection of Slab 3 at Site 3: longitudinal (top left), transverse (top right), diagonal 1 (bottom left), and diagonal 2 (bottom right)

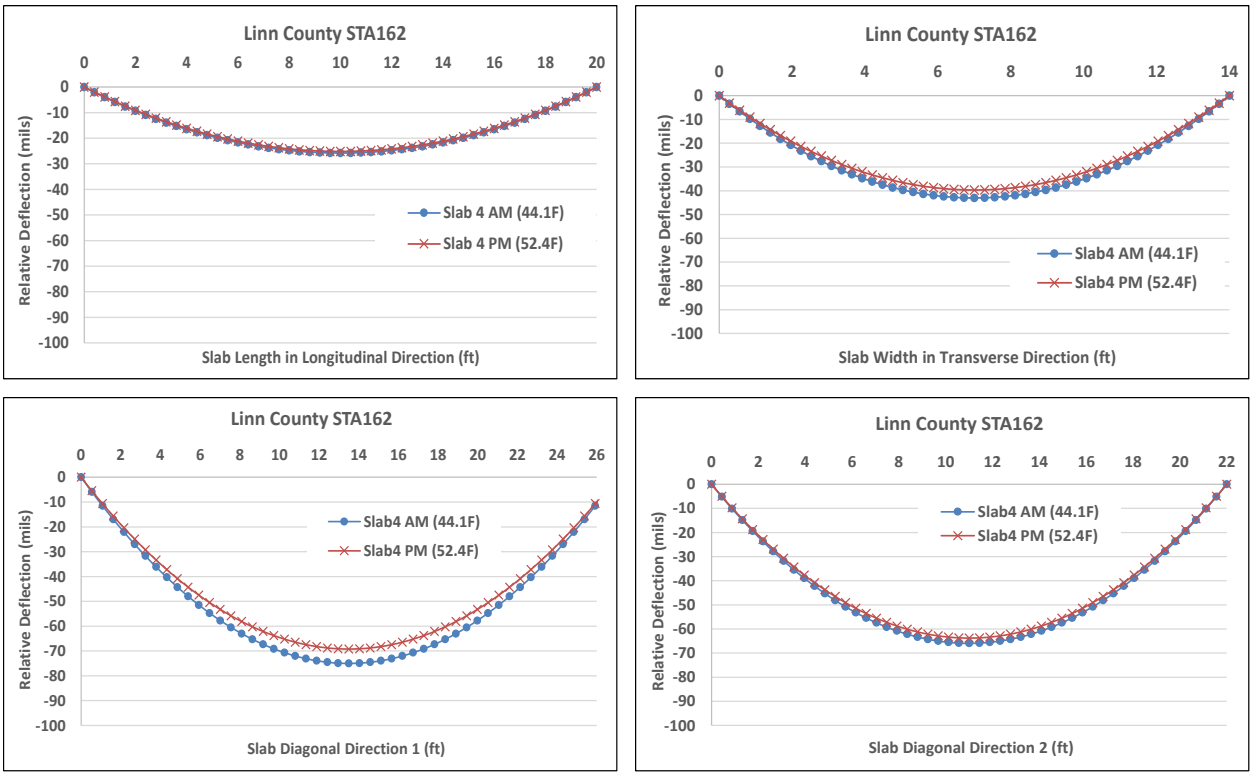

Figure 33. Morning and afternoon relative deflection of Slab 4 at Site 3: longitudinal (top left), transverse (top right), diagonal 1 (bottom left), and diagonal 2 (bottom right)

In Figure 30 through Figure 33, it can be seen that all slabs showed upward curling and warping during field investigation. The key findings are as follows:

- Along the longitudinal direction, the relative deflection is in the range of -43.7 to -14.8 mils.
- Along the transverse direction, the relative deflection is in the range of -48.9 to -38.3 mils.
- Along the diagonal directions, the relative deflection is in the range of -86.5 to -63.6 mils.
- The diagonal directions have the highest upward curling and warping compared to the longitudinal and transverse directions.
- The difference in relative deflection between adjacent slabs is within 19 mils.
- The average temperature for these slabs was 44.1°F in the morning of October 29, 2015 and 52.4°F in the afternoon of November 10, 2015.
- The relative deflection in the afternoon of November 10, 2015 was about 1.5 to 7 mils less than the relative deflection in the morning of October 29, 2015.

Site 4 - US 151 near Cedar Rapids, Linn County, STA183 (MP 33.15)

Pavement Design and Construction

The PCC pavement at this site was constructed on November 4, 1999, just three days after the construction at Site 3. Figure 34 illustrates the location of this site.

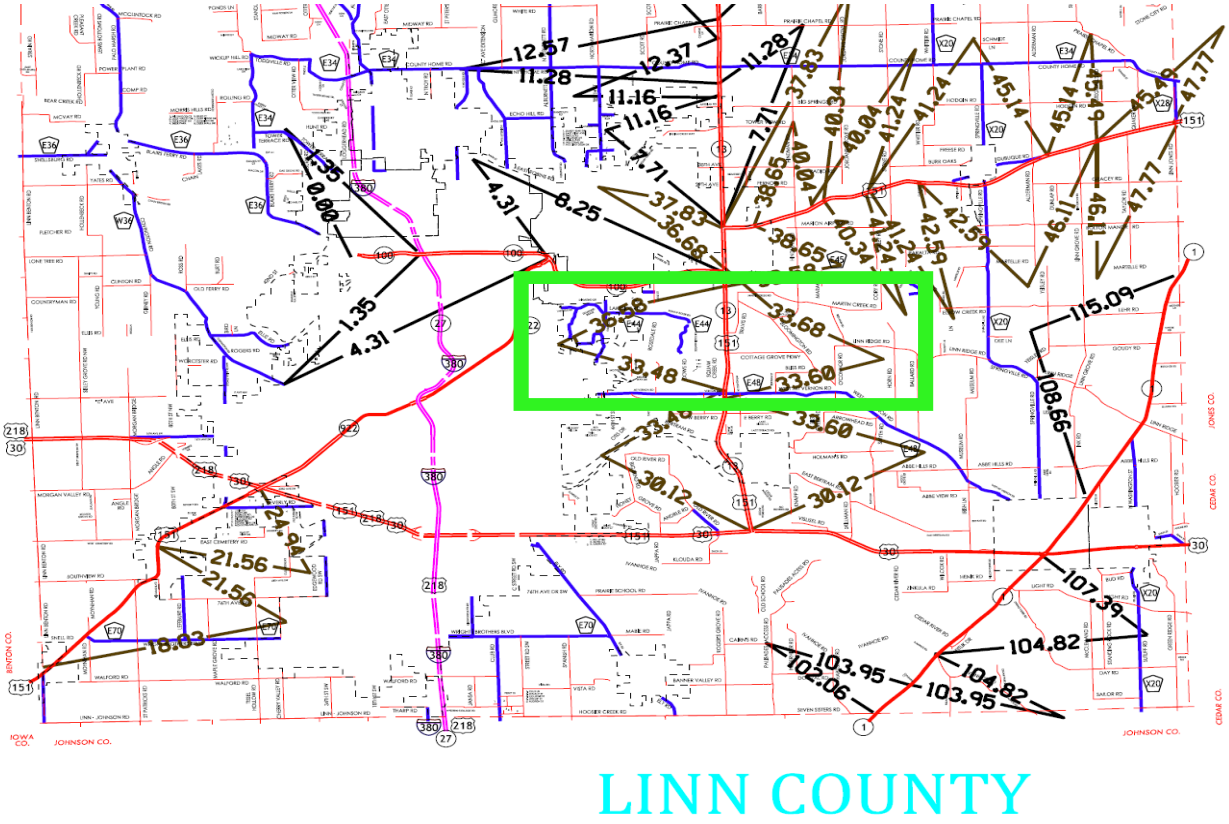

Iowa DOT 2014 Milepost book

Figure 34. Site 4 on US 151 near Cedar Rapids, Linn County, southbound

A 10 in. thick PCC pavement was built on top of an 8 in. thick granular subbase. The travel lane is 14 ft wide, and joint spacing is 20 ft. Additionally, the joint was constructed as skewed without any sealant. The granular shoulder was 9 ft wide.

Concrete paving started in the early morning at 8:00 a.m. using a slipform paver. Vibrators were used to consolidate the concrete. However, unlike at Site 3, cold weather protection was not adopted during construction at this site. On the day of construction, the weather was sunny, but the maximum ambient temperature was 64°F and the minimum ambient temperature was 29°F during paving. These temperatures were slightly lower than the ambient temperatures during construction at Site 3.

Pavement Materials

Table 10 summarizes the materials used in the concrete mixture for this site.

Table 10. Mix design of STA183 on US 151 near Cedar Rapids, Linn County

Component	Description	Batch Weight
Portland cement	Lafarge Type SM (SG =3.10)	479 lbs/yd^3
GGBFS		
Fly ash	ISG RES-Louisa Type C (SG =2.68)	85 lbs/yd^3
Coarse aggregate	Springville Crushed Limestone Grad #4 (SG =2.63, Absorption= 4.5~9%)	1,673 lbs/yd^3
Fine aggregate	Grad #1 (SG =2.64)	1,424 lbs/yd^3
Water		236 lbs/yd^3
Admixture 1	Brett AEA 92	2.0 fl. oz/cwt
Admixture 2	Brett WR-91	2.0 fl. oz/cwt
Water/cementitious ratio		0.42
Air content		7.7%

fl. oz/cwt = fluid ounces per hundred pounds of cement. Absorption depends on the specific gravity of the materials for this site.

Similar to Site 3, Class C fly ash was added to occupy 15% of the total weight of the cementitious materials in order to improve concrete workability and durability. Furthermore, water reducer was used, which produced an average w/cm ratio of 0.42. Moreover, air-entraining agent was added to the concrete mixture, and the average air content was 7.7%.

Field Investigation Description

Field investigations at Site 4 on US 151 in Linn County near Cedar Rapids were conducted in the morning at 10:00 a.m. on October 29, 2015. Another field investigation was performed in the afternoon at 2:30 p.m. on November 10, 2015. At this site, the scans for the selected PCC slabs were performed at STA183 on US 151. No cracks were observed in these slabs. Field investigation activities conducted at this site were the same as the activities conducted at Site 1. Figure 35 presents some of the activities performed during this field investigation.

Figure 35. Field investigation on US 151 near Cedar Rapids, Linn County, STA183 (MP 33.15)

Figure 36 and Figure 37 illustrate the calculated relative deflections at STA183, US 151 near Cedar Rapids, Linn County. Two slabs were selected to compare the measurements taken in the morning of October 29, 2015 and in the afternoon of November 10, 2015.

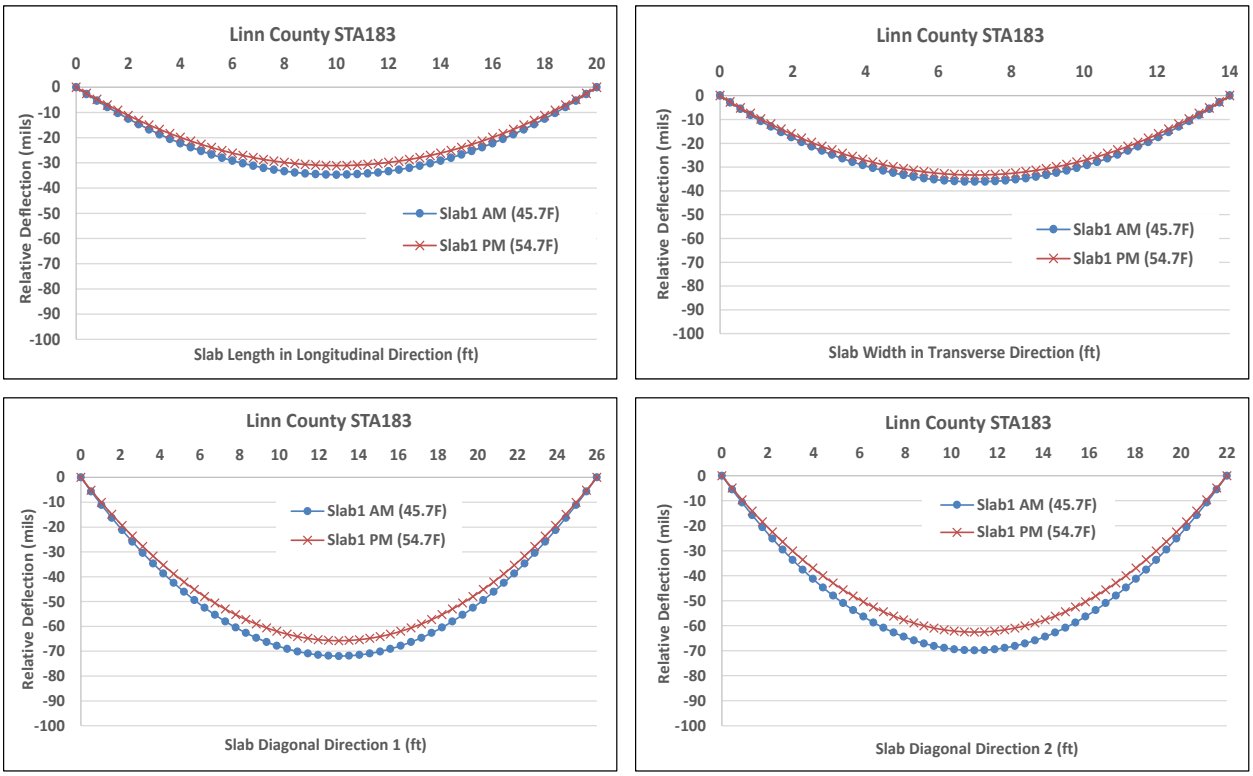

Figure 36. Morning and afternoon relative deflection of Slab 1 at Site 4: longitudinal (top left), transverse (top right), diagonal 1 (bottom left), and diagonal 2 (bottom right)

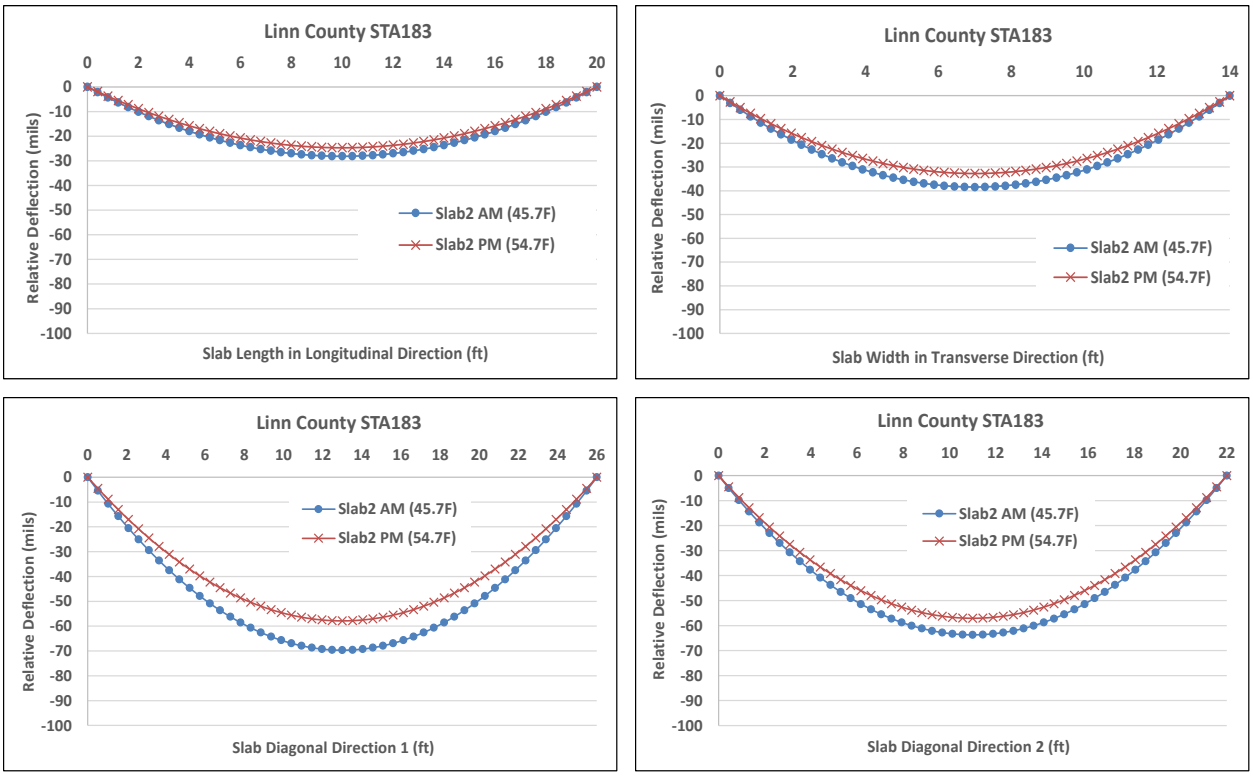

Figure 37. Morning and afternoon relative deflection of Slab 2 at Site 4: longitudinal (top left), transverse (top right), diagonal 1 (bottom left), and diagonal 2 (bottom right)

In Figure 36 and Figure 37, it can be seen that the two slabs showed upward curling and warping during field investigation. The key findings at this site are as follows:

- Along the longitudinal direction, the relative deflection is in the range of -34.7 to -24.7 mils.
- Along the transverse direction, the relative deflection is in the range of -38.4 to -32.7 mils.
- Along the diagonal directions, the relative deflection is in the range of -71.9 to -57.1 mils.
- Diagonal directions have the highest upward curling and warping compared to the longitudinal and transverse directions.
- The difference in relative deflection between adjacent slabs is within 8 mils.
- The average slab temperature was 45.7°F in the morning of October 29, 2015 and 54.7°F in the afternoon of November 10, 2015.
- The relative deflection in the afternoon of November 10, 2015 was about 2 to 7 mils less than the relative deflection in the morning of October 29, 2015.

Site 5 - US 30 near Cedar Rapids, Linn County, STA463 (MP 261.2)

Pavement Design and Construction

The PCC pavement at this site was constructed around the May 15, 1999. Figure 38 illustrates the location of this site.

Iowa DOT 2014 Milepost book

Figure 38. Site 5 on US 30 near Cedar Rapids, Linn County STA463 (MP 261.2), westbound

The PCC layer was 10 in. thick and built on top of a 10.5 in. thick granular subbase. The travel lane was 14 ft wide. The joint spacing was cut to be approximately 20 ft wide and sealed by asphalt sealant. Skewed joints were adopted for this site. Additionally, the granular shoulder was 10 ft wide. In the measured slab, longitudinal cracks were found in about every other slab.

Construction started in the early morning around 8 a.m. A slipform paver was used for concrete paving. The day of construction was sunny, with a maximum ambient temperature of 77.5°F and a minimum ambient temperature of 42.8°F.

Pavement Materials

Table 11 summarizes the materials used in the concrete mixture for this site.

It can be seen that 20% Class C fly ash was added to improve concrete properties such as workability and durability. Furthermore, water reducer was used, which produced an average w/cm ratio of 0.43.

Table 11. Mix design of STA463 on US 30 near Cedar Rapids, Linn County

Component	Description	Batch Weight
Portland cement	Lafarge Type 1SM (SG =3.10)	451 lbs/yd^3
GGBFS		
Fly ash	ISG Resource, Inc. (SG =2.68)	113 lbs/yd^3
Coarse aggregate	SO. Cedar Rapids Crushed Limestone Grad#3 (SG =2.66, Absorption= 2.6%)	1,702 lbs/yd^3
Fine aggregate	Wendling A57520 Grad#1 (SG =2.65)	1,447 lbs/yd^3
Water		240 lbs/yd^3
Admixture 1	Daravair 1,000	4.0 fl. oz/cwt
Admixture 2	WRDA-82	3.5 fl. oz/cwt
Water/cementitious ratio		0.43
Air content		Not available

fl. oz/cwt = fluid ounces per hundred pounds of cement

Field Investigation Description

Field investigations at Site 5 on US 30 in Linn County near Cedar Rapids were conducted in the morning at 11:00 a.m. on October 29, 2015. Another field investigation was performed in the afternoon at 1:00 p.m. on November 10, 2015. At this site, the scans for the selected PCC slabs were performed at STA463 on US 30. Longitudinal cracks that went through several slabs were observed in the traffic lane. Field investigation activities were the same as the activities conducted at Site 1. Figure 39 presents some of the activities performed during this field investigation.

Figure 39. Field investigation on US 30 in Linn County, STA463 (MP 261.2)

Data Analysis and Key Findings

Figure 40 through Figure 43 illustrate the calculated relative deflections at STA463, US 30 near Cedar Rapids, Linn County. Four slabs were selected to compare the measurements taken in the morning of October 29, 2015 and in the afternoon of November 10, 2015.

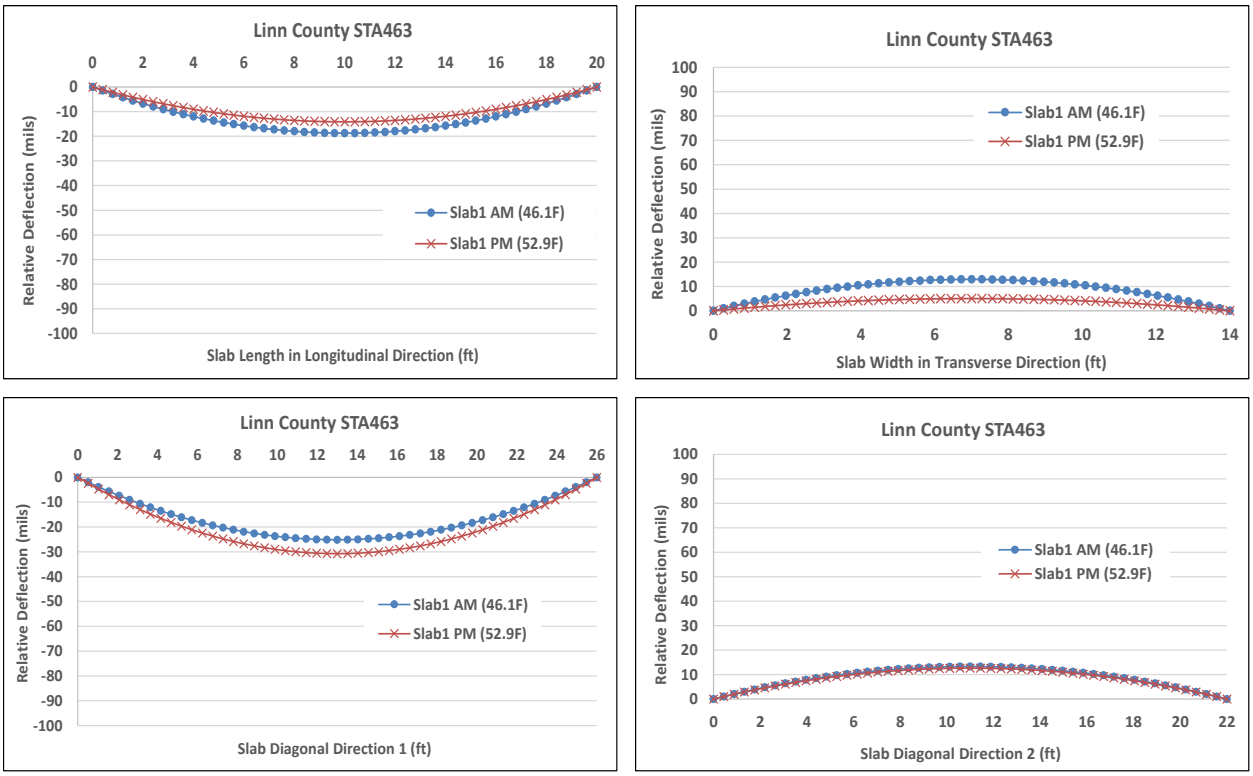

Figure 40. Morning and afternoon relative deflection of Slab 1 at Site 5: longitudinal (top left), transverse (top right), diagonal 1 (bottom left), and diagonal 2 (bottom right)

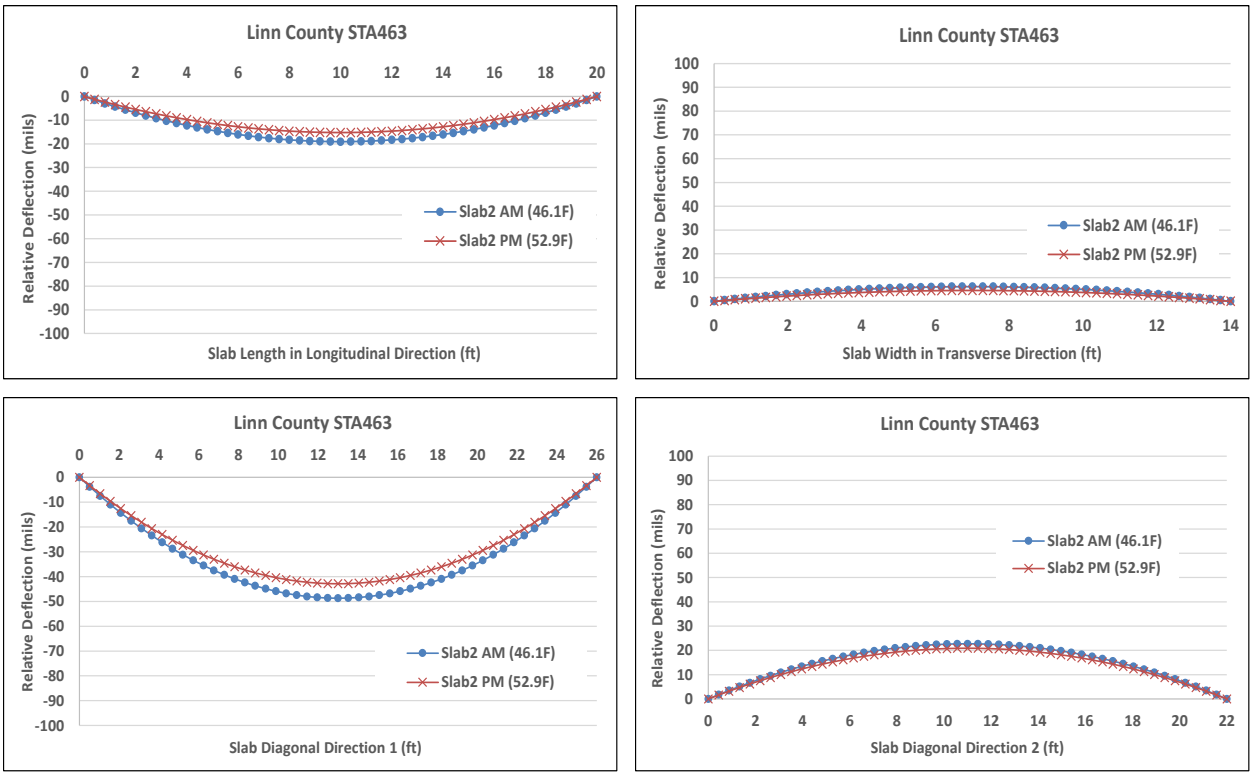

Figure 41. Morning and afternoon relative deflection of Slab 2 at Site 5: longitudinal (top left), transverse (top right), diagonal 1 (bottom left), and diagonal 2 (bottom right)

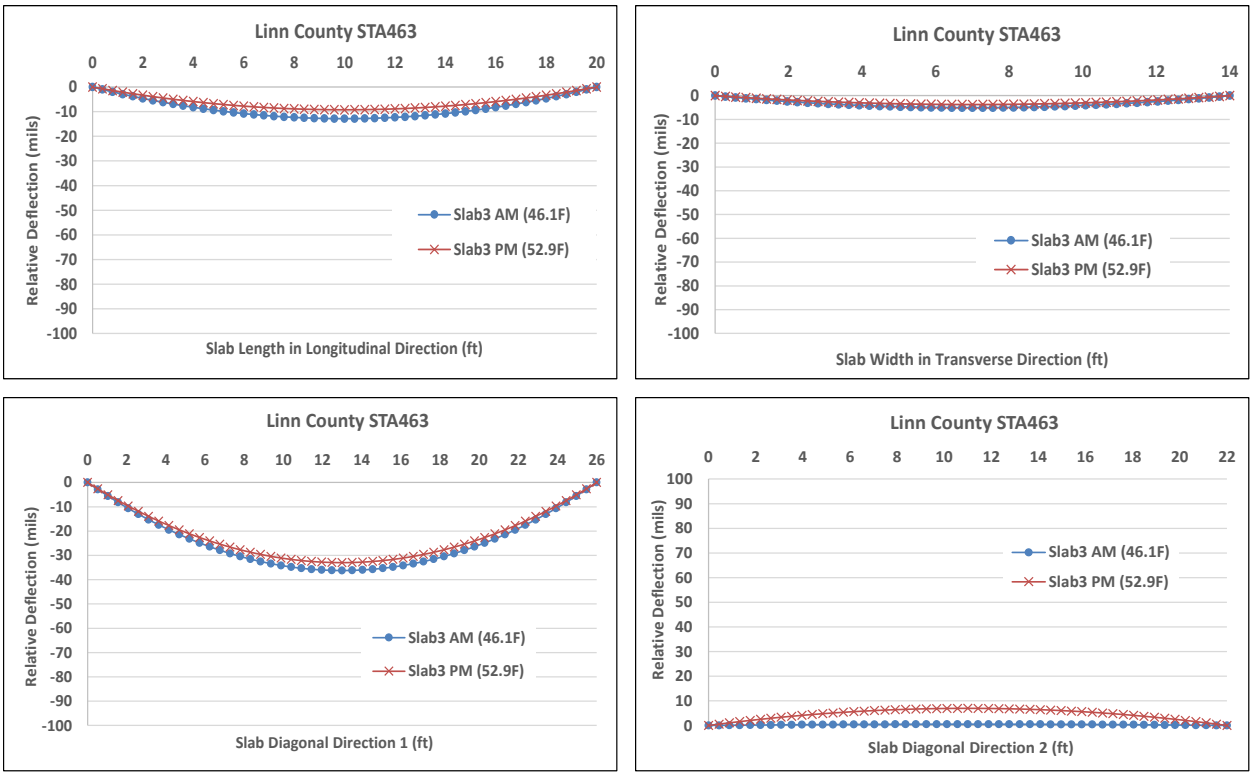

Figure 42. Morning and afternoon relative deflection of Slab 3 at Site 5: longitudinal (top left), transverse (top right), diagonal 1 (bottom left), and diagonal 2 (bottom right)

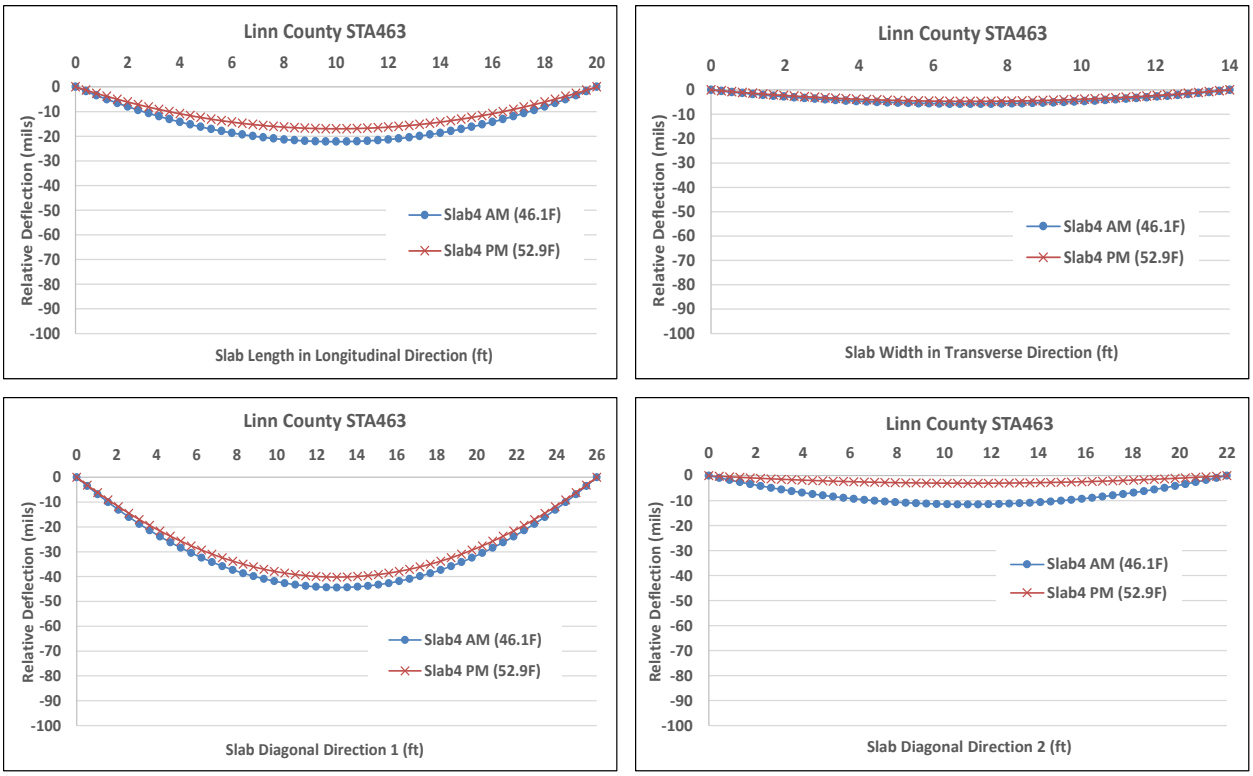

Figure 43. Morning and afternoon relative deflection of Slab 4 at Site 5: longitudinal (top left), transverse (top right), diagonal 1 (bottom left), and diagonal 2 (bottom right)

In Figure 40 through Figure 43, it can be seen that Slabs 1 and 2 at this site showed upward curling and warping along the longitudinal direction and downward curling and warping along the transverse direction. For the two diagonal directions 1 and 2 (see Figure 18) of the two slabs, one diagonal direction showed upward curling and warping while the other showed downward curling and warping. Slab 3 showed similar deflection to Slabs 1 and 2, except that Slab 3 had upward curling and warping in the transverse direction. Slab 4 only showed upward curling and warping. The key findings for this site are as follows:

- Along the longitudinal direction, the relative deflection is in the range of -22.2 to -9.2 mils.
- Along the transverse direction, the relative deflection is in the range of -3.7 to +12.9 mils.
- Along the diagonal directions, the relative deflection is in the range of -48.7 to +22.7 mils.
- Diagonal directions have highest curling and warping.
- The difference in relative deflection between adjacent slabs is within 17 mils.
- The average temperature calculated for these slabs was 46.1°F in the morning and 52.9°F in the afternoon.
- The relative deflection in the afternoon of November 10, 2015 is about 1 to 8 mils less than the relative deflection in the morning of October 29, 2015.

Site 6 - US 30 near Toledo, Tama County STA113 (MP 194.6)

Pavement Design and Construction

This site is located at the border of Tama County. The pavement at this section was paved at 3:00 p.m. in the afternoon of July 13, 2005. Figure 44 illustrates the location of this site.

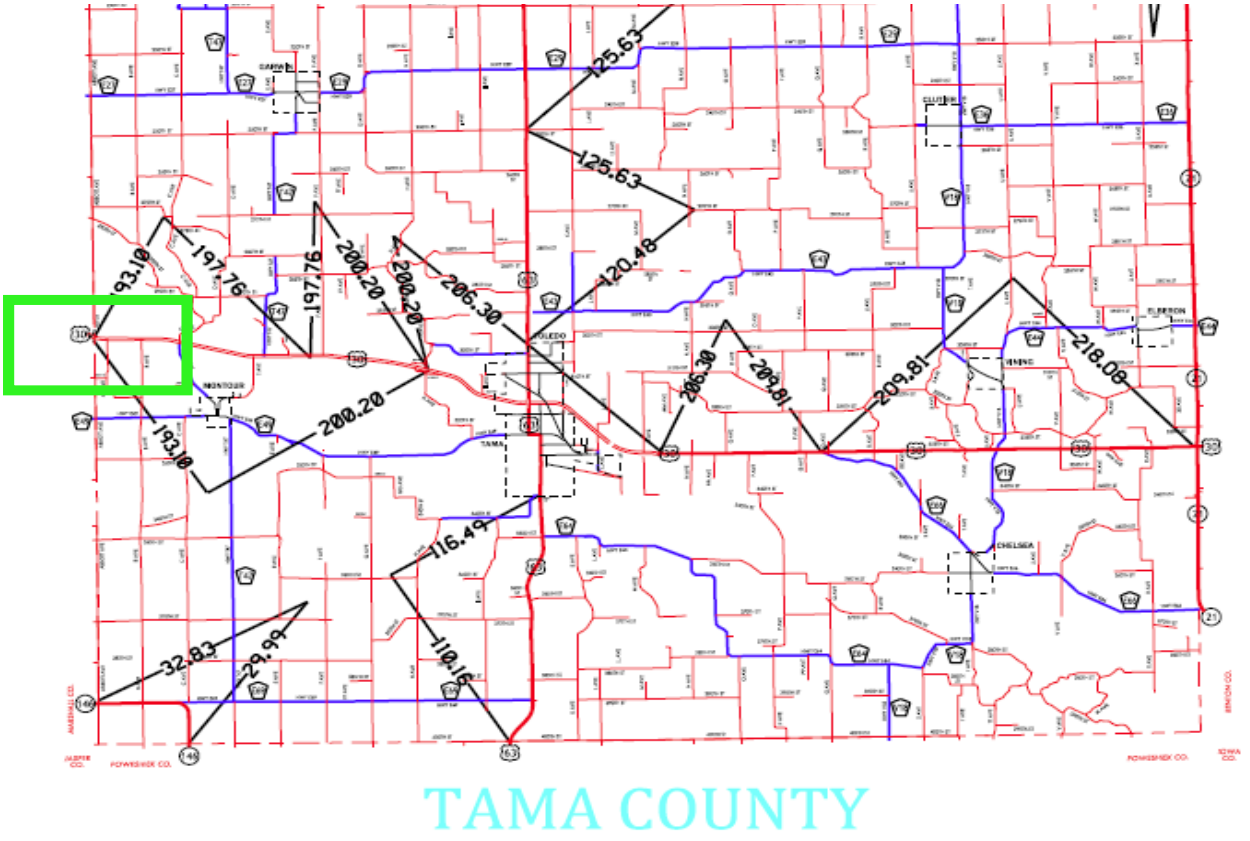

Iowa DOT 2014 Milepost book

Figure 44. Site 6 on US 30 near Toledo, Tama County STA113 (MP 194.6), eastbound

At this site, a 10 in thick JPCP was constructed on top of a 6 to 10 in. open-graded granular base. The concrete was paved by a concrete spreader and paver. Concrete was first transported by the haul trucks that traveled on-site and then graded and fed into the spreader. The paver was then applied to level off the fresh concrete. Dowel baskets were placed prior to concrete paving at transverse joints to hold smooth dowel bars 18 in. long and 1.5 in. in diameter. The dowels were placed approximately every 12 in. in the baskets. A transverse joint was cut approximately every 20 ft during the early age. The early-age saw cut was 1.25 in. deep. As for the longitudinal joints, size #5 tie bars with a 35 in. length and a 0.63 in. diameter were inserted every 2.5 ft. The longitudinal joints were cut 3.4 in. deep by conventional saws. The passing lane and travel lane were approximately 12 ft and 14 ft wide, respectively. It should be noted that the travel lane is about 2 ft wider than the passing lane because it is now more or less general practice in Iowa to

construct the travel lane to be 2 ft wider than the passing lane. Moreover, a HMA shoulder was placed next to the traffic lane.

Pavement Materials

Table 12 summarizes the materials used in the concrete mixture for this site.

Table 12. Mix design of STA113 on US 30 near Toledo, Tama County

Component	Description	Batch Weight
Portland cement	Ash Grove (Louisville, NE) - Type I/II	448 lbs/yd^3
GGBFS		
Fly ash	Ottumwa Generating Station - Type C (SG =2.61)	112 lbs/yd^3
Coarse aggregate	Wendling - Montour #86002 (SG =2.61, Absorption= 2.4%)	1,539 lbs/yd^3
Fine aggregate	Manatt - Flint #86502 (SG =2.66)	1,272 lbs/yd^3
Water		224 lbs/yd^3
Admixture 1	Daravair 1,400	3.92 oz/yd^3
Admixture 2	WRDA 82	19.6 oz/yd^3
w/cm ratio		0.40
Air content		6.0

The CTE measured from the field-fabricated cylinders was 5.35×10-6 Ɛ/°F. Class C fly ash was added to occupy 20% of the total weight of the cementitious materials in order to improve concrete workability and durability. Furthermore, water reducer was used, which produced an average w/cm ratio of 0.4. Air-entraining agent was added to the concrete mixture, and the average air content was 6%.

Field Investigation Description

Field investigations at Site 6 on US 30 in Toledo, Tama County were conducted in the morning at 11:00 a.m. on November 10, 2015. At this site, the scans for the selected PCC slabs were performed at STA113 on US 30 Highway. No cracks were found in the traffic lane. Field investigation activities were the same as the activities conducted at Site 1. Figure 45 presents some of the activities performed during this field investigation.

Figure 45. Field investigation on US 30 near Toledo, Tama County STA113 (MP 194.6)

Data Analysis and Key Findings

Figure 46 through Figure 49 illustrate the calculated relative deflections at STA113, Toledo, Tama County. Four slabs were selected to investigate the measurements taken in the morning of November 10, 2015.

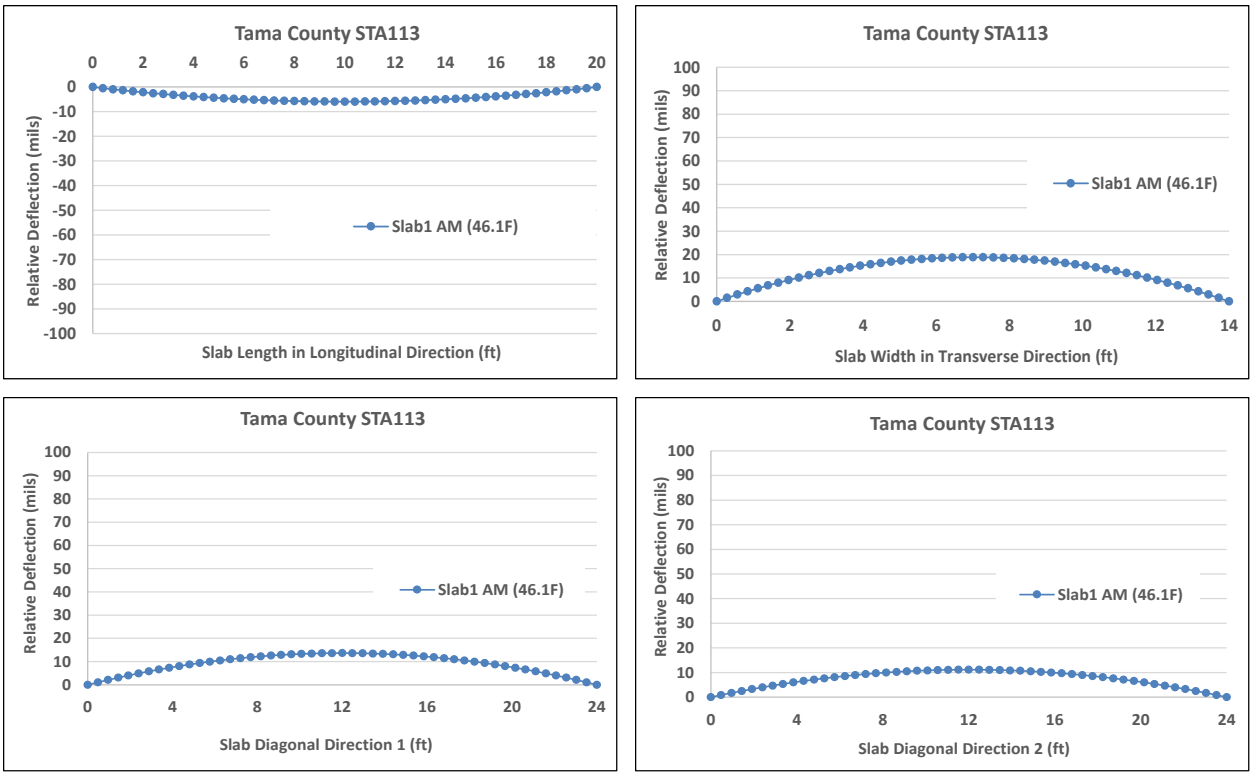

Figure 46. Morning relative deflection of Slab 1 at Site 6: longitudinal (top left), transverse (top right), diagonal 1 (bottom left), and diagonal 2 (bottom right)

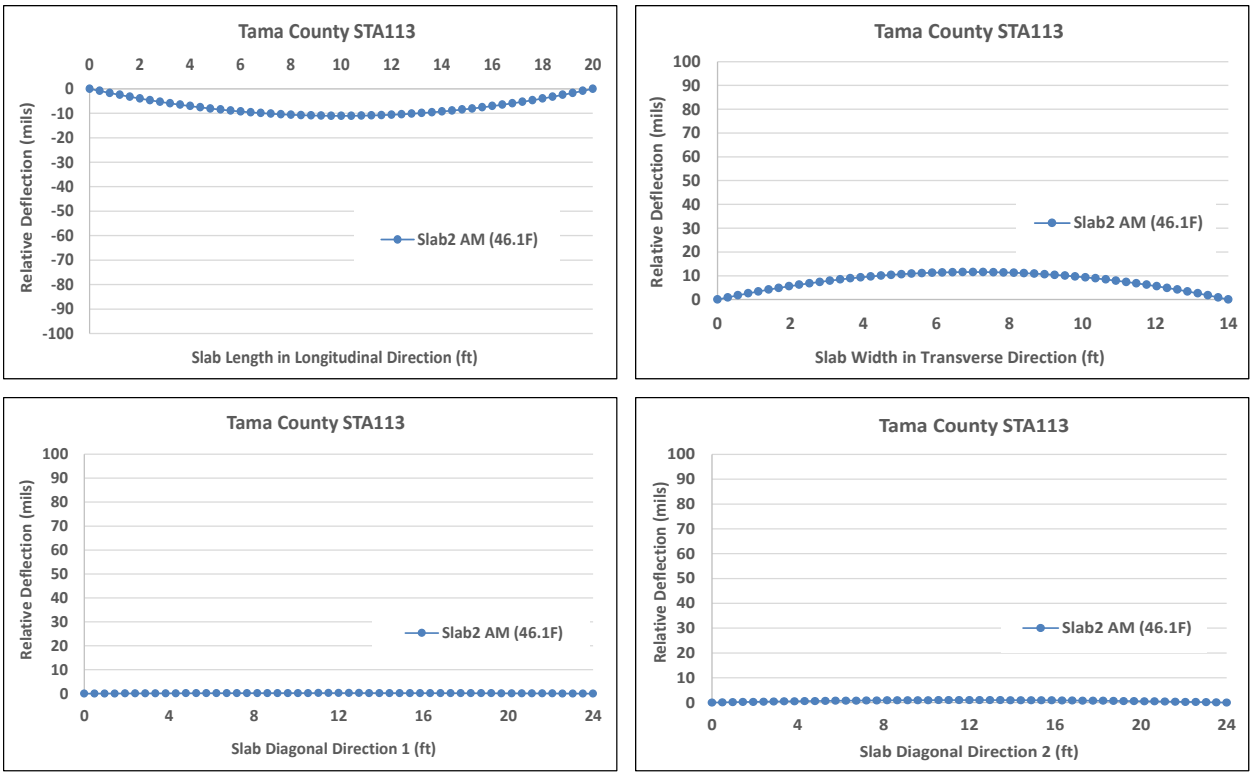

Figure 47. Morning relative deflection of Slab 2 at Site 6: longitudinal (top left), transverse (top right), diagonal 1 (bottom left), and diagonal 2 (bottom right)

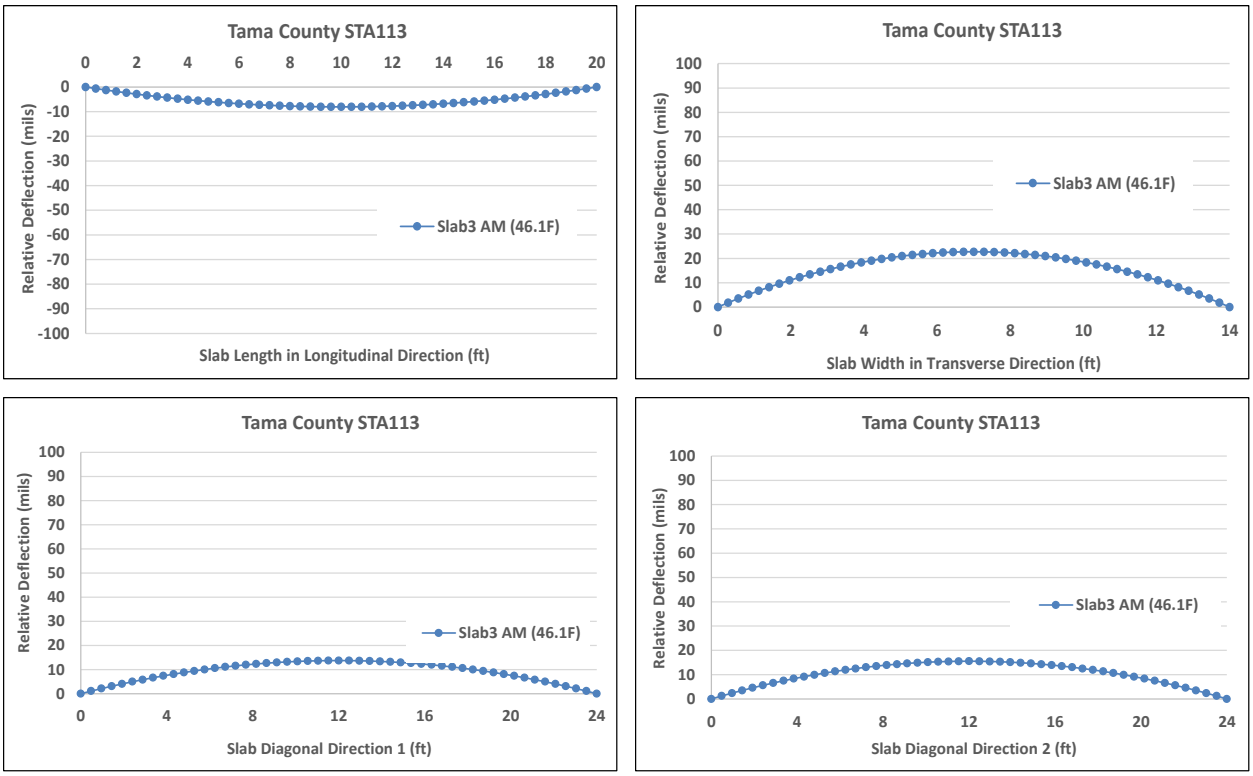

Figure 48. Morning relative deflection of Slab 3 at Site 6: longitudinal (top left), transverse (top right), diagonal 1 (bottom left), and diagonal 2 (bottom right)

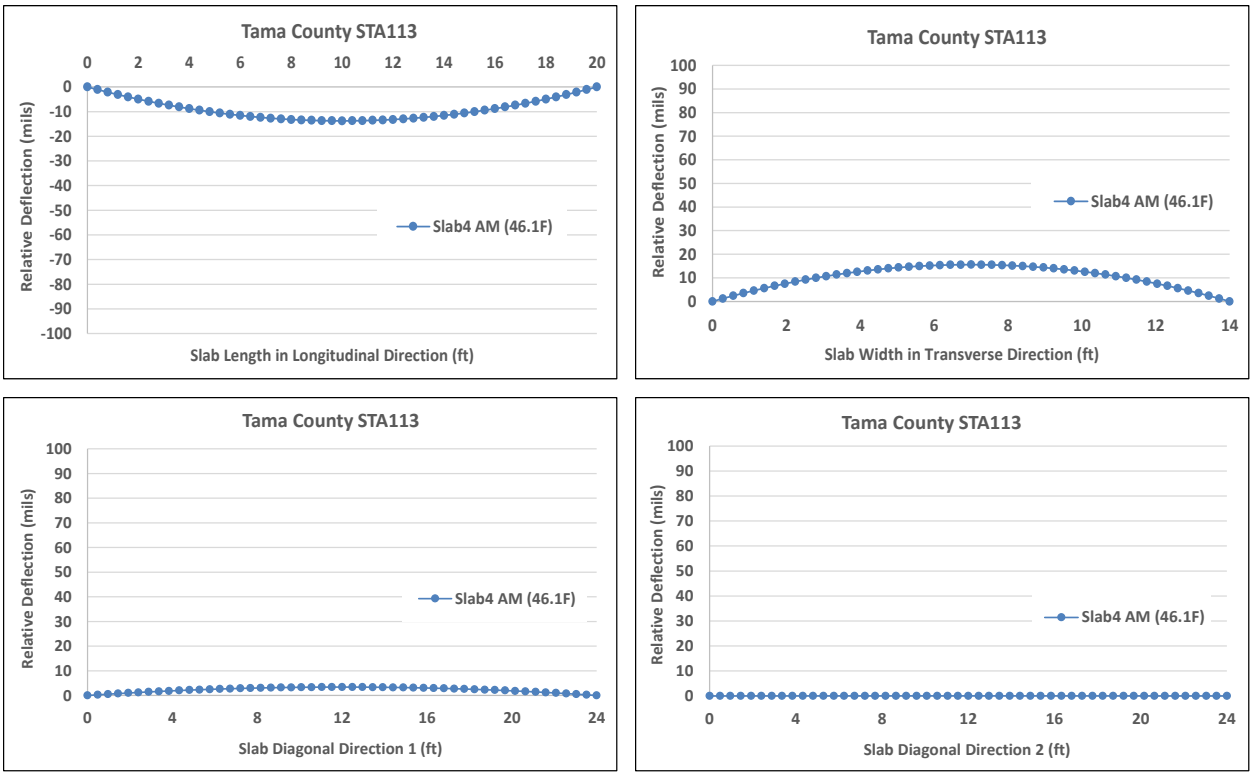

Figure 49. Morning relative deflection of Slab 4 at Site 6: longitudinal (top left), transverse (top right), diagonal 1 (bottom left), and diagonal 2 (bottom right)

In Figure 46 through Figure 49, it can be seen that all the slabs showed upward curling and warping along the longitudinal direction and showed downward curling and warping along the transverse and diagonal directions. The deflection shape of the entirety of Slab 1 can be seen in the 3D fitted slab surface, shown in Figure 50. More detailed discussions on 3D slab surfaces can be found in the following chapters.

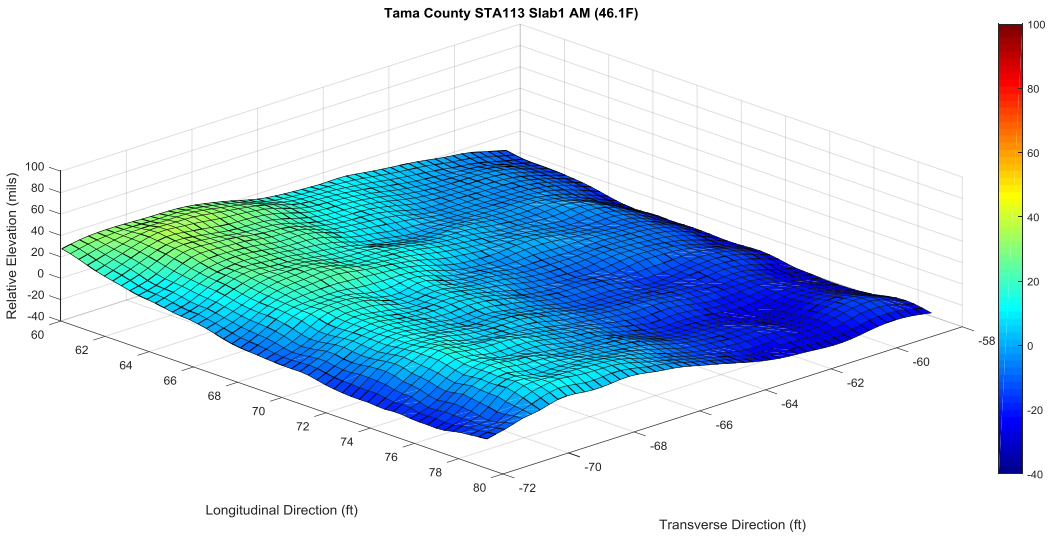

Figure 50. 3D simulation of Slab 1 at STA113 on US 30 near Toledo, Tama County

The key findings at this site are as follows:

- Along the longitudinal direction, the relative deflection is in the range of -13.8 to -5.9 mils.
- Along the transverse direction, the relative deflection is in the range of +11.6 to +22.7 mils.
- Along the diagonal directions, the relative deflection is in the range of +0. 04 to +15.5 mils.
- The transverse direction has the highest curling and warping.
- The difference in relative deflection between adjacent slabs is within 10 mils.
- The average temperature calculated for these slabs was 46.1°F in the morning.
- This site was also investigated in a previous study (Ceylan et al. 2007), and the degree of curling and warping at the early age of the pavement was found to be as follows:
  - Along the transverse direction, the measurements in the morning are in the range of -23 to -13 mils.
  - Along the transverse direction, the measurements in the afternoon are in the range of -9 to +7 mils.
  - Along the diagonal directions, the measurements in the morning are in the range of -42 to -14 mils.
  - Along the diagonal directions, the measurements in the afternoon are in the range of -2 to +7 mils.
  - In the morning, the negative temperature difference (surface temperature < bottom temperature) was in the range of -3.5 to -11°F.
  - In the afternoon, the positive temperature difference (surface temperature > bottom temperature) was in the range of +8.3 to +14 °F was observed.
  - The measured surface temperature was in the range of +97 to +120 °F.
  - The equivalent temperature difference was in the range of -8 to +12 °F.

In a previous study by Ceylan et al. (2007), the degree of curling and warping at this site was measured seven days after pavement construction. It was seen that this site originally showed upward curling and warping in the morning and then subsequently showed either a flat condition

or downward curling and warping in the afternoon when the surface temperature increased. However, the recent field investigation on November 10, 2015 showed that the slab shape was either flat or had some curvature, which is probably due to the following reasons:

- The degree of curling and warping at the early age of the pavement is in the range of -42 to -14 mils, which is relatively smaller than the typical value, which is in the range of 60 to 150 mils observed by other researchers (Jeong and Zollinger 2005, Lederle et al. 2001, Rao et al. 2001, Yu and Khazanovich 2001).
- Due to a relatively low degree of upward curling and warping at the early age of the pavement, the overall measured profile at the early age tended to be flat, which implied a relatively low degree of built-in curling during concrete set. Another possible reason is the effect of creep, which is produced by the stresses from the surrounding restraints and can counteract the effect of shrinkage deformation (upward warping)
- When the degree of upward curling and warping is low, the slab shape can easily reverse from an upward curvature to a downward curvature if the surface temperature of the slab is higher than the temperature at the bottom.

DISCUSSION

The impacts of curling and warping on JPCP performance are discussed in this chapter by comparing the average degree of measured curling and warping with the JPCP performance index records in *2014 Iowa DOT Test Sections by Milepost* (referred to as the Iowa DOT Milepost Book). Many factors identified in the literature review can affect curling and warping behavior. Among these factors, some can be controlled to mitigate the degree of curling and warping. These factors include PCC mix design–related variations, JPCP design-related features, and JPCP construction-related variations. The effects of these factors on curling and warping behavior are discussed in this chapter.

Impacts of Curling and Warping on JPCP Performance

Table 13 illustrates the average degree of curling and warping along the diagonal directions at each site.

Table 13. Comparison of pavement performance

Site No.	Site Information	Average Relative Deflection (mils) AM	Average Relative Deflection (mils) PM	IRI (in./mile)	PCI	Crack
Site 1	**US 30, Story County, MP 152.2, STA 1422, Eastbound**	-20.5	-21.5	N/A	N/A	
Site 2	**US 30, Story County, MP 158.95, STA 2207, Westbound**	-13.0	-13.5	92.5	83	
Site 3	**US 151, Linn County, MP 32.75, STA 162, Southbound**	-73.0	-70.7	130.5	73	Yes
Site 4	**US 151, Linn County, MP 33.15, STA 183, Southbound**	-68.8	-60.8	130.5	73	
Site 5	**US 30, Linn County, MP 261.2, STA 463, Westbound**	-33.2	-30.0	135.6	72	Yes
Site 6	**US 30, Tama County, MP 194.6, STA113, Eastbound**	+7.3	N/A	83.6	91	

"-" and "+" represent upward and downward curling and warping, respectively. N/A is not available.

In this table, the degree of curling and warping is represented by relative deflection. A positive value represents upward curling and warping, while a negative value represents downward curling and warping. Additionally, the IRI and Pavement Condition Index (PCI) from the 2014

Iowa DOT Milepost Book are also listed for the purposes of discussion. Based on Table 13, the key findings are as follows:

- Site 3 at STA162 of US 151 in Linn County and Site 4 at STA183 of US 151 in Linn County have the highest degree of upward curling and warping.

- Site 5 at STA 463 of US 30 in Linn County has a lower degree of upward curling and warping than Sites 3 and 4 but a higher degree than the other sites.

- Site 2 at STA1422 of US 30 and Site 1 at STA2207 of US 30 in Story County have the lowest degree of upward curling and warping. Site 6 at STA113 of US 30 in Tama County has the lowest degree of downward curling and warping.

- Lower PCI and higher IRI values were identified for Site 3, Site 4, and Site 5, and these sites showed relatively higher degrees of curling and warping than Site 2 and Site 6. Cracks were also observed at Site 3 and Site 5 during field investigations. These results indicate that the degree of curling and warping may influence overall JPCP performance.

Effects of PCC Mix Design–Related Variations on Curling and Warping

Table 14 compares PCC mix design information used at the investigated sites to see the effects of mix design on the degree of curling and warping.

Table 14. Comparison of mix design parameters

Site No.	Site Information	Coarse Agg. lbs/yd^3	Fine Agg. lbs/yd^3	Cement lbs/yd^3	Fly Ash lbs/yd^3	Water lbs/yd^3	w/cm
Site 1	**US 30, Story County, MP 152.2, STA 1422, Eastbound**	1,403	1,307	448	112	225	0.40
Site 2	**US 30, Story County, MP 158.95, STA 2207, Westbound**	1,653	1,446	457	114	250	0.44
Site 3	**US 151, Linn County, MP 32.75, STA 162, Southbound**	1,675	1,415	479	85	222	0.40
Site 4	**US 151, Linn County, MP 33.15, STA 183, Southbound**	1,673	1,424	479	85	236	0.42
Site 5	**US 30, Linn County, MP 261.2, STA 463, Westbound**	1,702	1,447	451	113	240	0.43
Site 6	**US 30, Tama County, MP 194.6, STA113, Eastbound**	1,539	1,272	448	112	224	0.40

Coarse aggregates used in Site 1 have an absorption of 1.1%; Coarse aggregates used in Site 2 have an absorption of 2.6%; Coarse aggregates used in Site 3 have an absorption of 2.6%; In Site 4, the absorption of coarse aggregates is from 4.5% to 9% depending on the specific gravity of the materials; Coarse aggregates used in Site 5 have an absorption of 2.6%; Coarse aggregates used in Site 6 have an absorption of 2.4%.

Higher amounts of cement along with lower amounts of fly ash were used at Site 3 at STA162 of US 151 and Site 4 at STA183 of US 151 in Linn County, both of which showed higher degrees of curling and warping.

Generally, the amounts of cementitious materials and their paste products are related to the hydration process and shrinkage. Using less cement and more SCMs such as fly ash can help reduce the potential for shrinkage (Rao and Roesler 2005a, Smiley and Hansen 2007). Lower degrees of curling and warping were observed at the sites in Story County and Tama County, where less cement and more fly ash was used.

However, no clear relation between the degree of curling and warping and the aggregate contents were observed. Note that aggregate properties related to shrinkage include absorption, gradation, and the coarseness of the aggregates (Taylor and Wang 2014).

Effects of JPCP Design-Related Features on Curling and Warping

Table 15 compares JPCP design features used at the investigated sites.

Table 15. Comparison of pavement design parameters

Site No.	Site Information	Slab Length	Slab Width	Slab Thickness	Slab Shape	Subbase Thickness / Type	Shoulder
Site 1	**US 30, Story County, MP 152.2, STA 1422, East**	20 ft	14 ft	10 in.	Rectangular	10 in./ Granular	HMA
Site 2	**US 30, Story County, MP 158.95, STA 2207, West**	20 ft	14 ft	10 in.	Skewed	10 in./ Granular	Granular
Site 3	**US 151, Linn County, MP 32.75, STA 162, South**	20 ft	14 ft	10 in.	Skewed	10.5 in./ Granular	Granular
Site 4	**US 151, Linn County, MP 33.15, STA 183, South**	20 ft	14 ft	10 in.	Skewed	8 in./ Granular	Granular
Site 5	**US 30, Linn County, MP 261.2, STA 463, West**	20 ft	14 ft	10 in.	Skewed	10.5 in./ Granular	Granular
Site 6	**US 30, Tama County, MP 194.6, STA113, East**	20 ft	14 ft	10 in.	Rectangular	10 in./ Granular	HMA

As seen in Table 15, all sites have similar slab lengths, widths, and thicknesses. However, it has been well recognized that thicker and shorter slabs usually exhibit less curling and warping (Cement Concrete & Aggregates Australia 2006, Rao and Roesler 2005a).

Two sites (Site 1 and Site 6) have rectangular slab shapes and HMA shoulders while the other sites have skewed slab shapes (Site 2, Site 3, Site 4, and Site 5) and granular shoulders. Among the four sites having skewed slab shapes and granular shoulders, threes sites (Site 3, Site 4, and Site 5) in Linn County showed relatively higher degrees of upward curling and warping and worse JPCP performance (in terms of IRI and PCI).

Limited studies have been conducted on the effect of skewed joints (or skewed slab shape) on PCC curling and warping. Through numerical analysis, Rasmussen et al. (2007) demonstrated that skewed joints effectively increase the slab dimensions and consequently result in higher

curling and warping stresses and deflections at the corners than in slabs with a rectangular shape. However, both HMA shoulders and granular shoulders are untied (or disconnected) shoulder types, which have low load transfer efficiency (LTE) values. Therefore, the higher degree of upward curling observed at three sites (Site 3, Site 4, and Site 5) in Linn County could be more related to slab shape than shoulder type.

Effects of JPCP Construction-Related Variations on Curling and Warping

Weather conditions and the time at which paving occurs during construction can influence curling and warping, especially at the early age. Table 16 compares the JPCP construction conditions at the investigated sites.

Table 16. Comparison of construction conditions

Site No.	Site Information	CY	Month	Time	Weather	Ambient Temp.	Other
Site 1	**US 30, Story County, MP 152.2, STA 1422, East**	2013	May	8 a.m.	Sunny	85°F	Chemical curing compound
Site 2	**US 30, Story County, MP 158.95, STA 2207, West**	1995	June	7 a.m.	Sunny	78°F	Chemical curing compound
Site 3	**US 151, Linn County, MP 32.75, STA 162, South**	1999	November	8 a.m.	Sunny	67°F	Cold weather protection was adopted during construction; a right-turn lane was added in 2015
Site 4	**US 151, Linn County, MP 33.15, STA 183, South**	1999	November	8 a.m.	Sunny	64°F	N/A
Site 5	**US 30, Linn County, MP 261.2, STA 463, West**	1999	May	8 a.m.	Sunny	78°F	N/A
Site 6	**US 30, Tama County, MP 194.6, STA113, East**	2005	July	3 p.m.	Sunny	90°F	Chemical curing compound

CY is construction year. N/A is not available.

Because ambient temperature may indicate overall weather conditions as well as the time of paving, the variations in ambient temperatures during the construction of the investigated sites are discussed below.

Ambient temperatures (ranging from 64°F to 78°F) during construction for Site 2 to Site 5 are not cases for hot or cold weather concreting. This indicates that ambient temperatures during

construction for these sites are not significant factors causing variations in the degrees of curling and warping among these sites.

Ambient temperatures of about 85°F to 90°F during construction at Site 1 and Site 6 may be within the temperature range that is likely to influence the degree of curling and warping at early ages. However, these sites were not seen to experience high degrees of curling and warping in this study. Plausible explanations for these behaviors are as follows:

- Site 1 experienced heavy rains one day after construction, which may have mitigated drying shrinkage at the early age and consequently led to lower degrees of curling and warping during its service life.

- Unlike other sites, Site 6 was constructed in the late afternoon (i.e., 3 p.m.) and hardened during the night with a low temperature gradient (less than 5°F between the top and bottom of the slab). Such a low temperature difference during the hardening period may result in a low degree of built-in upward curling, which could be recovered during the pavement's service life due to creep behaviors from the slab weight and dowel bar constraints, as addressed in a previous chapter. Although a low degree of built-in upward curling for this site would not cause overall JPCP performance issues, a high degree of built-in upward curling could lead to poor JPCP performance, as demonstrated through MEPDG analysis by Ceylan (2014) at a JPCP site on I-80 (see Figure 51).

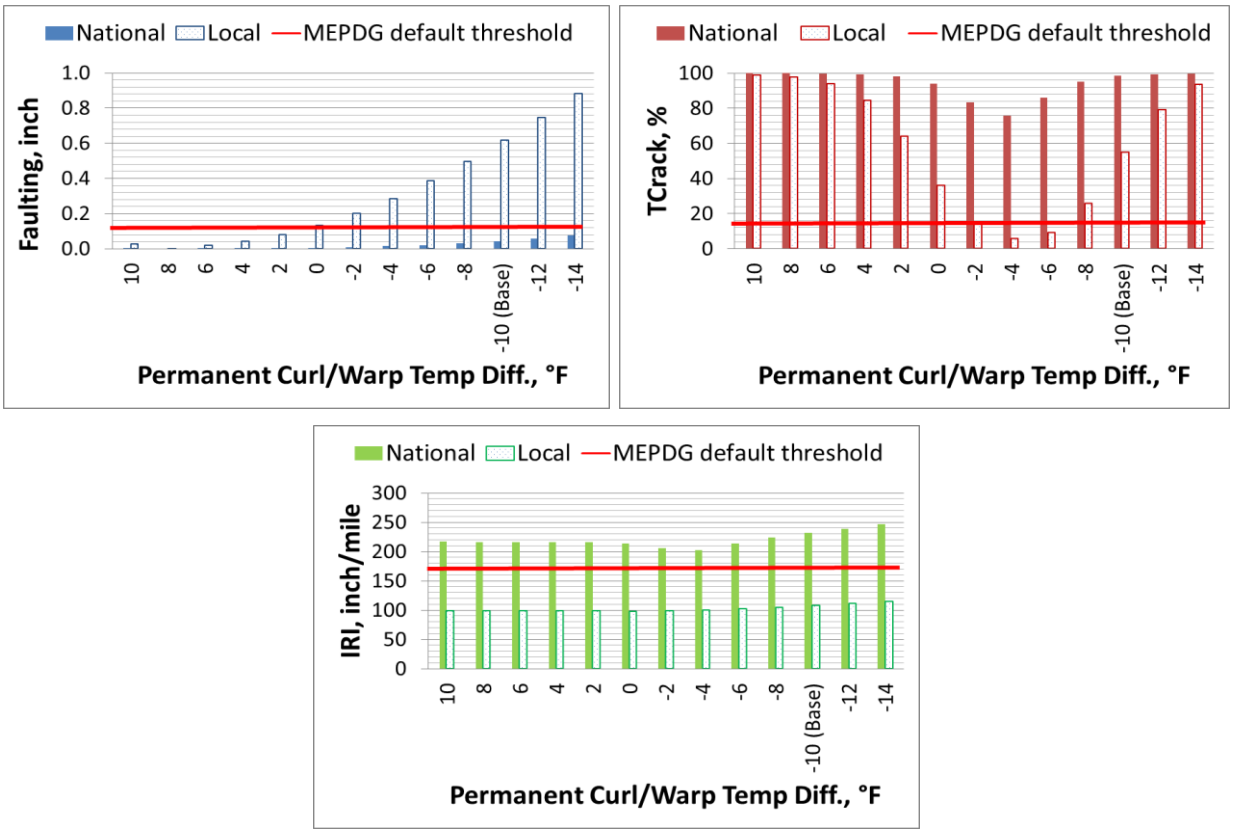

Ceylan 2014

Figure 51. Effect of permanent curling and warping temperature difference on MEPDG performance predictions for I-80 JPCP site: faulting (top left), transverse cracking (top right), and IRI (bottom)

FEASIBILITY STUDY ON 3D MODELING USING POINT CLOUD DATA

Conventional pavement profile measuring devices, such as a dipstick and walking profilometer, can only measure the profile along a certain path. However, a LiDAR device can provide the curvature shape for the entire slab. The following steps were undertaken for 3D modeling using the point cloud data set from the LiDAR device used in this study (Alhasan et al. 2015a, Alhasan et al. 2015b):

1. Eliminate the noise points from the original point cloud.
2. "Dig" the single slab out from the point cloud.
3. Import the point cloud of the slab into the graphing software package.
4. Check the shape of the point cloud in a top-view model and then select the reference point to calculate the rotation angle.
5. Develop the 2D rotation matrix to rotate the point cloud for further 3D modeling.
6. After rotation, calculate the center point of the point cloud for the development of a 3D rotation matrix.
7. Develop a series of 3D rotation matrices based on the calculated center point and rotation angle.
8. Reduce the sample size and then apply surface fitting.
9. Calculate the center of the fitted surface and then shift the whole point cloud vertically to make sure the elevation at the center is 0.
10. Develop another 3D rotation matrix to eliminate the crown for the slab.
11. Calibrate the elevation for all the points in the point cloud to calculate the relative elevation of each point with respect to the elevation of the center point.
12. Apply the surface fitting again for the calibrated point cloud to produce the finalized 3D-modeled surface.

Figure 52 and Figure 53 illustrate examples of slabs modeled in 3D.

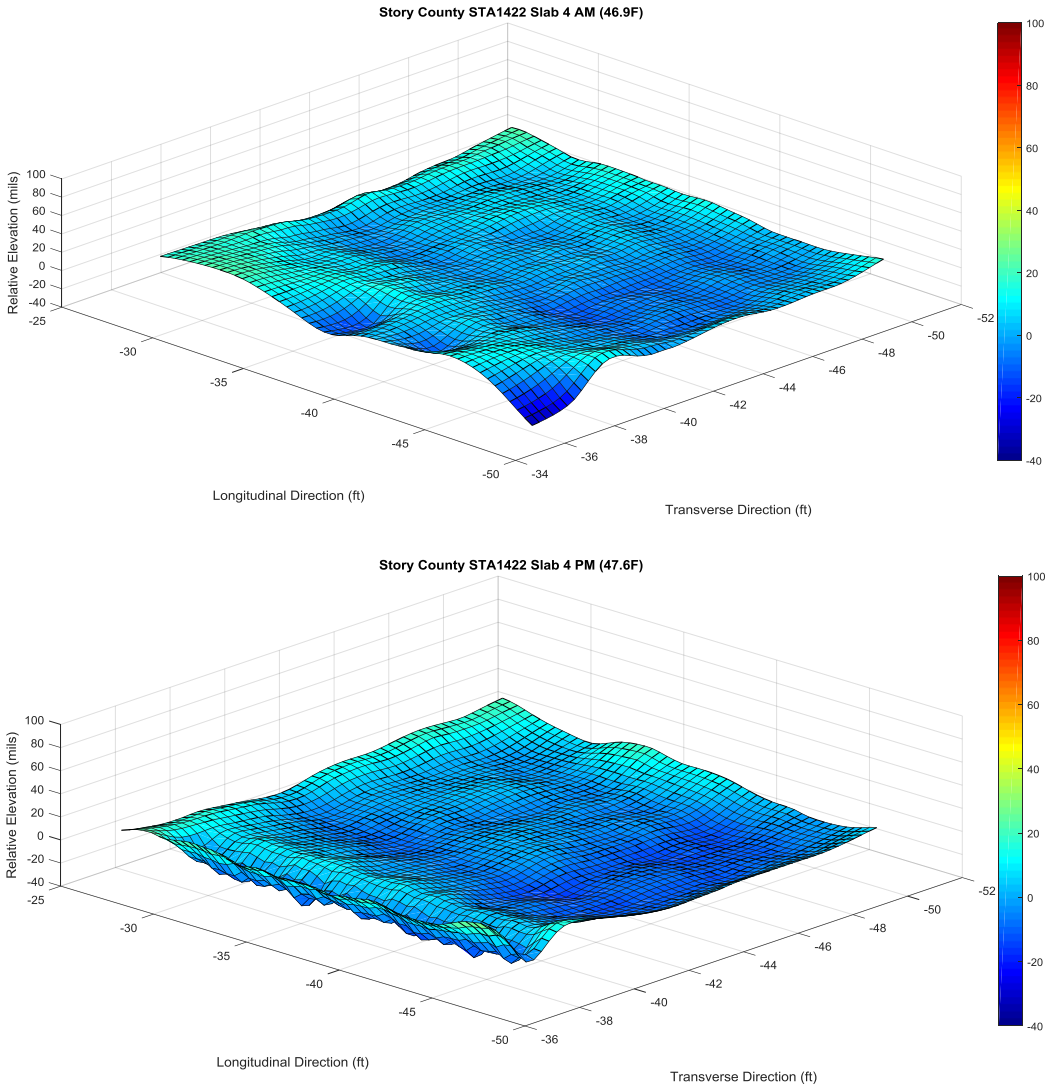

Figure 52. 3D modeling of Slab 4 at Site 1 in Story County at STA1422: slab in the morning (top) and slab in the afternoon (bottom)

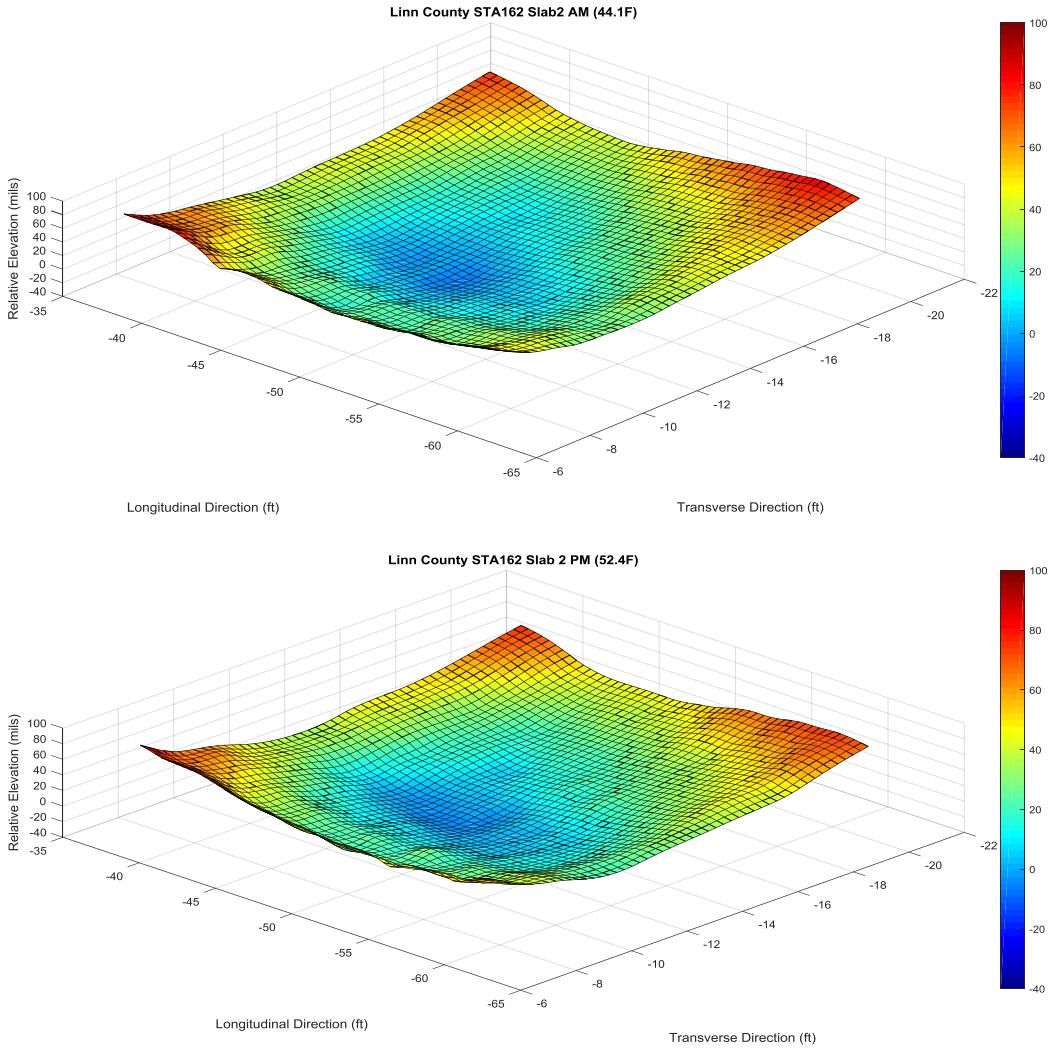

Figure 53. 3D modeling of Slab 2 at Site 3 in Linn County at STA162: slab in the morning (top) and slab in the afternoon (bottom)

The Slab 4 from Site 1 at STA1422 in Story County was selected for 3D modeling because of the relatively low degree of curling and warping observed at that site. Slab 2 from Site 3 at STA162 in Linn County was also used for 3D modeling because of the high degree of observed curling and warping. As an additional example, Slab 1 from Site 6 at STA113 in Tama County was also modeled (see Figure 50) because it showed downward curling and warping.

In Figure 52 and Figure 53, the slabs modeled from Site 1 and Site 3 show upward curling and warping. The vertical elevation was calculated as relative elevation with respect to the elevation of the center, which was shifted to be zero. Colors were assigned to the relative elevation values to show the contrast between elevations. The color distribution illustrates that the slab selected from Site 3 shows more upward curling and warping compared to the selected slab from Site 1.

The 3D modeling of the point cloud is able to provide a visualization of the overall curvature

shape of the slab. The advantages of using this 3D modeling method for curling and warping are as follows:

- The overall curvature shape of the slab is provided for curling and warping analysis. In contrast, the conventional method can just measure the slab profile along a certain line.
- The degree of curling and warping at a certain point, along a certain path, or within a certain area can be easily extracted.
- This method can provide good visualization so that the points that have the highest and lowest curling and warping can be easily found.
- The color distribution can show a direct comparison among different slabs.
- The same point cloud used for 3D modeling has the potential to be used for other applications as well, such as IRI, cross slopes, and crack detection (see Table 17).

Table 17. Research studies focusing on using LiDAR systems for pavement inspection

Research Study	LiDAR Device	Applications	Software
Chang et al. 2006	Mensi GS100	IRI	PointScape, RealWork
Johnson et al. 2010	Lecia ScanStation II	IRI	Lecia Cyclone
Olson and Chin 2012	Riegl VZ-400 3D	Cross slopes, IRI	ProVAL
Tsai and Li 2012	HD 3D laser profiler	Crack detection	N/A
Alhasan et al. 2015a	Trimble CX 3D STLS	Roughness	MATLAB

CONCLUSIONS AND RECOMMENDATIONS

Conclusions

The primary objectives of this study were to investigate the curling and warping behavior of existing PCC pavements and to provide suggestions for mitigating curling and warping. In order to investigate the curling and warping behavior of the slabs in existing PCC pavements, field investigations were performed on PCC pavements at six sites with various ages, slab shapes, shoulders, concrete mix designs, paving seasons and times, and weather conditions during construction. A LiDAR device was used to measure the surface profile of the identified slabs, and the deflections along the longitudinal, transverse, and diagonal directions were calculated based on the point cloud data obtained by the LiDAR device. The conclusions from this project are summarized below.

Conclusions from the Literature Review

- Curling and warping can influence PCC pavement performance. The factors that can impact curling and warping behavior include slab temperature and moisture gradients, shrinkage, built-in curling, creep, slab geometry, concrete materials and mix characteristics, the type of underlying layers, and on-site weather conditions.
- The mitigation strategies for PCC curling and warping can broadly be categorized into material selection, mix design, pavement design, and construction practices.
- Material selection can have a significant influence on curling and warping. The use of coarse aggregates with a larger maximum aggregate size, higher specific gravity, lower CTE, and lower water absorption is desired. The use of fine aggregates with coarser particles and lower water absorption is also desired. Moreover, cement with lower C_3A (a tricalcium aluminate) and alkali content can help reduce warping. Use of SCMs such as fly ash can help reduce curling and warping as well.
- Concrete mix design containing more coarse aggregates and less paste can result in less warping of PCC slabs. Additionally, a moderate w/cm ratio is desired, because a higher w/cm ratio can lead to higher drying shrinkage, while a lower w/cm ratio can lead to higher autogenous shrinkage.
- Pavement design can have an influence on curling and warping. Thicker and shorter slabs result in a lower degree of curling and warping. Concrete slabs with a typical joint spacing of 20 ft in Iowa suffer from relatively higher levels of curling and warping stresses compared to slabs with 15 ft or shorter joint spacing in other parts of the country.
- A soft underlying base course results in less curling, while a base with good drainage result in less warping. However, repeated traffic loading may induce more tensile stresses in a soft base course.
- Construction of PCC pavements at relatively higher ambient temperatures, in lower ambient RH conditions, or in higher winds can result in higher curling and warping. Construction during the latter half of the day or at nighttime helps reduce the duration of time the fresh concrete is exposed to strong solar radiation, which thereby reduces the degree of built-in curling and warping.

- The upward curvature (most noticeable at PCC slab corners) can be up to 1 in. (2.5 cm). Suprenant and Malisch (1999) indicate that when the amount of curling is less than 0.25 in., cracking is usually not so excessive as to disqualify a PCC slab.

Conclusions from the Field Investigations

- The three sites (Site 3, Site 4, and Site 5) in Linn County show a higher degree of upward curling and warping than the two sites (Site 1 and Site 2) in Story County. Site 6 in Tama County shows a low degree of downward curling and warping.
- The degree of curling and warping may influence the overall performance of JPCP. The sites with higher degrees of observed curling and warping (Site 3, Site 4, and Site 5) also have lower PCI and higher IRI values. Meanwhile, Site 2 and Site 6, which have lower degrees of observed curling and warping, have higher PCI and lower IRI values.
- Cracks were observed at the sites having both a high degree of curling and warping and higher traffic volumes (Site 3 and Site 5). This could be attributed to the combined effect of environmental and traffic loads, because the tensile stresses induced by a high degree of curling and warping can be magnified when combined with high traffic loads.
- A high degree of built-in curling may result in a higher degree of curling and warping over the service life of a JPCP and consequently may lead to poor performance.
- The PCC pavements at the sites showing higher degrees of curling and warping (Sites 3 and 4) were found to have more cement and less fly ash. Correspondingly, the PCC pavements at the sites showing lower degrees of curling and warping (Site 1, Site 2, and Site 6) were found to have less cement and more fly ash.
- In concrete mix design, the amounts of cement and fly ash are significant factors for minimizing warping. This is because the amounts of cementitious materials and their paste products are directly related to the hydration process and shrinkage.
- Slab shape (i.e., rectangular or skewed) can also affect the degree of curling and warping. Among four sites having skewed slab shapes, three sites (Site 3, Site 4, and Site 5) in Linn County showed a higher degree of upward curling and warping and worse JPCP performance. The skewed joints effectively increase the slab dimensions and consequently result in higher curling and warping stresses and deflections at the corners than in slabs with a rectangular shape (Rasmussen et al. 2007).
- The time at which paving occurs and weather conditions during the paving and curing periods influence curling and warping at the early age.
- Construction during the latter half of the day helps reduce the amount of time that the fresh concrete is exposed to strong solar radiation, which consequently reduces built-in curling. A low degree of built-in curling may be recovered during the service life of the pavement due to creep behavior from the slab weight and the dowel bar constraints. The findings from Site 6 (US 30 in Tama County) are indicative of such behavior.
- Subsequent wetting cycles after pavement construction can help reduce warping. Site 1 had a higher ambient temperature (85°F) during paving but showed a relatively lower degree of curling and warping. This may be because of the heavy rains that occurred just one day after construction at Site 1, which might have mitigated early-age drying shrinkage and consequently led to a lower degree of curling and warping during its service life.

Recommendations

Based on the study findings, the following are the highlighted recommendations for further research:

- Further research is needed to validate the preliminary findings of this study by utilizing a larger number of concrete pavement systems from Iowa highways and county and city roads to determine which factors (through a sensitivity study) have the most influence on the curling and warping behavior of PCC pavements and how pavement design engineers and contractors can minimize the degree of curling and warping to extend the service life of Iowa PCC pavement systems. The PCC pavements investigated in this study were mainly selected from Iowa highways, whose pavement design features are different from those of Iowa county and city roads (which, for example, have thinner PCC slabs). Note that thicker and shorter PCC slabs can result in a relatively lower degree of curling and warping. In addition, the number of PCC pavements selected and the relevant data collected were not sufficient for validating the recommendations derived from the literature review. For example, the curling and warping literature suggests that water absorption of coarse aggregate is a significant mix design variable affecting the degree/magnitude of warping, but little reported information exists on the water absorption properties of the coarse aggregate used in Iowa PCC pavements that can validate this literature review finding. Therefore, a more comprehensive follow-up study on the impact of curling and warping on Iowa concrete pavement is recommended.
- The current 3D modeling algorithm described in this study is a semi-automated process. Further research and improvements are needed to fully automate the algorithm to process the data more quickly.
- It is recommended that other beneficial applications of LiDAR related to pavement inspection, such as pavement roughness, cross slope, and crack detection, be investigated.
- Further research is needed to investigate the feasibility of using LiDAR devices for built-in curling measurement.
- It is recommended that other LiDAR platforms, such as airborne laser scanners and mobile laser scanners, be investigated for pavement inspection in the future.
- It is recommended that the pavement surface be scanned by a LiDAR device after concrete placement to obtain the initial point cloud. This “original” point cloud can be used to calculate the true degree of curling and warping in the future and help align subsequent scans to the initial scan. This practice could eliminate the necessity for 3D rotation matrices in the 3D modeling method, which tend to reduce the prediction accuracy because the reference coordinates are hypothetical.

REFERENCES

AASHTO. 2008. *Mechanistic-Empirical Pavement Design Guide: A Manual of Practice*. American Association of State Highway and Transportation Officials, Washington, DC.

AASHTO. 2013. AASHTOWare Pavement ME Design. American Association of State Highway and Transportation Officials, Washington, DC. www.me-design.com/MEDesign/Index.html. Last accessed December 30, 2015.

Ahmed, I., M. H. Rahman, S. M. Seraj, and A. M. Hoque. 1998. Performance of plain concrete runway pavement. *ASCE Journal of performance of constructed facilities*, 12(3): 145–152.

Alhasan, A., D. J. White, and K. De Brabanter. 2015a. Spatial pavement roughness from stationary laser scanning. *International Journal of Pavement Engineering*: 1–14.

Alhasan, A., D. White, and K. De Brabanter 2015b. Quantifying Unpaved Road Roughness from Terrestrial Laser Scanning. *Transportation Research Record: Journal of the Transportation Research Board* 2523: 105–114.

Aitcin, P. C., and P. K. Mehta. 1990. Effect of coarse aggregate characteristics on mechanical properties of high-strength concrete. *Materials Journal* 87(2): 103–107.

Al-Nasra, M., and L. R. Wang. 1994. Parametric study of slab-on-grade problems due to initial warping and point loads. *ACI Structural Journal* 91(2): 198–210.

Altoubat, S. 2010. Early age creep and shrinkage of concrete with Shrinkage Reducing Admixtures (SRA). *Jordan Journal of Civil Engineering* 4(3): 281–291.

Altoubat, S. A., and D. A. Lange. 2001. Creep, shrinkage, and cracking of restrained concrete at early age. *ACI Materials Journal* 98(4): 323–331.

ARA, Inc. 2004. *Guide for Mechanistic-Empirical Design of New and Rehabilitated Pavement Structures*. Draft Final Report, NCHRP Project 1-37A. Transportation Research Board, National Research Council, Washington, DC.

Asbahan, R. E. 2009. Effects of the built-in construction gradient and environmental conditions on jointed plain concrete pavements. PhD dissertation, University of Pittsburgh, PA.

Babaei, K., and R. L. Purvis. 1995. *Prevention of Cracks in Concrete Bridge Decks: Report on Laboratory Investigation of Concrete Shrinkage*. Report PA-FHWA-95-004+89-01. Pennsylvania Department of Transportation, Harrisburg, PA.

Bradbury, R. D. 1938. *Reinforced Concrete Pavements*. Wire Reinforcement Institute, Washington, DC.

Bazant, Z. 1988. *Mathematical Modeling of Creep and Shrinkage of Concrete*. John Wiley & Sons Ltd., New York, NY.

Bazant, Z. P. 2001. Prediction of concrete creep and shrinkage: past, present and future. *Nuclear Engineering and Design* 203(1):27–38.

Bazant, Z. P., G. Cusatis, and L. Cedolin. 2004. Temperature effect on concrete creep modeled by microprestress-solidification theory. *ASCE Journal of Engineering Mechanics*, 130(6): 691–699.

Bazant, Z. P., and S. T. Wu. 1974. Creep and shrinkage law for concrete at variable humidity. *ASCE Journal of the Engineering Mechanics Division*, 100(6): 1183–1209.

Bissonnette, B., E. K. Attiogbe, M. A. Miltenberger, and C. Fortin. 2007. Drying shrinkage, curling, and joint opening of slabs-on-ground. *ACI Materials Journal* 104(3): 259–267.

Burrows, R. D. 1998. *The Visible and Invisible Cracking of Concrete*. American Concrete Institute Monograph No. 11. MI. American Concrete Institute, Farmington Hills, MI.

Caltrans. 2011. Chapter 15: Terrestrial laser scanning specification. *Caltrans Surveys Manual*. California Department of Transportation, Sacramento, CA. www.dot.ca.gov/hq/row/landsurveys/SurveysManual/15_Surveys.pdf. Last accessed January 2, 2016.

Carlson, R. W. 1938. Drying shrinkage of concrete as affected by many factors. *Proc., of the American Society for Testing and Materials, ASTM,* Vol. 38, Part. II: 419–440.

Cement Concrete & Aggregates Australia. 2002. *Drying Shrinkage of Cement and Concrete*. www.boral.com.au/brochures/ordering/PDF/DS2002DryingShrinkage.pdf?pdfName=DS2002DryingShrinkage.pdf. Last Accessed July 7, 2016.

Cement Concrete & Aggregates 2006. *Curling of Concrete Slabs*. 59.167.233.142/publications/pdf/Curling.pdfAustralia. Last accessed July 7, 2016.

Ceylan, H., S. Kim, K. Gopalakrishnan, and K. Wang. 2007. Environmental effects on deformation and smoothness behavior of early age jointed plain concrete pavements. *Transportation Research Record: Journal of the Transportation Research Board* 2037: 30–39.

Ceylan, H., K. Gopalakrishnan, S. Kim, C. W. Schwartz, and R. Li. 2013. Global sensitivity analysis of jointed plain concrete pavement mechanistic–empirical performance predictions. *Transportation Research Record: Journal of the Transportation Research Board* 2367: 113–122.

Ceylan, H. 2014. Performance evaluation of a jointed plain concrete pavement using mechanistic-empirical pavement design guide: A case study. Paper presented at the 93rd annual meeting of the Transportation Research Board, Washington, DC.

Ceylan, H., R. F. Steffes, K. Gopalakrishnan, S. Kim, S. Yang, and K. Zhuang. 2016. *Development and Evaluation of a Portable Device for Measuring Curling and Warping in Concrete Pavements*. Institute for Transportation, Iowa State University, Ames, IA.

Chang, G. K., S. M. Karamihas, R. O. Rasmussen, D. Merritt, and M. Swanlund. 2008. Quantifying the impact of jointed concrete pavement curling and warping on pavement unevenness. Paper presented at the 6th symposium on pavement surface characteristics (SURF), Potoroz, Slovenia.

Chang, J., K. Chang, and D. Chen. 2006. Application of 3D laser scanning on measuring pavement roughness. *Journal of Testing and Evaluation* 34 (2): 83–91.

Channakeshava, C., F. Barzegar, and G. Z. Voyiadjis. 1993. Nonlinear FE analysis of plain concrete pavements with doweled joints. *ASCE Journal of Transportation Engineering,* 119(5): 763–781.

Childs, L. D. and J. W. Kapernick. 1958. Tests of Concrete pavements on gravel subbases. *ASCE Journal of Highway Division,* 84, HW3.

Choubane, B., and M. Tia. 1992. Nonlinear temperature gradient effect on maximum warping stresses in rigid pavements. *Transportation Research Record: Journal of the Transportation Research Board* 1370: 14–24.

Choubane, B., and M. Tia. 1995. Analysis and verification of thermal-gradient effects on concrete pavement. *ASCE Journal of Transportation Engineering,* 121(1): 75–81.

Chung, Y. 2012. Thermal stress analysis of jointed plain concrete pavements containing fly ash and slag. PhD dissertation, Louisiana State University, LA.

Chung, Y., and A. H. C. Shin. 2015. Local calibration of EICM using measured temperature gradients and numerical analysis. *International Journal of Pavement Research and Technology* 8(4): 259–266.

Darter, M. I., and E. J. Barenberg. 1977. *Design of Zero-Maintenance Plain Jointed Concrete Pavement, Volume 1: Development of Design Procedures.* Report FHWA-RD-77-111. Federal Highway Administration, Washington, DC.

Davids, W. G. 2001. 3D finite element study on load transfer at doweled joints in flat and curled rigid pavements. *ASCE International Journal of Geomechanics,* 1(3): 309–323.

Dere, Y., A. Asgari, E. D. Sotelino, and G. C. Archer. 2006. Failure prediction of skewed jointed plain concrete pavements using 3D FE analysis. *Engineering Failure Analysis* 13(6): 898–913.

Eisenmann, J., and G. Leykauf. 1990. Effect of paving temperatures on pavement performance. Paper presented at the 2nd International Workshop on Theoretical Design of Concrete Pavements, Spain.

FDOT. 2012. *Terrestrial Mobile LiDAR Surveying & Mapping Guidelines*. Florida Department of Transportation, Tallahassee, FL. www.dot.state.fl.us/surveyingandmapping/documentsandpubs/20120823_TML_Guidelines.pdf. Last accessed December 30, 2015.

Franta, D. P. 2012. Computational analysis of rigid pavement profiles. PhD dissertation, University of Minnesota, MN.

Grasley, Z. C., A. D. Lange, and M. D. D'Ambrosia. 2006. Internal relative humidity and drying stress gradients in concrete. *Materials and Structures* 39(9): 901–909.

Hajibabaee, A., and M. T. Ley. 2015. The impact of wet curing on curling in concrete caused by drying shrinkage. *Materials and Structures*: 1–11.

Hall, K., and S. Tayabji. 2011. *Coefficient of Thermal Expansion in Concrete Pavement Design*. The Advanced Concrete Pavement Technology (ACPT) Products Program, Office of Pavement Technology, Federal Highway Administration. www.fhwa.dot.gov/pavement/concrete/pubs/hif09015/hif09015.pdf. Last Accessed May 22, 2016.

Hansen, W., and Y. Wei. 2008. *PCC Pavement Acceptance Criteria for New Construction When Built-In Curling Exists*. Research Report RC-1481. Michigan Department of Transportation, Lansing, MI.

Hansen, W., Y. Wei, D. L. Smiley, Y. Peng, and E. A. Jensen. 2006. Effects of paving conditions on built-in curling and pavement performance. *International Journal of Pavement Engineering* 7(4): 291–296.

Hansen, W., Y. Wei, abd E. Schlangen. 2008. Moisture warping in jointed plain concrete pavements. Paper presented at the 9th International Conference on Concrete Pavements, San Francisco, CA.

Harik, I. E., P. Jianping, H. Southgate, and D. Allen. 1994. Temperature effects on rigid pavements. *ASCE Journal of Transportation Engineering,* 120 (1): 127–143.

Harr, M. E. 1958. Warping stresses and deflections in concrete slabs. Thesis, Purdue University.

Hatt, W. K. 1925. The effect of moisture on concrete. *ASCE Transactions of the American Society of Civil Engineers* 89(1): 270-307.

Hiller, J. E., and J. R. Roesler. 2005. Determination of critical concrete pavement fatigue damage locations using influence lines. *ASCE Journal of Transportation Engineering,* 131(8): 599–607.

Holt, E., and M. Leivo. 2004. Cracking risks associated with early age shrinkage. *Cement and Concrete Composites* 26(5): 521–530.

Huang, Y. H. 2004. *Pavement Analysis and Design*. 2nd Edition. Pearson Education, Inc., New Jersey.

Hudson, W. R., and P. R. Flanagan. 1987. An examination of environmental versus load effects on pavements. *Transportation Research Record: Journal of the Transportation Research Board* 1121: 34–39.

Hveem, F. N. 1949. *A Report of an Investigation to Determine Causes for Displacement and Faulting at the Joints in Portland Cement Concrete Pavements on California Highways*. California Division of Highways, Sacramento, CA.

Iowa Department of Transportation. 2014. *2014 Test Sections by Milepost Book.* www.iowadot.gov/Construction_Materials/investigations/milepost.html. Last Accessed May 28, 2016.

Janssen, D. J., and M. B. Snyder. 2000. Temperature-moment concept for evaluating pavement temperature data. *ASCE Journal of Infrastructure Systems* 6(2): 81–83.

Jeong, J. H., and D. G. Zollinger. 2005. Environmental effects on the behavior of jointed plain concrete. *ASCE Journal of Transportation Engineering*, 131(2): 140–148.

Johnson, A. M., B. C. Smith, W. H. Johnson, and L. W. Gibson. 2010. *Evaluating the Effect of Slab Curling on IRI for South Carolina Concrete Pavements*. South Carolina Department of Transportation, Columbia, SC, and Federal Highway Administration. ntl.bts.gov/lib/46000/46200/46247/SPR_688.pdf.

Kim, S., H. Ceylan, and K. Gopalakrishnan. 2007. Initial smoothness of concrete pavements under environmental loads. *Magazine of Concrete Research* 59(8): 599–609.

Kim, S., H. Ceylan, and K. Gopalakrishnan. 2008. Smoothness variations of early-age jointed plain concrete pavements. *Canadian Journal of Civil Engineering* 35(12): 1388–1398.

Kim, S., K. Gopalakrishnan, H. Ceylan, and K. Wang. 2010. Early-age response of concrete pavements to temperature and moisture variations. *The Baltic Journal of Road and Bridge Engineering* 5(3): 132–138.

Kim, S., K. Gopalakrishnan, and H. Ceylan. 2011. A simplified approach for predicting early-age concrete pavement deformation. *Journal of Civil Engineering and Management* 17(1): 27–35.

Kosmatka, S. H., B. Kerkhoff, and W. C. Panarese. 2002. *Design and control of concrete mixtures*. 14th Edition. Portland Cement Association, Skokie, IL.

Kovler, K. 1999. A new look at the problem of drying creep of concrete under tension. *ASCE Journal of Materials in Civil Engineering*, 11(1): 84–87.

Kuo, C. M. 1991. The effects of temperature loading on the rigid pavement slabs. Thesis, National Cheng Kung University, Taiwan.

Kuo, C., K. Hall, and M. Darter. 1996. Three-dimensional finite element model for analysis of concrete pavement support. *Transportation Research Record: Journal of the Transportation Research Board* 1505: 119–127.

Kuo, C. M. 1998. Effective temperature differential in concrete pavements. *ASCE Journal of Transportation Engineering*, 124(2): 112–116.

Lafarge North America. *Concrete Slab Curling*. www.lafarge-na.com/wps/portal/na/en/3_A_11_5-Curling_of_Concrete_Slabs. Last accessed March 3, 2016.

Lederle, R. E., R. W. Lothschutz, and J. E. Hiller. 2011. *Field Evaluation of Built-In Curling Levels in Rigid Pavements*. Report MN/RC 2011-16. Minnesota Department of Transportation, St. Paul, MN.

Lee, Y. H., and M. I. Darter. 1994a. Loading and curling stress models for concrete pavement design. *Transportation Research Record: Journal of the Transportation Research Board* 1449: 101–113.

Lee, Y. H., and M. I. Darter. 1994b. New predictive modeling techniques for pavements. *Transportation Research Record: Journal of the Transportation Research Board* 1449: 234–245.

Lee, Y. H. 1999. TKUPAV: stress analysis and thickness design program for rigid pavements. *ASCE Journal of Transportation Engineering,* 125(4): 338–346.

Leonards, G. A., and M. E. Harr. 1959. Analysis of concrete slabs on ground. *ASCE Journal of the Soil Mechanics and Foundations Division,* 85(3): 35–58.

Liang, R. Y., and Y. Z. Niu. 1998. Temperature and curling stress in concrete pavements: analytical solutions. *ASCE Journal of Transportation Engineering,* 124(1): 91–100.

Lim, S., and S. D. Tayabji. 2005. Analytical technique to mitigate early-age longitudinal cracking in jointed concrete pavements. Paper presented at the 8th International Conference on Concrete Pavements, Colorado Springs, CO.

Mahboub, K. C., Y. Liu, and D. L. Allen. 2004. Evaluation of temperature responses in concrete pavement. *ASCE Journal of Transportation Engineering,* 130(3): 395–401.

Masad, E., R. Taha, and B. Muhunthan (1996). Finite-element analysis of temperature effects on plain-jointed concrete pavements. *ASCE Journal of Transportation Engineering,* 122(5): 388–398.

McCracken, J. K. 2008. Seasonal analysis of the response of jointed plain concrete pavements to FWD and truck loads. Thesis, University of Pittsburgh, PA.

McCracken, J. K., Asbahan, R. E., and J. M. Vandenbossche. 2008. *S.R.-22 Smart Pavement: Response Characteristics of a Jointed Plain Concrete Pavement to Applied and Environmental Loads – Phase II Final Report*. Report FHWA-PA-2008-007-22021-2B-013. University of Pittsburgh, Pittsburgh, PA.

Mehta, P. K. 1986. *Concrete: Structure, Properties and Materials*. 1st Edition. Prentice Hall, NJ.

Merritt, D. K., G. K. Chang, H. N. Torres, K. Mohanraj, and R. O. Rasmussen. 2015. *Evaluating the Effects of Concrete Pavement Curling and Warping on Ride Quality*. Report CDOT-2015-07. Colorado Department of Transportation, Denver, CO.

Mindess, S., J. F. Young, and D. Darwin. 2003. *Concrete*. 2nd Edition. Pearson Education, Inc., NJ.

Nantung, T. E. 2011. *High Performance Concrete Pavement in Indiana*. Report FHWA/IN/JTRP-2011/20. Indiana Department of Transportation, Division of Research and Development, West Lafayette, IN.

Nassiri, S. 2011. Establishing permanent curl/warp temperature gradient in jointed plain concrete pavements. PhD dissertation, University of Pittsburgh, PA.

Olson, M. J., and A. Chin. 2012. *Inertial and Inclinometer Based Profiler Repeatability and Accuracy Using the IRI Model*. Report SPR 744. Oregon Department of Transportation Research Section and Federal Highway Administration, Washington, DC.

Park, J. Y., W. S. Yeom, S. H. Kim, and J. H. Jeong. 2015. Environmental load for design of airport concrete pavements. *Institution of Civil Engineers-Transport* 168(2): 139–149.

Perenchio, W. F. 1997. The drying shrinkage dilemma. *Concrete* Construction 42: 379–383.

Powers, T. C. 1959. Causes and control of volume change. *Journal of the PCA Research and Development Laboratories* 1(1): 29–39.

Powers, T. C., L. E. Copeland, and H. M. Mann. 1959. Capillary continuity of discontinuity in cement paste. *Portland Cement Association R & D Laboratories Bull. No*. 110: 2–12.
Rao, C., E. J. Barenberg, and M. B. Snyder. 2001. Effects of temperature and moisture on the response of jointed concrete pavements. Paper presented at the 7th International Conference on Concrete Pavements, Orlando, FL.
Rao, S., and J. R. Roesler. 2005a. *Characterization of Effective Built-in Curling and Concrete Pavement Cracking on the Palmdale Test Sections*. University of Illinois at Urbana-Champaign, Urbana, IL.
Rao, S., and J. R. Roesler. 2005b. Characterizing effective built in curling from concrete pavement field measurements. *ASCE Journal of Transportation Engineering*, 131 (4): 320–327.
Rasmussen, R. O., A. Agosto, and S. Cramer. 2007. *Analysis of Concrete Pavement Joints to Predict the Onset of Distress*. The Transtec Group, Inc., Austin, TX.
Rivero-Vallejo, F., and B. F. McCullough. 1976. *Drying shrinkage and temperature drop stresses in jointed reinforced concrete pavement*. Report CFHR 3-8-75-177-1. Texas State Department of Highways and Public Transportation, Austin, TX.
Schindler, A. K., and F. B. McCullough. 2002. Importance of concrete temperature control during concrete pavement construction in hot weather conditions. *Transportation Research Record: Journal of the Transportation Research Board* 1813: 3–10.
Schmitt, T. R., and D. Darwin. 1999. Effect of material properties on cracking in bridge decks. *ASCE Journal of Bridge Engineering*, 4(1): 8–13.
Schwartz, C. W., R. Li, S. Kim, H. Ceylan, and K. Gopalakrishnan. 2011. *Sensitivity Evaluation of MEPDG Performance Prediction*. Contractor's Final Report of NCHRP 1-47 project. University of Maryland and Iowa State University, College Park, MD, and Ames, IA.
Shadravan, S., C. Ramseyer, and T. H. K. Kang. 2015. A long-term restrained shrinkage study of concrete slabs on ground. *Engineering Structures* 102: 258-265.
Siddique, Z., and M. Hossain. 2005. Finite element analysis of PCCP curling and roughness. Paper presented at the 8th International Conference on Concrete Pavements, Colorado Springs, CO.
Smiley, D., and W. Hansen. 2007. *Investigation of Early Cracking on Selected JPCP Projects*. Report RC-1501. Michigan Department of Transportation, Lansing, MI.
Smith, K. D., D. G. Peshkin, A. L. Mueller, E. Owusu-Antwi, and M. I. Darter. 1991. *Evaluation of Concrete Pavements in the Phoenix Urban Corridor, Volume 1: Final Report*. Report FHWA-AZ91-264-II. Federal Highway Administration, Washington, DC.
Suprenant, B. A. 2002. Why slabs curl. *Construction International* 24(3): 57–61.
Suprenant, B. A., and W. R. Malisch. 1999. Repairing curled slabs. *Concrete Construction* 9: 58–65.
Taylor, P., and X. Wang. 2014. *Concrete Pavement Mixture Design and Analysis (MDA): Factors Influencing Drying Shrinkage*. National Concrete Pavement Technology Center, Ames, IA.
Teller, L. W., and E. C. Sutherland. 1935. The structural design of concrete pavements, part 2: Observed effects of variations in temperature and moisture on the size, shape, and stress resistance of concrete pavement slabs. *Public Roads* 16(9): 169–197.
Thomlinson, J. 1940a. Temperature variations and consequence stress produced by daily and seasonal temperature cycles in concrete slabs. *Concrete Constructional Engineering* 36(6): 298–307.

Thomlinson, J. 1940b. Temperature variations and consequence stress produced by daily and seasonal temperature cycles in concrete slabs. *Concrete Constructional Engineering* 36(7): 352–360.

Tsai, Y. C. J., and F. Li. 2012. Critical assessment of detecting asphalt pavement cracks under different lighting and low intensity contrast conditions using emerging 3D laser technology. *ASCE Journal of Transportation Engineering*, 138 (5): 649–656.

Vandenbossche, J. M. 2003. *Interpreting Falling Weight Deflectometer Results for Curled and Warped Portland Cement Concrete Pavements*. University of Minnesota, St. Paul, MN.

Vandenbossche, J. M., F. Mu., J. J. Gutierrez., and J. Sherwood. 2010. An evaluation of the built-in temperature difference input parameter in the jointed plain concrete pavement cracking model of the Mechanistic–Empirical Pavement Design Guide. *International Journal of Pavement Engineering* 12(3): 215–228.

Wei, Y., and W. Hansen. 2011. Characterization of moisture transport and its effect on deformations in jointed plain concrete pavement. *Transportation Research Record: Journal of the Transportation Research Board* 2240: 9–15.

Wells, S. A. 2005. Early age response of jointed plain concrete pavements to environmental loads. Thesis, University of Pittsburgh, PA.

Westergaard, H. M. 1926. Analysis of stressed in concrete pavements due to variations of temperature. *Highway Research Board Proceedings* 6: 201-215.

Westergaard, H. M. 1927. Analysis of stressed in concrete pavements caused by variations of temperature. *Public Roads* 8(3): 54–60.

William, G. W., and S. N. Shoukry. 2001. 3D finite element analysis of temperature-induced stresses in dowel jointed concrete pavements. *The International Journal of Geomechanics* 1(3): 291–307.

Wilson, M. L., and S. H. Kosmatka. 2011. *Design and Control of Concrete Mixtures*. 15th Edition. Portland Cement Association, Skokie, IL.

Xi, Y., Z. P. Bazant, and H. M. Jennings. 1994. Moisture diffusion in cementitious materials adsorption isotherms. *Advanced Cement Based Materials* 1(6): 248–257.

Yang, S. 2014. Health monitoring of pavement system using smart sensing technologies. Thesis, Iowa State University, IA.

Yinghong, Q. 2011. Numerical study on the curling and warping of hardened rigid pavement slabs. PhD dissertation, Michigan Technological University, MI.

Yoder, E. J., and M. W. Witczak. 1975. *Principles of Pavement Design*. 2nd Edition. John Wiley & Sons, NY.

Ytterberg, R. F. 1987. Shrinkage and curling of slabs on grade, Part II: Warping and curling. *Concrete International* 9(5)54–61.

Yu, H. T., and L. Khazanovich. 2001. Effects of construction curling on concrete pavement behavior. Paper presented at the 7th International Conference on Concrete Pavements, Orlando, FL.

Yu, H. T., L. Khazanovich, and M. I. Darter. 2004. Consideration of JPCP curling and warping in the 2002 design guide. Paper presented at the 83rd Annual Meeting of the Transportation Research Board, Washington, DC.

Zaghloul, S., T. White, and T. Kuczek. 1994. Evaluation of heavy load damage effect on concrete pavements using three-dimensional, nonlinear dynamic analysis. *Transportation Research Record: Journal of the Transportation Research Board* 1449: 123–133.

Zeller, M. J. 2014. *Contractor Quality and Contractor Buy-In in Minnesota*. Presentation to the National Concrete Consortium, Fall Meeting, Omaha, NE, September 10, 2014. www.cptechcenter.org/ncc/TTCC-NCC-2014.cfm. Last Accessed March 2, 2016.

Zhang, J., T. F. Fwa, K. H. Tan, and X. P. Shi. 2003. Model for nonlinear thermal effect on pavement warping stresses. *ASCE Journal of Transportation Engineering*, 129(6): 695–702.

APPENDIX A. PHOTO LOG OF SITE 1 IN STORY COUNTY

Figure 54. Field investigation at Site 1 on US 30 near Ames, Story County, STA1422 (MP 152.20) on October 28, 2015 (morning)

Figure 55. Pavement at Site 1 on US 30 near Ames, Story County, STA1422 (MP 152.20) on October 28, 2015 (morning)

Figure 56. Field investigation at Site 1 on US 30 near Ames, Story County, STA1422 (MP 152.20) on October 28, 2015 (afternoon)

Figure 57. Pavement at Site 1 on US 30 near Ames, Story County, STA1422 (MP 152.20) on October 28, 2015 (afternoon)

APPENDIX B. PHOTO LOG OF SITE 2 IN STORY COUNTY

Figure 58. Field investigation at Site 2 on US 30 near Nevada, Story County, STA2207 (MP 159.85) on October 28, 2015 (morning)

Figure 59. Pavement at Site 2 on US 30 near Nevada, Story County, STA2207 (MP 159.85) on October 28, 2015 (morning)

Figure 60. Field investigation at Site 2 on US 30 near Nevada, Story County, STA2207 (MP 159.85) on October 28, 2015 (afternoon)

Figure 61. Pavement at Site 2 on US 30 near Nevada, Story County, STA2207 (MP 159.85) on October 28, 2015 (afternoon)

APPENDIX C. PHOTO LOG OF SITE 3 IN LINN COUNTY

Figure 62. Field investigation at Site 3 on US 151 near Cedar Rapids, Linn County, STA162 (MP 32.75) on October 29, 2015 (morning)

Figure 63. Pavement at Site 3 on US 151 near Cedar Rapids, Linn County, STA162 (MP 32.75) on October 29, 2015 (morning)

Figure 64. Field investigation at Site 3 on US 151 near Cedar Rapids, Linn County, STA162 (MP 32.75) on November 10, 2015 (afternoon)

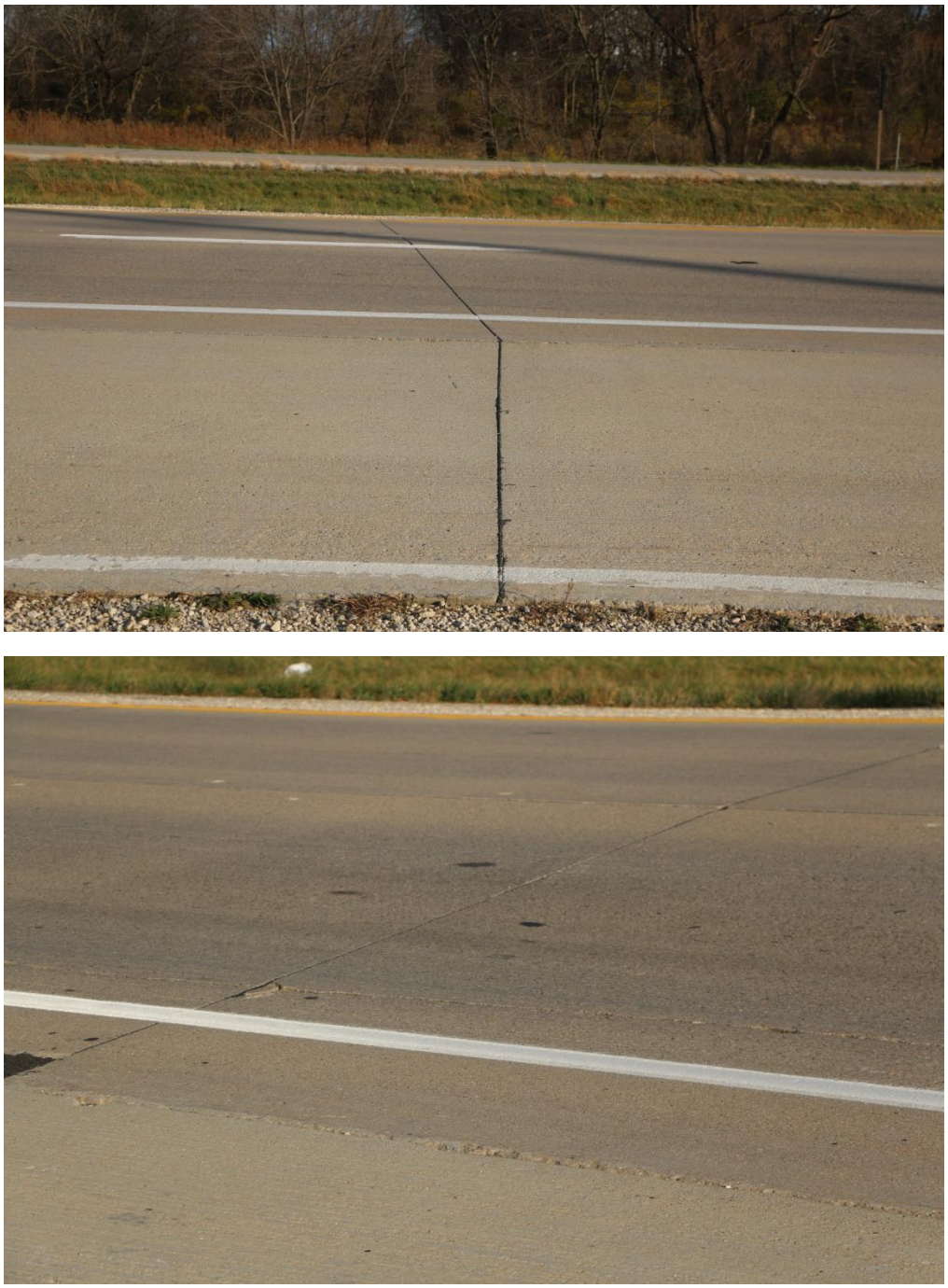

Figure 65. Pavement at Site 3 on US 151 near Cedar Rapids, Linn County, STA162 (MP 32.75) on November 10, 2015 (afternoon)

Figure 66. Slabs with cracks observed at Site 3

Figure 67. Transverse (top) and longitudinal (bottom) cracks at Site 3

APPENDIX D. PHOTO LOG OF SITE 4 IN LINN COUNTY

Figure 68. Field investigation at Site 4 on US 151 near Cedar Rapids, Linn County, STA183 (MP 33.15) on October 29, 2015 (morning)

Figure 69. Pavement at Site 4 on US 151 near Cedar Rapids, Linn County, STA183 (MP 33.15) on October 29, 2015 (morning)

Figure 70. Field investigation at Site 4 on US 151 near Cedar Rapids, Linn County, STA183 (MP 33.15) on November 10, 2015 (afternoon)

Figure 71. Pavement at Site 4 on US 151 near Cedar Rapids, Linn County, STA183 (MP 33.15) on November 10, 2015 (afternoon)

APPENDIX E. PHOTO LOG OF SITE 5 IN LINN COUNTY

Figure 72. Field investigation at Site 5 on US 30 near Cedar Rapids, Linn County, STA463 (MP 261.2) on October 29, 2015 (morning)

Figure 73. Pavement at Site 5 on US 30 near Cedar Rapids, Linn County, STA463 (MP 261.2) on October 29, 2015 (morning)

Figure 74. Field investigation at Site 5 on US 30 near Cedar Rapids, Linn County, STA463 (MP 261.2) on November 10, 2015 (afternoon)

Figure 75. Pavement at Site 5 on US 30 near Cedar Rapids, Linn County, STA463 (MP 261.2) on November 10, 2015 (afternoon)

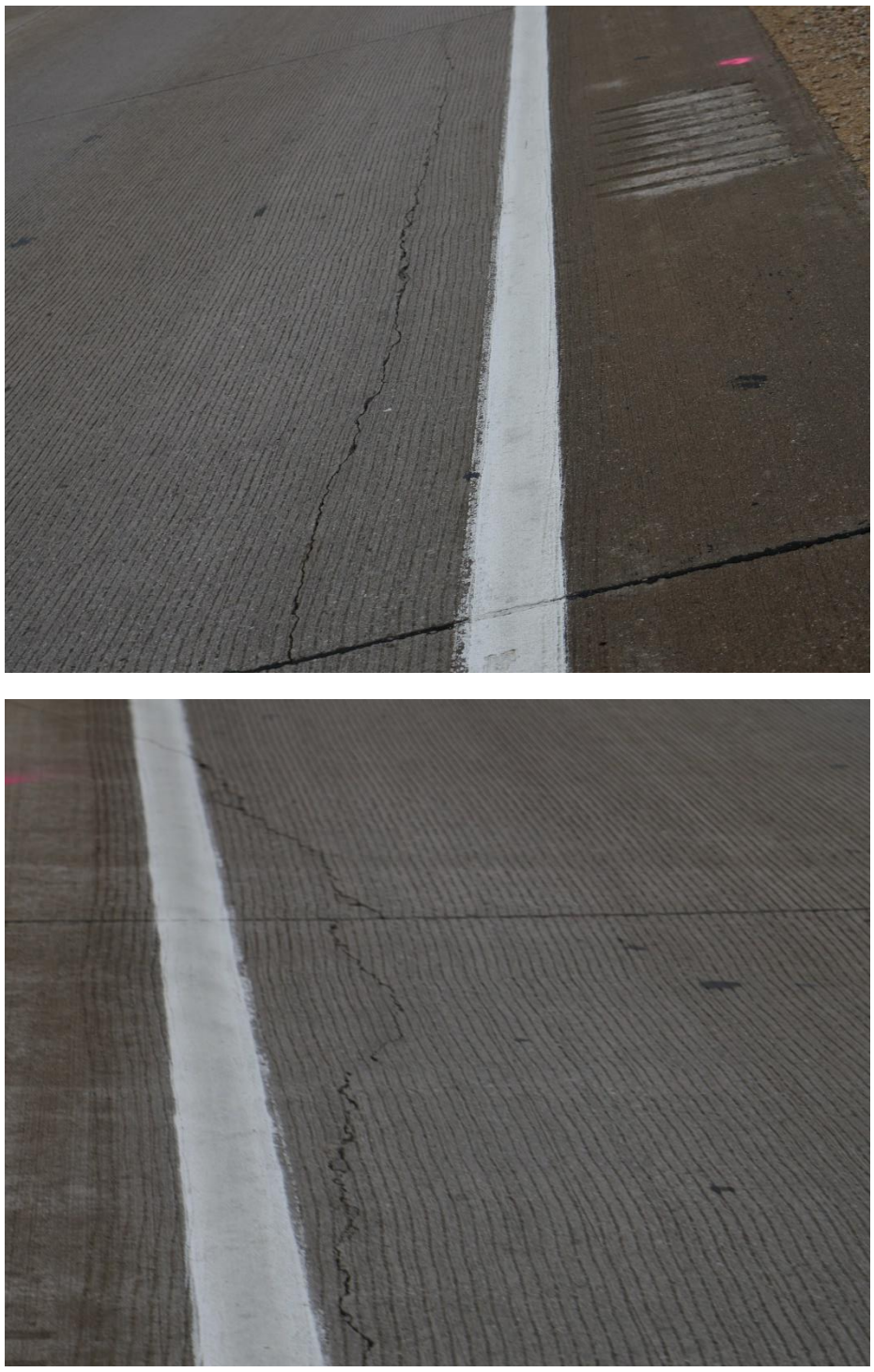

Figure 76. Slabs with cracks observed at Site 5

Figure 77. Longitudinal cracks at Site 5

APPENDIX F. PHOTO LOG OF SITE 6 IN TAMA COUNTY

Figure 78. Field investigation at Site 6 on US 30 near Toledo, Tama County, STA113 (MP 194.6) on November 10, 2015 (morning)

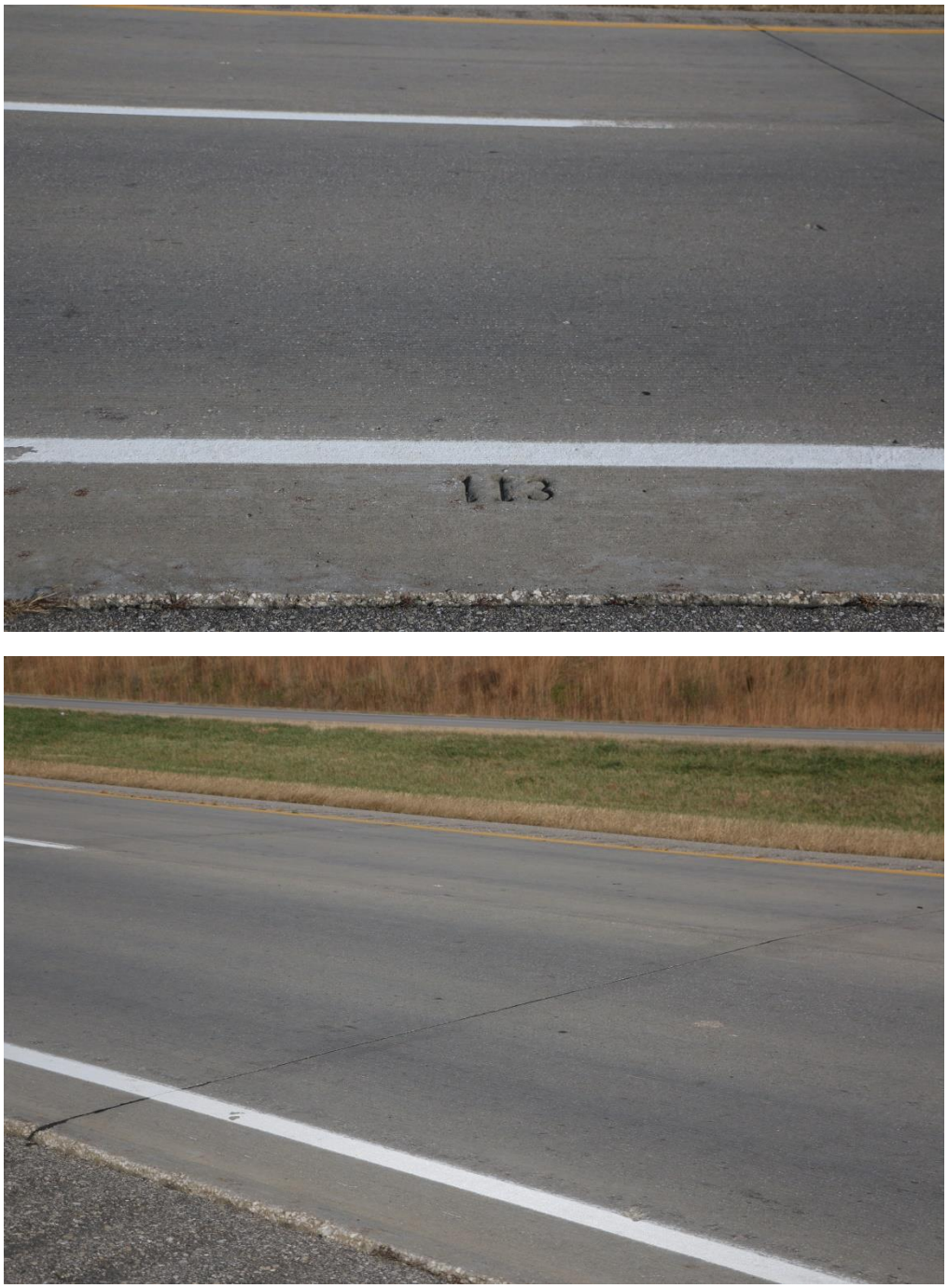

Figure 79. Site 6 on US 30 near Toledo, Tama County, STA113 (MP 194.6) on November 10, 2015 (morning)